localized spin fluctuations in some dilute alloy systems

j.e. van dam

L
1C
L0

LOCALIZED SPIN FLUCTUATIONS IN SOME

DILUTE ALLOY SYSTEMS

LOCALIZED SPIN FLUCTUATIONS IN SOME DILUTE ALLOY SYSTEMS

PROEFSCHRIFT

ter verkrijging van de graad van Doctor in de Wiskunde en Natuurwetenschappen aan de Rijksuniversiteit te Leiden, op gezag van de Rector Magnificus Dr. A.E. Cohen, Hoogleraar in de Faculteit der Letteren, volgens besluit van het college van Dekanen te verdedigen op woensdag 17 januari 1973 te klokke 15.15 uur.

door

JAN EGBERT VAN DAM
geboren te 's-Gravenhage in 1942

Krips Repro - Meppel

PROMOTOR : PROF. DR. C.J. GORTER

COREFERENT: DR. G.J. VAN DEN BERG

This investigation is part of the research programs of the "Stichting voor Fundamenteel Onderzoek der Materie (FOM)", which is financially supported by the "Nederlandse Organisatie voor Zuiver-Wetenschappelijk Onderzoek (ZWO)" and by the "Centrale Organisatie voor Toegepast Natuurwetenschappelijk Onderzoek (TNO)".

Aan mijn ouders

To my parents

Contents page

Chapter 4

The magnetic susceptibility of Pd-Cr and Pt-Cr alloys

GENERAL INTRODUCTION.

The work described in this section is concerned with the study of dilute magnetic alloys. The presence of small amounts of localized moments in a metal gives rise to a wide variety of phenomena [1]) which, since about 1966, are labeled with the name "*Kondo effect*".

In order to explain these phenomena several models of an impurity state in a metal have been used. The Anderson model [2]) assumes a large difference between purity and host metal, considering an extra d-orbital for the localized electron and assuming the conduction electrons to be mainly of s-character. The Wolff [3]) and Friedel [4]) model suggest the localized state to be due to resonant scattering of the conduction electrons by the impurity potential, resulting in a virtual bound state. Although these two models seem to be very different they are closely related to each other [5]). The extra orbital overlapping the conduction band in energy in the Anderson model can be considered also as a virtual bound state.

The possibility of a magnetic moment on the impurity site can be discussed using e.g. the Anderson model. It turns out that the magnetic properties of the virtual bound state are determined by two parameters:

1. the Coulomb repulsion between electrons of opposite spin, U.
2. the width of the virtual bound state, Δ.

The first interaction favours the formation of a local moment, while the second interaction opposes it. Consequently if U/Δ is sufficiently large a local moment exists, and if U/Δ is small, the impurity is non-magnetic. These two limiting cases have been considered in the s-d model [6]) and the localized spin fluctuation (LSF) model [7]).

The regime for $U/\Delta \sim 1$ has not yet been treated satisfactorily. Many attempts have been made but these are revised a few times per year. We will therefore only consider the LSF model in some detail, because of its simplicity and its success in explaining many experimental data.

The localized spin fluctuation (LSF) model.

The basic assumption of the LSF model is the existence of a characteristic time τ_{sf}, (corresponding to the lifetime of the fluctuations of the localized spin) which governs the magnetic behaviour of the impurity. When the LSF's are faster than the fluctuations induced by the temperature, one observes (in a static experiment) a non-magnetic behaviour. However, when the temperature

increases the LSF will eventually be slower than the thermal fluctuations and the LSF cannot be distinguished from a genuine spin, i.e. a magnetic behaviour is observed. The transition between the non-magnetic and the magnetic regime is smooth (no phase transition, because of a small number of degrees of freedom) and occurs near the spin fluctuation temperature, T_{sf}, which is determined by the relation $kT_{sf} = \hbar\tau_{sf}^{-1}$. Using the s-d model Nagaoka [8]) suggested for the first time the occurrence of a non-magnetic (singlet) ground state, the transition to this state taking place over many decades in temperature around a certain temperature, the Nagaoka-Suhl-Abrikosov temperature, later known as the Kondo temperature T_K. By identifying T_{sf} with T_K (the Kondo temperature), a connection was made between the LSF model and the s-d model.

From the above discussion it is clear that, within the LSF model, the magnetic properties of an impurity in a metal depend on the measuring conditions [9]). Considering only essentially static measurements (i.e. at frequencies much less than the spin fluctuation frequency) this means that only the value of the temperature relative to T_{sf} determines whether one observes magnetic or non-magnetic behaviour. The value of the localized spin itself is not affected, as might be intuitively deduced from the notion of "spin-compensation" used for many years.

The temperature dependence of the various properties of the dilute alloy is predicted to be very similar to that of the free electron gas in a metal, i.e. simple power laws. The main difference is in the value of the spin fluctuation temperature: T_F, the Fermi temperature, for the pure metal and T_{sf} for the dilute alloy. For example, in a pure metal one calculates for $T << T_F$ a temperature-independent spin susceptibility ("Pauli susceptibility"), while for $T >> T_F$ a Curie-law behaviour is obtained. In the dilute magnetic alloy one therefore expects an enhanced (about a factor T_F/T_{sf}) Pauli susceptibility for $T << T_{sf}$ and a Curie law behaviour for $T >> T_{sf}$. For intermediate temperatures the susceptibility can be described by a Curie-Weiss law, $\chi = c/(T + \Theta)$, where Θ has a value of the same order as that of T_{sf}.

Alloy systems

a. Au-V, Pd-Cr and Pt-Cr.

We have measured the static magnetic susceptibility of Au-V, Pd-Cr and Pt-Cr alloys. (see chapter I and 4). Our work was part of a combined effort of the Metals Group at the Kamerlingh Onnes Laboratory to study the various properties of these systems. Resistivity results were obtained by Star et al.[10]) and specific heat measurements performed by Boerstoel et al.[10]).

The main interest of this effort was to determine as accurately as possible the temperature dependence of the various properties far below T_K (or T_{sf}). Information about this behaviour was badly needed because at the time (about 1968) several, very different theoretical predictions existed. For example, the temperature dependence of the impurity resistivity (ρ) was calculated (at T = 0) to result in $|d\rho/dT| = \infty$ [11]) or $|d\rho/dT| = 0$ [7]). This ambiguity, which results in observable differences at higher temperatures also, has been resolved in favour of the latter prediction by the very accurate measurements of Star et al. [10]). However, before the conclusion of "simple power law" could be drawn, it was observed that only for alloys with a concentration below a certain value (c_o) it is allowed to compare experiments and theoretical predictions. In the theoretical models possible magnetic interactions between the impurities were not taken into account, consequently the alloys should also exhibit single impurity effects, which requires $c < c_o$. Analysis of electrical resistivity and the specific heat showed c_o to be approximately equal to T_K/T_F.

The choice of the systems to be studied was therefore motivated by the high Kondo temperatures which had been reported. (Au-V: 300 K; Pd-Cr: 30 K[+]) This enables one to study the properties far below T_K in an easily accessible temperature range and also for reasonably high concentrations, up to about 0.5 at.%.

b. Pd-Ni.

We have measured the specific heat of some dilute Pd-Ni alloys in order to check a suggestion that LSF effects would be at the origin of the anomalous temperature dependence of the effective Debye temperature. Our results are presented and discussed in chapter 2. The idea of local spin fluctuations was first suggested by Lederer and Mills [13]) in connection with the explanation of the properties of Pd-Ni. From a comparison of the properties of Pd-Ni and Pd-Cr in terms of the LSF model we conclude that these systems are behaving very similarly.

c. pure Pd.

For the analysis of the Pd-Cr measurements we also measured the susceptibility of pure Pd. The temperature dependence of χ is anomalous, exhibiting a broad maximum around 85 K in the χ versus T curve. Many attempts have been

[+] this value turned out to be much larger: $T_K \simeq 300$ K, a similar value was obtained for Pt-Cr.

made to explain this feature. We give a discussion of some results and compare our data with a recent bandstructure calculation by Andersen [12]) in chapter 3. The magnitude of the susceptibility is very high, which is the origin of many interesting phenomena, like the occurrence of ferromagnetism in very dilute Pd alloys. We have measured several Pd samples to study a possible influence of electron scattering on the value of χ. These results are also reported in chapter 3, which serves as a guide to the analysis of the Pd-Cr and Pd-Ni alloys.

REFERENCES

1. See the following review papers on experiments about the Kondo effect:
   - van den Berg, G.J., in "Progress in Low Temperature Physics" (C.J. Gorter, ed.) vol. 4, p. 194 (North-Holland Publishing Co., Amsterdam, 1964)
   - Daybell, M.D. and Steyert, W.A., Rev. Mod. Phys. 40 (1968) 380.
   - Heeger, A.J., in Solid State Physics series (Seitz, F., Turnbull, D. and Ehrenreich, H., eds.) vol. 23, p. 283 (Academic Press, New York, 1969).
   - van Dam, J.E. and van den Berg, G.J., Phys. Stat. Sol. (a) 3 (1970) 11.
   - Rizzuto, C., in Reports on Progress in Physics, to be published.
   - Wohlleben, D. and Coles, B.R.; Narath, A.; Daybell, M.D., and several other authors in "Magnetism" (Suhl, H., ed.) vol. 5, to be published.
2. Anderson, P.W., Phys. Rev. 124 (1961) 41.
3. Wolff, P.A., Phys. Rev. 124 (1961) 1030.
4. Friedel, J., Nuovo Cim. Suppl. 7 (1958) 287.
5. Rivier, N., thesis, University of Cambridge, 1968; see also Rivier, N. and Zitkova, J., Advances in Physics, 20 (1971) 143.
6. For a discussion of the s-d model see: Fischer, K., in "Springer Tracts in Modern Physics" (G. Höhler, ed.) vol. 54, p. 1 (Springer Verlag, Berlin, 1970).
7. See e.g. Rivier, N. and Zuckermann, M.J., Phys. Rev. Letters 21 (1968) 904.
8. Nagaoka, Y., Phys. Rev. 138 (1965) A1112.
9. This point of view has been stressed particularly by Wohlleben and Coles in their forthcoming paper, see ref. 1.
10. Star, W.M., thesis, University of Leiden, 1971; Star, W.M., Physica 58 (1972) 623; Star, W.M., de Vroede, E. and van Baarle, C., Physica 59 (1972) 128 (Communications Kamerlingh Onnes Lab., Leiden, No. 390 b and and c).
11. Hamann, D.R., Phys. Rev. 158 (1967) 570.
12. Andersen, O.K., Phys. Rev. B2 (1970) 883.
13. Lederer, P. and Mills, D.L., Phys. Rev. 165 (1968) 837.

CHAPTER 1

MAGNETIC SUSCEPTIBILITY OF SOME Au-V ALLOYS *

Abstract

The magnetic susceptibility of some Au-V alloys (0.2, 0.3, 0.5, 1.0, 2.0 and 10.0 at.%V) has been measured from 2 K to 293 K. The temperature dependence of the impurity susceptibility of the most dilute samples (0.2 and 0.3 at.%V) can be described, for $T < 50$ K, by $\chi(T) = \chi(0)(1 - AT^2)$. This result is discussed in the light of existing theoretical predictions for the behaviour of a Kondo system. It turns out that the magnetic susceptibility can be considered to arise from a virtual bound state having a width comparable to kT_K. Our results for more concentrated alloys indicate the existence of V atoms with stronger and weaker local magnetic properties than isolated V atoms. It is suggested that this concentration-dependent behaviour can be explained by assuming that nearest-neighbour V atoms have a decreased local susceptibility, while next-nearest V atoms show an increased local susceptibility.

1.1. Introduction

From several experiments on Au-V alloys one can deduce that this system behaves like a Kondo alloy with a characteristic temperature T_K ("Kondo temperature") of about 300 K [1]. Therefore it is a suitable system to study the behaviour of various properties (e.g. resistivity, specific heat) below the Kondo temperature. As the theoretical predictions for the behaviour below T_K differ widely †, one hopes that careful experiments can provide an answer as to which theory is correct.

Recently it was shown that experimental evidence on several Kondo systems [2] supports theories which predict a simple power-law behaviour. This experimental evidence was, however, restricted to resistivity data and specific-heat results. The temperature dependence below T_K of the magnetic susceptibility (this will be referred to in the rest of this work simply as susceptibility)

* The main part of this chapter has already been published in Physica [77].
† Recently a kind of convergence seems to have set in (see section 1.5).

is still uncertain. There are several reasons for this.

First of all, the presence of small amounts of magnetic impurities (e.g. Fe) has a large influence on the susceptibility at low temperatures ($T \leq 20$ K).

Secondly, all kinds of clustering, of metallurgical or statistical origin, can play a dominant role [3].

Finally, the determination of the susceptibility as a function of temperature is about two orders of magnitude less accurate than that of the resistivity. For this reason, fitting the susceptibility data to a certain theoretical expression generally has less significance than is usually assumed. For example, a fit to a formula of the Curie-Weiss type seems to be always possible, provided the tamperature range is sufficiently limited.

Although the exact temperature dependence of the susceptibility is difficult to establish experimentally, one might hope to solve the fundamental problem of the low-temperature behaviour at least qualitatively, i.e. whether or not the susceptibility diverges at $T = 0$.

Susceptibility measurements on the Cu-Fe system by Tholence and Tournier [4] indicate that the susceptibility remains finite, in contrast to some earlier work by Daybell and Steyert [5,1b].

For the Au-V system also a non-divergent behaviour has been found by several authors [1b]. This is confirmed by our measurements, which show in addition a $-T^2$ temperature dependence at low temperatures and for low concentrations (see section 1.4). Besides the temperature dependence of the susceptibility it is of importance to study the concentration dependence. If one compares experimental results with theoretical expressions for the Kondo effect, one should be sure to have single-impurity effects (i.e. behaviour proportional to the concentration). Only for the single impurity effects do the present theories hold.

Since in the resistivity and the specific heat of Au-V alloys a peculiar type of concentration dependence was observed [6,7], it seems worthwhile to look for this effect in the susceptibility also. Previous measurements of the susceptibility of Au-V alloys (see section 1.3) have not shown such a concentration effect, but we have been able to observe it. We propose an explanation of this effect, which generalizes a model that has been suggested earlier [8] to describe concentration-dependent behaviour in Au-V alloys (see section 1.5).

In section 1.2 we describe the experimental set-up; in section 1.3 previous measurements on the Au-V system are reviewed; in section 1.4 we present our results on the susceptibility, which are discussed and compared with various theories in section 1.5. The conclusions are summarized in section 1.6.

1.2. Description of the experimental arrangement

In this section an experimental set-up is described, which allows the measurement of the magnetic susceptibility in the temperature range from 2 K to room temperature. The Faraday method is used for these measurements, since this method is best suited for measuring dilute alloys. A sketch of the experimental set-up is shown in figs. 1 and 2. In the following a detailed description of the different sections of this set-up will be given.

1.2.1. *Cryostat*. The cryostat consists essentially of two concentric tubes which are mainly constructed from german silver. The inner tube (Ø = 1 cm) connects the vacuum housing of the balance on top of the cryostat with the

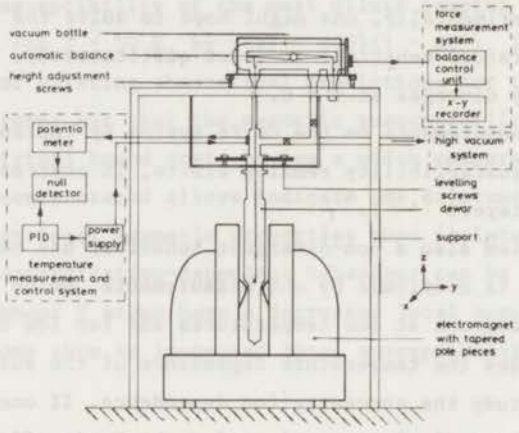

Fig. 1. Schematical view of the susceptibility set-up. PID = Proportional, Integrating and Differentiating device. The origin of the coordinate system is halfway between the edges of the pole pieces.

sample chamber at the lower end of the cryostat. The outer tube surrounds the inner tube over most of its length and provides the possibility of evacuating the space between inner and outer tube. The sample chamber, made from copper, is then connected with the cooling fluid outside the outer tube through a stainless-steel section of the inner tube (see fig. 2) and a large brass flange which serves as a heat sink. This construction allows one to control the temperature of the sample chamber in the temperature range above those provided by the cooling liquids (He, H_2 and N_2) (see section 1.2.5). The lowest sections of the outer and inner tubes can be removed for access to the sample. These sections are attached to the outer and inner tubes by flanges with indium O-ring high vacuum seals. The sample is placed in a Teflon sample holder, which

has the form of a little bucket. An eye on the lid of this bucket is hooked on the balance suspension wire (high-purity copper, Ø = 0.1 mm). The choice of Teflon material and pure-copper wire was motivated by their low and nearly

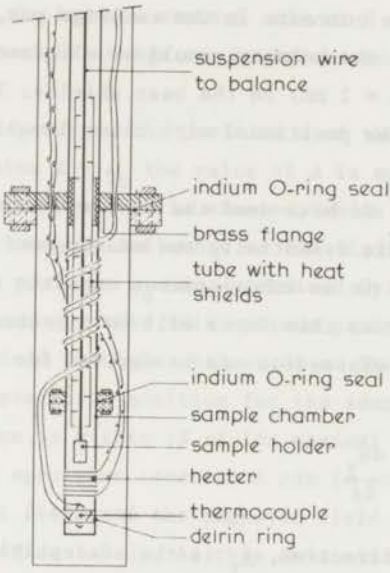

Fig. 2. Diagram of the lower section of the cryostat.

temperature-independent susceptibilities [9]). Indeed the force on the empty sample holder (bucket and suspension wire) turned out to be only slightly temperature-dependent at low temperatures (about 10% change in the force when decreasing the temperature from 77 to 2 K).

On the sample chamber a heater (200 Ω) is wound with insulated constantan wire (Ø = 0.1 mm). Also on the sample chamber one of the thermocouple junctions, spotwelded into a gold foil, is attached. A ring made of Delrin is mounted around this gold foil. By contracting at temperatures below room temperature this ring ensures good thermal contact of the thermocouple with the sample chamber. In order to avoid ground loops in the measuring circuit the sample chamber has been electrically insulated by applying GE varnish or nitrocellulose lacquer. The various electrical leads (heater, thermocouple etc.) are thermally anchored on the stainless-steel section of the inner tube before reaching room temperature. The thermocouple leads are fed through a seal with open pins without any soldering (the seal is made vacuum-tight with sealing

wax). The other leads are soldered to a high-vacuum metal-glass seal.

Inside the inner tube a small tube with many radiation shields was fitted (see fig. 2). This provides a stable temperature gradient along the suspension wire between the heat sink (brass flange) and the sample chamber. By fitting this small tube, unstable gas currents in the exchange gas, which cause spurious forces [10]) detected by the balance, could be eliminated. The suspension wire passes through holes (Ø = 2 mm) in the heat shields. The cryostat is mounted on a platform which can be positioned with three levelling screws.

1.2.2. *Force measurement.* We have used the Faraday method of measuring the susceptibility. This method is essentially the measurement of the force exerted on a small sample placed in an inhomogeneous magnetic field. By choosing a special form of the pole pieces this force will be directed along the z axis (see fig. 1). The following expression can be derived for the force in this case [11]):

$$F_z = v(\chi_v - \chi_o)H_y \frac{dH_y}{dz} \qquad (1)$$

where F_z is force in the z direction, χ_v is the susceptibility of the sample per unit volume, χ_o is the susceptibility of the surrounding medium, per unit volume, v is the volume of the sample, H_y is the magnetic field in the y direction (see fig. 1). The surrounding medium used in our experiments is purified helium gas (about 100 torr at room temperature), which has a very small susceptibility per unit volume (-8.4×10^{-12} emu/cm^3) at 20 °C and 760 torr. Compared to the susceptibilities of most of the samples (e.g. Cu: -9.7×10^{-9} emu/cm^3) one can safely neglect χ_o. Introducing χ_m, the susceptibility per unit mass, the expression for the force then reads:

$$F_z = m\chi_m H_y \frac{dH_y}{dz} = Am\chi_m, \qquad (2)$$

where m is the mass of the sample and $A = H_y(dH_y/dz)$. If A and m are known, χ_m can be directly calculated from the force measurement using formula (2).

The force is measured as an apparent weight change by a commercially available automatic microbalance (Cahn, type RG). The sensitivity of this balance is claimed to be 0.1 μg, but in our set-up it is limited to about 1 μg.

The accuracy of the balance readings under ideal conditions is about 0.05%. This corresponds to an accuracy in the apparent weight change of about 0.1% to 0.3%, depending on the value of the apparent weight change, which is a diffe-

rence of the two balance readings (without and with field).

The output from the balance control unit is detected by an X-Y recorder (Hewlett-Packard 2D-2M), which is used as a null instrument. The X input is used in "time" function, the Y input being in the potentiometric mode. From the dial readings of the balance control unit at H = 0 and H = H_i ($2 < H_i < 16$ kOe) the apparent weight change can be calculated directly, once the balance has been calibrated.

The value of A depends on the position z of the sample for a certain magnetic field. For a value $z = z_o$ the value of A is maximal. At this position the maximal force on the specimen is exerted, while the variation of A with z is minimal, and therefore the influence of the finite size of the sample is smallest. The optimum position z_o was determined by measuring the force as a function of z. It turned out that this optimum position shifted slightly with increasing magnetic field to higher values of z. Therefore a "mean" value of z_o was chosen as the preferred position for the sample ($\bar{z}_o$ = +3.30 cm). For this position the force is within 1% of its maximal value for every field.

The value of the apparatus constant A can in principle be determined by measuring the magnetic field and the magnetic field gradient at the position of the sample (see section 1.2.3). As this determination (especially of the gradient dH_y/dz) is not very accurate, it has been done by measuring the force on a sample with accurately known susceptibility. Calibration measurements were performed at room temperature on high purity (Cominco) gold (6 N+) and on (4 N) tantalum from "Johnson Matthey". Using the values $\chi_m(Ta) = +0.849 \times 10^{-6}$ emu/g[12,13]) and $\chi_m(Au) = -0.143 \times 10^{-6}$ emu/g[14]) the factor A has been determined for 14 different magnetic fields in the range 2 - 16 kOe.

To take into account the uncertainty of the sample position at low temperatures due to the contraction of the suspension wire (see section 1.2.5) measurements were also carried out at 77.5 K. This resulted in slightly different (0.5%) values for A.

By this calibration procedure all measured susceptibilities, calculated with formula (2), are relative to the values of the "standard" specimens Au and Ta we have used.

As a check on the absolute accuracy the susceptibilities of some pure metals (Pt and Cu) have been determined and compared to the values recently obtained by other authors (see table 1.1). As can be noted the agreement between these values is rather good.

1.2.3. *Magnetic field calibration.* The inhomogeneous magnetic field necessary for the Faraday method is produced by an Oerlikon (C 30) electromagnet

TABLE 1.1

Summary of susceptibility data for Cu and Pt *

Pt		Cu	
χ_m (10^{-6} emu/g)	Ref.	χ_m (10^{-6} emu/g)	Ref.
0.985	15	0.0858	18
1.013	16	0.0860	19
0.971	12	0.0863	this work
0.979	17		
0.982	this work		

* T = 293 K.

with tapered pole pieces, $\emptyset$ = 200 mm, like those designed by Heyding et al. [20]. These pole pieces provide a relatively large region (5 x 5 mm) of constant (i.e. within 1%) value for $H_y(dH_y/dz)$. This decreases the errors due to finite sample size and deviations of the sample position from the "standard" position $\bar{z}_o$.

The magnet current is supplied by a stabilized power supply ($1:10^5$). The value of the current can be dialled on a digital remote control box. In our experiments we have always used values of the magnet current which were multiples of 10 A.

The magnetic field strength as a function of magnet current has been determined with a small coil of known dimensions. The voltage induced in this coil by rotating it by 180^o was detected by a ballistic galvanometer. From this voltage the value of the magnetic field could be calculated, after calibrating the galvanometer with a known flux change by reversing a current in a calibrated self-inductance. The accuracy of this method is about 1%. The procedure described above was checked, using flat pole pieces, by determining the magnetic field with NMR techniques. Agreement between the two methods was within the experimental error of the coil method.

The magnetic field strength has been determined for several values of z to get an impression of the profile of the magnetic field. From a plot of H_y^2

vs. z (see fig. 3) one can deduce a value for $H_y(dH_y/dz)$ at $z = z_o$. The values are about 10% smaller than determined by the force measurement (see section 1.2.2), which is most probably due to errors in the graphical evaluation [21]).

The maximum field with a pole gap of 6.0 cm, at $z = z_o$, is 16 kOe (I_{magnet} = 140 A).

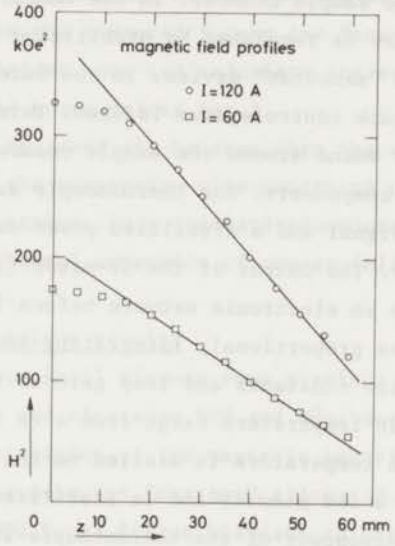

Fig. 3. Variation of H^2 along the z axis, for a pole gap of 60 mm.

1.2.4. *Temperature measurement, calibration and regulation.* The temperatures in the ranges provided by liquid helium, hydrogen or nitrogen have been deduced from the vapour pressures (mercury manometer) using for He the T_{58} table [22]), for H_2 the table by Durieux and Van Dijk [23]) and for N_2 a table by Henning and Otto [24]).

In the intermediate temperature ranges from 2 K to 293 K the temperature is obtained with an Au-Fe (0.03 at.% Fe) vs. Chromel thermocouple. The thermocouple wires (Ø = 0.08 mm) are enamel insulated as supplied by Johnson Matthey The properties and advantages are described in the literature [25,26]).

The thermal e.m.f. was measured by means of a potentiometer (Leeds and Northrup, type K5) with a μV-meter (Fluke, model 845AB) as null detector. The sensitivity of this measurement is about 0.2 μV corresponding to about 0.01 K. The thermocouple has been calibrated in the ranges provided by the liquid coolants (He, H_2, N_2) and with a calibrated platinum thermometer from 20 K up to room temperature *. In the range from 4 to 14 K a graphical interpolation of V_{emf} vs. T was made using

* The calibrated Pt-thermometer was kindly provided by the thermometry group of our laboratory.

the data of a calibrated Au-Fe (0.03 at.%) vs. chromel thermocouple [27]). The relative accuracy of the temperature determination is estimated to be about 1% over the whole temperature range.

The temperature of the sample, which temperature can be assumed to be the same as that of the sample chamber within 1% [10]), can be regulated by controlling the temperature of the sample chamber. In the temperature ranges of liquid He, H_2 or N_2 the temperature is regulated by stabilizing the vapour pressure of the cooling liquid by a "manostat" device. In the intermediate temperature ranges an electronic feedback controlsystem is used. This system regulates the current through the heater wound around the sample chamber. The feedback loop consists of the following components: the thermocouple as sensor, the μV-meter as detector of the error signal and a stabilized power supply (Hewlett-Packard model 6202B) as controller. The output of the μV-meter (1 V for a full-scale deflection) passes through an electronic network before it acts on the power supply. This network allows proportional, integrating and differentiating actions. By adjusting the time constants and loop gain of this feedback system it can be used in the whole temperature range from 4 to 293 K. When the voltage corresponding to a certain temperature is dialled on the potentiometer this temperature is reached in a few minutes and is stabilized quickly.

The change in the thermopower of the thermocouple in an applied magnetic field causes a shift in the regulated temperature, which can be neglected for our purpose. ($\Delta T/T \approx 1\%$ at 4 K, decreasing rapidly at higher temperatures [25]).)

1.2.5. *Experimental procedure and operation.* The sample (maximum dimensions: a cylinder of 4 x 3 mm) is placed in the sample holder, which is suspended by a wire hanging down from one arm of the balance. The balance is placed in the equilibrium position by counter weights on a pan hanging on the other arm.

The optimum position of the sample is then obtained by adjusting screws on the balance housing. The position of the sample is read by a cathetometer.

By visual inspection of the clearance of the suspension wire from the inner sections of the cryostat and by observing the recorder trace, the cryostat is aligned to the suspension wire with the adjusting screws on the cryostat platform. Now the sample chamber and outer can are mounted to the cryostat with bolts; indium O-rings provide for a vacuum-tight connection. The inner and outer tubes and the vacuum bottle surrounding the balance are then evacuated to about 5×10^{-5} torr to remove the oxygen. The apparatus is subsequently filled with purified helium gas ($p \approx 100$ torrr at room temperature) which provides a proper exchange of heat between the sample, the sample chamber and cooling fluid.

The helium gas is purified by absorption in an active charcoal trap, cooled with liquid hydrogen.

The susceptibility can now be measured from 2 to 293 K. At each temperature the force on the sample is recorded for several of the 14 field strengths, in the range from 2 to 16 kOe, which have been used in this experiment. In this way any possible field dependence of the susceptibility could be checked. Having subtracted from the measured forces the force exerted on the suspension wire and the sample holder, one can calculate the susceptibility according to formula (2), using the known values for A.

It is necessary to lower the balance when the cryostat is cooled down to low temperatures, as the suspension wire contracts upon cooling. This is done as a function of temperature in a standard procedure, estimating the contraction from the known thermal expansion of copper ($\Delta l/l \approx 0.3\%$ [28]).

1.3. Discussion of previous results

In this section we shall discuss some previous susceptibility measurements [8]) on the Au-V system and also some NMR and Mössbauer effect results which are essential for the explanation of the magnetic behaviour of Au-V. Kume [29]) published susceptibility data for four Au-V alloys (0.3; 1.0; 1.1 and 2 at.%V) in the range 1.4 - 1000 K. He fitted his data to the following formula (to judge from his figure 3 this fit is only valid from 20 to 300 K):

$$\chi(T) = \chi_{Au} + \frac{Nc\mu_{eff}^2}{3k(T + \Theta)}, \qquad (3)$$

where $\chi(T)$ is the susceptibility of the alloy per mole, χ_{Au} the susceptibility of the Au per mole, μ_{eff} the magnetic moment of the V atom, c the concentration of V atoms, N Avogadro's number, k Boltzmann's constant and Θ is the effective Curie-Weiss temperature. The fit resulted in values for μ_{eff} and Θ of 3.0 μ_B and +290 K, respectively. The value of Θ was found to be independent of concentration and was assumed to be equal to the Kondo temperature (T_K).

Below 20 K deviations from the fit were noted, which Kume ascribed to magnetic impurities (like Fe). Although the Au used as starting material contains about 10 ppm Fe and the contribution of V could be 2 ppm (for the 1.1 at.% this figure will be much larger) this contamination is probably not the only cause of the deviations (see below).

Kume gave also an alternative description of his data according to the following formula:

$$\Delta\chi = \frac{Nc\mu_{eff}^2(T)}{3kT} = \frac{Nc\mu_B^2 p_{eff}^2(T)}{3kT} . \qquad (4)$$

In this formula it is assumed that μ_{eff} is temperature dependent. Using his susceptibility data Kume then calculated $\mu_{eff}(T)$. At temperatures of about 1000 K μ_{eff} becomes temperature independent(Curie-law behaviour), while μ_{eff} decreases gradually to zero as the temperature decreases to zero ("spin compensation").

Creveling and Luo [8]) measured the susceptibility of many Au-V samples in the concentration range 0.05 - 20 at.%V from 0.4 to 293 K. The purity of their starting materials is for Au: 99.999$^+$% and for V: 99.97%. They discovered that the heat treatment of the samples could substantially influence the results. Creveling and Luo could fit their data to a formula of the following form:

$$\chi = \chi_o + C/(T + \Theta) . \qquad (5)$$

Contrary to the analysis by Kume they assumed χ_o to be an adjustable parameter, like Θ and C. Thus one allows for a temperature-independent contribution of the V atoms and a possible effect of alloying on the host susceptibility. In trying to explain their results Creveling and Luo assumed that only a fraction of the V atoms is "magnetic", in the sense that these atoms contribute to the temperature-dependent term in eq. (5). This suggestion, which was first put forward by Vogt and Gerstenberg [30]), is made plausible by a model in which V atoms without nearest neighbours ("isolated" V atoms) have a local moment. This moment is quenched by the presence of another V atom on a nearest-neighbour site. The strong influence of the local environment on the magnetic properties of the V atoms has been demonstrated by many experiments on the compound Au_4V. For an extensive discussion see refs. 8 and 31. In the ordered phase Au_4V is ferromagnetic ($T_c \simeq 60$ K), while in the disordered phase the ferromagnetism has disappeared. Mössbauer-effect measurements by Cohen et al. [31]) substantiated suggestions that the ferromagnetic behaviour of ordered Au_4V is due to local moments on the V atoms. Furthermore they could deduce from their data that in the disordered phase the local moment on the V atoms disappears. The disappearance of the local moment was shown not to be due to a transition of the d electrons of V to an s-like conduction band. Cohen et al. explained this disappearance on the basis of the Anderson model, suggesting that a small increase in the level width (due to crystal-field interac-

tions in the disordered phase) leads to the "collapse" of the moment. The validity of this local environment model for disordered Au-V alloys was confirmed by NMR and spin-lattice relaxation-time measurements by Narath and Gossard [32]. By a careful analysis of their data they could extract the magnetic properties of the "magnetic" and "nonmagnetic" V sites, suggesting the difference to be simply a difference in spin-fluctuation lifetimes. Another important conclusion concerned the possible existence of an impurity-induced long-range spin polarization of the conduction electrons, as suggested by Heeger et al. [33]. Narath and Gossard showed by experiments on Au(Ag)-V alloys that this long-range polarization is not present in Au-V alloys [32]. The observed interactions leading to transitions between "magnetic" and "nonmagnetic" V atoms are in fact found to be of short-range character. Contrary to the observations of Creveling and Luo [8], it appeared that different heat treatment had no effect on the line shape of a 1.0 at.%V alloy [32].

1.4. Experimental results

1.4.1. *Sample preparation.* The alloys were prepared in an induction furnace by melting appropriate amounts of the starting materials Au and V (Au: Cominco 6N+; V: Johnson Matthey 4N). Use was made of high-purity alumina (Al_2O_3) crucibles. The alloys were kept liquid under pure argon atmosphere for about 30 minutes. One sample (no. 7) has been prepared from less pure Au (5N) in a radiation furnace.

The samples have been spark cut from the melt in the form of cylinders (4 x 3 mm). Two samples (3 and 5) were cut from large samples used for specific-heat measurements by Boerstoel et al. [7,2a]. One sample (no. 2) was cut from the same melt from which Star et al. obtained their resistivity specimen [2b,34]. For this alloy zone-refined V was used. After annealing at 1000 °C the samples were quenched in water or slowly cooled to room temperature.

It turned out that the susceptibility results of some alloys were strongly influenced by this heat treatment (see section 1.4.2). Before the samples were measured they were heavily etched in boiling aqua regia. In table 1.2 a summary of the sample characteristics is given. The analysis of the concentration of some samples has been performed by Dr. Kragten et al. (Natuurkundig Laboratorium, Amsterdam) using an atomic absorption spectrophotometric technique. The accuracy of this method is about 3%. For some samples the Fe contamination was determined, which is also shown in table 1.2. In all cases the Fe contamination was less than the detection limit (about 5 ppm). The nominal and

Table 1.2

Sample characteristics of Au-V alloys

Sample	Lab no.	Conc V(at.%) (nom.)	Conc V(at.%) (anal.)	Fe contamination	Homogenization process	Quenched
1	6899	0				no
2	6982	0.2	0.19			yes
3	68126	0.3	0.32		48 h, 1000°C	yes
4	6922	0.5	0.34		20 h, 1000°C	yes
5a	6895	1.0	0.93 *		48 h, 1000°C	no
5b		1.0			24 h, 1000°C	yes
6a	6935	2.0			24 h, 1000°C	no
6b		2.0		< 5 ppm	24 h, 1000°C	yes
7	67138	10.0	9.75		24 h, 1000°C	no
8		100.0		< 5 ppm		

* This value was checked by wet chemical analysis.

analytical concentrations of the samples do agree quite well, except for sample no. 4 and no. 5. The nominal concentration has been adopted for no. 4 on the basis of the value of $\Delta\chi$ (see fig. 12) and the analytical concentration for no. 5, since this value was also found by wet chemical analysis. The only difference between samples 5a and 5b (6a and 6b) is the difference in quenching after

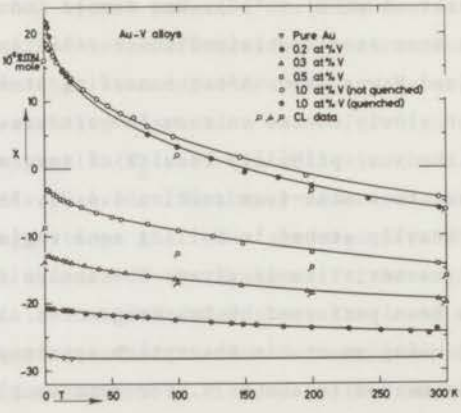

Fig. 4. Temperature dependence of the susceptibility for Au-V samples with a V concentration up to 1 at.%. The values indicated for χ are per mole of the alloy.

the annealing (homogenization process).

1.4.2. *Temperature dependence of the susceptibility.* In figs. 4, 5 and 6 the experimental results are shown for the susceptibility in the temperature range from 2 K to 295 K for the samples 1-5, 6 and 7, respectively. Some of these results were already discussed in a short paper [35]). The susceptibilities

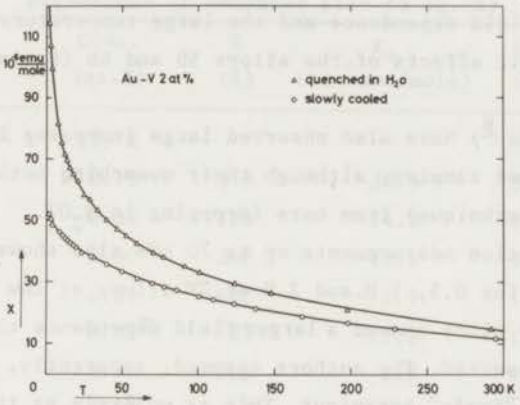

Fig. 5. Temperature dependence of the susceptibility of sample 6. The differences between the slowly cooled (s.c.) and the quenched (q) data for this sample are not due to Fe contamination (see text). At temperatures below 4 K the values of χ for 6b, obtained at 16 kOe have been plotted.

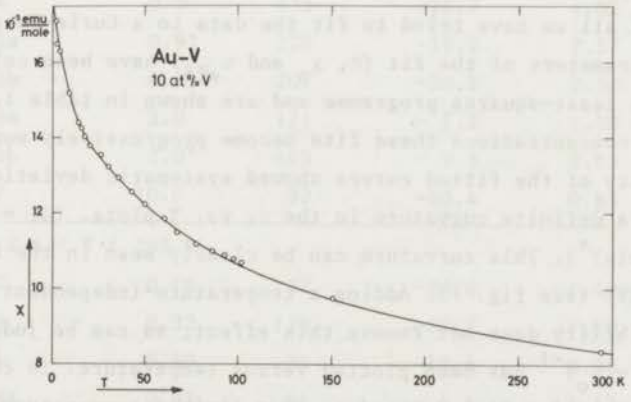

Fig. 6. Temperature dependence of the susceptibility for sample 7.

are field-independent up to 16 kOe, except for samples 5b and 6b, which show field-dependent behaviour at temperatures below about 8 K. The values plotted in figs. 4 and 5 are those determined in a magnetic field of 16 kOe. The

origin of this field dependence is uncertain. Contamination of the samples, which are identical to the samples 5a and 6a, during the quenching in H_2O is unlikely. This has been verified for sample 6b by analyzing it, see table 1.2. As expected, the supposed Fe contamination turned out to be less than the detection limit (5 ppm), which is far too small to explain the observed effect which would correspond to about 20 ppm Fe. The field dependence for the 1 at.%V alloy (no. 5b) is much smaller ($\simeq$ 2 ppm Fe).

Therefore, the field dependence and the large temperature dependence are most probably intrinsic effects of the alloys 5b and 6b (for a discussion see section 1.5.2.).

Creveling and Luo [8]) have also observed large increases in the temperature dependence for quenched samples, although their quenching method is very different (splat-cooling technique) from ours (dropping in H_2O).

Recent magnetization measurements up to 70 kOe also showed field-dependent susceptibilities [36]) for 0.5, 1.0 and 2.0 at.%V alloys at low temperatures ($T < 5$ K). The 2 at.%V alloy showed a larger field dependence than the more dilute alloys, as we have observed. The authors assumed, apparently, that the magnetic field influenced the "Kondo" behaviour. This is unlikely as the Kondo temperature is too large ($T_K \simeq 300$ K) for these fields to have a significant effect. However, the presence of V impurities having substantially lower T_K values might explain this behaviour qualitatively. This possibility will be discussed in the next subsection.

We have analyzed our data in several ways.

a) First of all we have tried to fit the data to a Curie-Weiss law (formula (5)). The parameters of the fit (Θ, χ_o and μ_{eff}) have been calculated by a computer with a least-squares programme and are shown in table 1.3. For alloys with higher concentrations these fits become progressively worse. Examination of the quality of the fitted curves showed systematic deviations from the data, indicating a definite curvature in the $\Delta\chi$ vs. T plots. ($\Delta\chi = \chi_{alloy} - (1 - c)\chi_{Au}$(emu/mole)*). This curvature can be clearly seen in the case of sample 5b (1 at.%V) (see fig. 7). Adding a temperature-independent term to the impurity susceptibility does not remove this effect, as can be judged from fig. 8, where $(\chi - \chi_o)^{-1}$ has been plotted versus temperature. To check these observations we have also fitted the data over limited temperature ranges, viz. 2-77.5 K and 90-295 K. The parameters resulting from the fits in the

---

*The notation (emu/mole) is used for the susceptibility of a mole of the *alloy*.

limited temperature ranges are shown also in table 1.3. In the "high"-temperature range (case B), a clear trend toward higher Θ values than those obtained in the "low"-temperature range (case C) can be deduced. Also the values of μ_{eff} are systematically higher in case B than in case C. The data which have

Table 1.3

Parameters of computer fits to eq.(5) *

Sample	Conc. (at.%)	Θ (K)	χ_o (10^{-6} emu/mole)	μ_{eff} (μ_B)
A:2 K < T < 295 K				
2	0.19	315	-28.5	3.21
3	0.32	225	-24.3	2.52
4	0.50	267	-23.7	2.91
5a	0.93	127	-13.9	1.87
5b	0.93[q]	85	-13.3	1.55
6a	2.0	115	- 2.7	1.55
6b	2.0[q]	62	+ 0.4	1.45
7	10.0	71	+64.9	0.75
B:90K < T < 295 K				
2	0.19	302	-28.3	3.12
3	0.32	454	-28.1	4.01
4	0.50	435	-28.2	4.02
5a	0.93	228	-19.2	2.57
5b	0.93[q]	207	-20.5	2.50
6a	2.0	171	- 7.7	1.90
6b	2.0[q]	145	- 9.3	2.05
7	10.0	92	+60.4	0.85
C:2 K < T < 295 K				
2	0.19	127	-24.6	1.45
3	0.32	123	-21.1	1.60
4	0.50	59	-12.4	0.95
5a	0.93	64	- 4.4	1.13
5b	0.93[q]	36	- 2.4	0.86
6a	2.0	57	+11.9	0.95
6b	2.0[q]	14	+24.2	0.73
7	10.0	37	+84.7	0.50

*The data listed in the appendix have been used for these fits.

been fitted were not corrected for the temperature dependence of the host. This causes an artificial temperature dependence of the impurity susceptibility at low temperatures which leads to too low values for Θ in case C. This correction is important for the most dilute samples (e.g. 2, 3 and 4). Only for the lowest concentration (0.19 at.%V) is there no difference between cases A and B, indicating the absence of a systematic curvature. It is important to note that χ_o for this sample has about the same value as that of pure Au (-28.1×10^{-6} emu/mole). When the concentration is increased χ_o is no longer equal to χ_{Au}, but

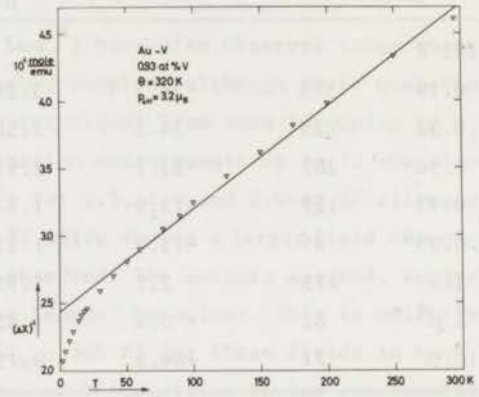

Fig. 7. Temperature dependence of the inverse of the impurity susceptibility $\Delta\chi$, $\Delta\chi(T) = \chi_{alloy}(T) - (1 - c)\chi_{host}(T)$, for sample 5.

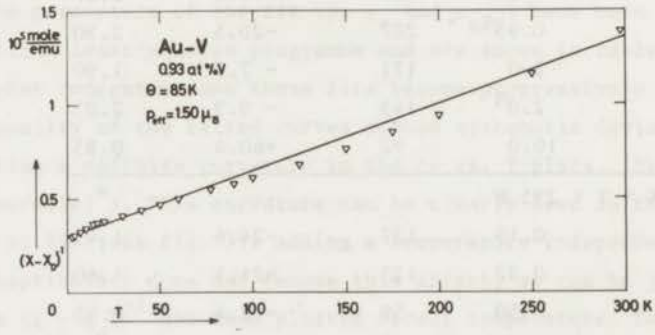

Fig. 8. Temperature dependence of the inverse of the susceptibility difference $\delta\chi$, $\delta\chi(T) = \chi_{alloy}(T) - \chi_o$, for sample 5. The value for χ_o was obtained from the computer fit (see table 1.3, case A).

increases monotonically (case A). This result has also been obtained by

Creveling and Luo[8]). However, in case B, for the three most dilute alloys (nos. 2, 3 and 4), χ_o turns out to be again equal to χ_{Au}. From this behaviour we conclude that in case A the increase of χ_o, at least for concentrations up to 1 at.%V, is due to the fitting procedure which has to "connect" the two regimes B and C * [37]). We shall discuss these concentration effects in the next subsection.

b) Secondly, we have calculated p_{eff} according to formula (4), assuming that p_{eff} is temperature dependent. The result for the most dilute alloys (c < 1 at.%V) is shown in fig. 9. It is clear that p_{eff} tends to zero with decreasing temperature. This is a characteristic feature of the Kondo effect ("spin compensation"). The data for the different concentrations do not fall on a universal curve. This is caused by uncertainties in the values of the concentration (error bars) and also by real concentration-dependent behaviour (see section 1.4.3).

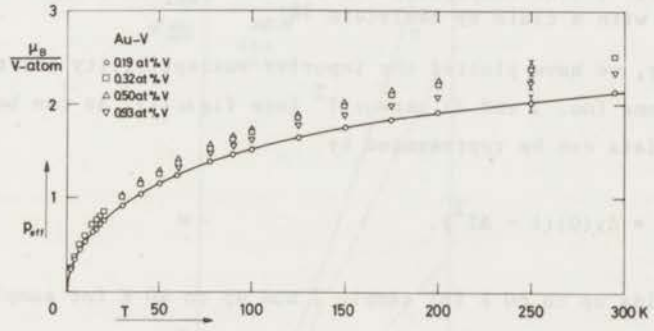

Fig. 9. Temperature dependence of p_{eff} as calculated with formula (4). At low temperatures the data points for the 0.50 and 0.93 at.% alloys coincide with those of the 0.32 at.% alloy, and have therefore been omitted from the figure.

The temperature dependence of p_{eff} determines the behaviour of the susceptibility near T = 0. It has been suggested by Edelstein [38]) that $\Delta\chi$ is proportional to $T^{-\frac{1}{2}}$ for Au-V alloys, a result he deduced from Kume's data [29]). If this were true, then $(p_{eff})^2 \propto T^{+\frac{1}{2}}$. From our data it follows that instead, $p_{eff} \propto T^{+\frac{1}{2}}$ (see fig. 10), which leads to a constant susceptibility at low temperatures (T < 20 K). This is an important result which fits into the picture which is emerging for the Kondo effect (see section 5). The divergent behaviour (e.g. $\chi \propto T^{-\frac{1}{2}}$ or $\chi \propto T^{-2/3}$), which is often observed is certainly due to inter-

* The author of ref. 37 has shown quite convincingly the artificial character of χ_o for the systems Rh-Mn, Mo-Fe, Mo-Co and Au-Fe.

action effects [39]). In Kume's results contamination (Fe) could also play a role, as Kume suggested [29]).

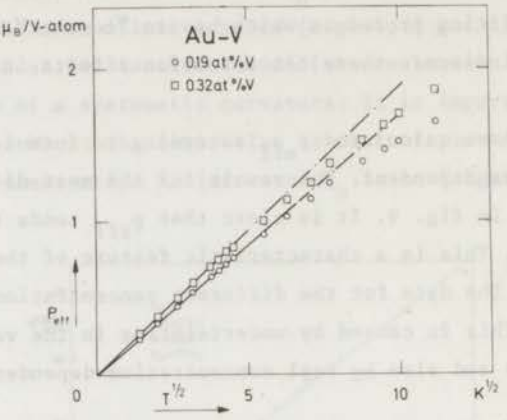

Fig. 10. Peff vs. $T^{\frac{1}{2}}$. At temperatures below 20 K p_{eff} is proportional to $T^{\frac{1}{2}}$, in disagreement with a claim by Edelstein [38]).

c) Finally, we have plotted the impurity susceptibility for the two lowest concentrations (no. 2 and 3) versus T^2 (see fig. 11). As can be seen in fig. 11, these data can be represented by

$$\Delta\chi(T) = \Delta\chi(0)(1 - AT^2). \qquad (6)$$

Equation (6) holds up to 60 K for sample 2 and up to 40 K for sample 3. This

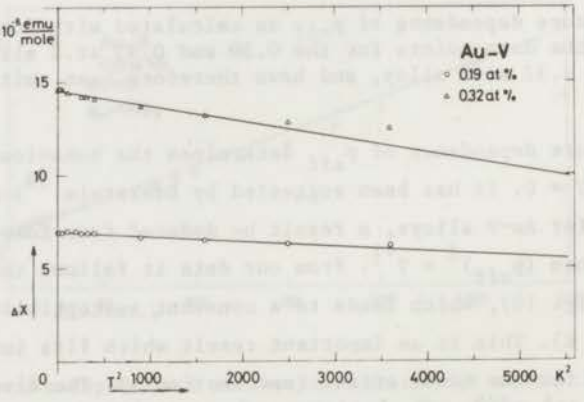

Fig. 11. The incremental susceptibility $\Delta\chi$ vs. T^2. From the slope of the solid line the value of T_K can be calculated. Note the deviations from the solid lines, starting at 60 K and 40 K for the 0.19 at.% and the 0.32 at.% alloy, respectively.

temperature dependence is consistent with that found for the specific heat [7,2]) and the resistivity [34]), which properties all show a simple power-law behaviour. The deviations at higher temperatures from formula (6) are to be expected since this formula would hold only for $T \ll T_K$. It should be noted that for sample 3 the deviation starts at a lower temperature than for sample 2. Also the slope (A) of $\Delta\chi$ vs. T^2 is larger for sample 3. This is indicative of interaction effects of the same kind as those observed in the resistivity [6]) and specific heat [7]) (see also sections 1.5 and 1.6).

1.4.3. *Concentration dependence.* As has already been noted in the previous subsection, the susceptibility results for Au-V alloys show deviations from proportionality with concentration. In fig. 12 our data for samples with concentration up to 1 at.%V are shown as a function of the analyzed or chemical

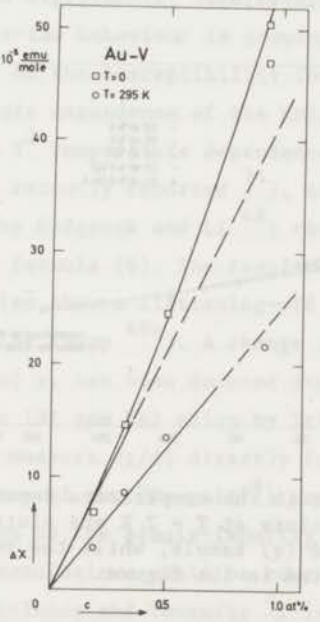

Fig. 12. Concentration dependence of the impurity susceptibility $\Delta\chi$ for quenched samples. (The data point at 47×10^{-6} is for a slowly cooled sample). A linear extrapolation (dashed line) from the low-concentration regime up to 1 at.% gives: $\Delta\chi(T = 0) = 42 \times 10^{-6}$ (emu/mole at.%V).

composition (no. 2: 0.19 at.%; no. 3: 0.32 at.%; no. 4: 0.5 at.% and no. 5: 0.93 at.%). The datum point for sample 2 deviates a little from an assumed proportionality of $\Delta\chi$ with c at T = 295 K. This led us to estimate the concentration for sample no. 2 to be 0.15 at.%V in ref. 35. In the case of sample no. 5

a trend becomes clear toward a larger increase of $\Delta\chi$ at T = 0, with increasing concentration than expected from $\Delta\chi \propto c$ (dashed lines in fig. 12). This trend is opposite to the behaviour of higher concentrations, for which $\Delta\chi(T = 0)$ increases slower than proportional to the concentration (see fig. 16). The latter behaviour has been reported in all previous measurements while the increase of $\Delta\chi$ faster than proportional to the concentration has not been noted before.

To eliminate the uncertainty in the values of the concentrations we have plotted $\Delta\chi(T)$ normalized at T = 295 K to the value of sample 3 (see fig. 13). One can see that the trend observed in fig. 12 can also be deduced from fig. 13. Two data points at T = 0 are also plotted for samples 6a and 6b. The quenched sample (no. 6b) shows an even larger temperature dependence than sample no. 5b. We have analyzed the data of Creveling and Luo [8]) for the dilute alloys in the same way (normalizing at T = 295 K). It turned out that for their data also $\Delta\chi$ (for homogenized samples) increases more rapidly than proportional to concentration for the 1 at.%V alloy.

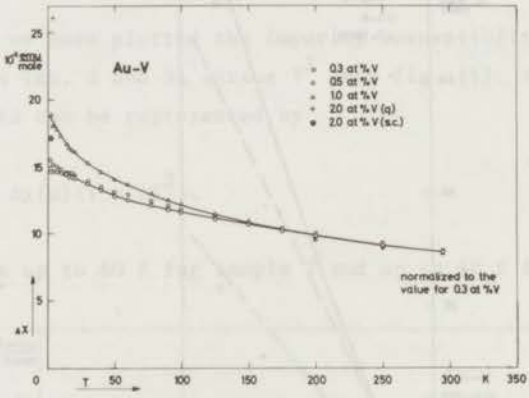

Fig. 13. Concentration effect in the temperature dependence of $\Delta\chi$. For the 2 at.%V alloy only two data points at T = 2 K are plotted: for the slowly cooled (s.c.) and the quenched (q) sample, while the room temperature values are also normalized as indicated in the figure.

1.5. Discussion

1.5.1. *Temperature dependence.* Our measurements, which are more accurate than the previous ones, have shown that for dilute alloys ($c \leq 0.3$ at.%) at temperatures far below T_K the impurity susceptibility flattens off to a constant value, $d\chi/dT$ becoming zero at T = 0. In a short paper [35]) we have reported that the low-temperature behaviour can be described by a T^2 dependence (see formula (6) and fig. 11). This kind of temperature dependence has been

theoretically predicted by several authors on the basis of different approaches to the Kondo problem [1,40].

Originally, this prediction was made in the local spin fluctuation (LSF) theory (e.g. ref. 53), but recently a T^2 dependence was also put forward on the basis of the Anderson model by Dworin [41], and by Schotte and Schotte [42] starting from the (anisotropic) s-d model developed by Anderson et al. [43]. So, the three principal approaches to the Kondo effect appear to give qualitatively the same predictions. The argument given by Dworin [41] about the factor $(1 - 3\eta^2)$, which would lead to a $\Delta\chi$ increasing with T^2, can be disregarded, as this factor should not appear in eq. (13) of ref. 53 (Rivier, private communication).

The divergent behaviour at T = 0, calculated several years ago for the s-d model [44] or suggested in a ground-state theory [45] can therefore be ruled out. This convergence of the theoretical predictions is an important result, which is in agreement with the experimental data obtained recently [1b,46]. The evidence for a simple power-law behaviour is growing.

The flattening-off of the susceptibility in Au-V has been confirmed by a study of the temperature dependence of the Knight shift by Narath et al. [47] in a 0.2 at.%V alloy. A T^2 temperature dependence of the V Knight shift of a 0.3 at.% Au-V alloy was recently reported [74], confirming our results. Susceptibility data on Al-Mn by Hedgcock and Li [48] revealed a temperature dependence of $\Delta\chi$ in agreement with formula (6). The results for $\Delta\chi$ of Ir-Fe (0.5 at.%Fe) by Guertin et al [49a] also show a flattening-off at low temperatures, substantiating earlier results by Knapp [49b]. A change in the slope of χ, which indicates a flattening-off of χ, has been deduced from the field dependence of the specific heat of a Cu-Fe (81 ppm Fe) alloy by Tripplet and Phillips [50]. An attempt by De Vroede to measure $d\chi/dT$ directly in a Cu-Fe (20 ppm Fe) alloy, demonstrated the dominance of the "Fe-pair"[4] contribution at temperatures below 3 K [51]. Separation of the single-impurity contribution is therefore uncertain. However, some conclusions could be reached, e.g. that the Curie-Weiss behaviour reported by Tholence and Tournier [4] is not consistent with the $d\chi/dT$ results: this conclusion was also drawn by Tripplet and Phillips [50].

The question whether the Kondo model (s-d model) or the LSF model is best suited to describe the actual state of affairs in real alloys seems to become an academic one. This conclusion is also reached by Narath [52]. Although for extreme examples like Cu-Mn ($T_K \approx 10$ mK) and Al-Mn ($T_K \approx 500$ K) differences might be expected, it turned out that for Au-V ($T_K \approx 300$ K) this is not the case [41]. The calculations by Schotte and Schotte [42] are particularly interes-

ting, as they predict a universal behaviour which, using the scaling theory of Anderson et al. [43]) can be calculated exactly from the so-called resonant-level model (RL model). The RL model ($U = 0$ and $E_d = 0$) has the characteristics of an unsplit virtual bound state, which is also the starting point of the LSF theories. In fact, the general expression for the susceptibility derived by Schotte and Schotte is the same as the one derived by Rivier and Zuckermann, eq. (11) of ref. 53. The only difference is in the use of Δ (width of the impurity state in the RL model) and τ_o^{-1} (inverse spin-fluctuation life time), which is related to the width of the actual virtual bound state. One can conclude from the expression of the RL model that the behaviour of the local "magnetic" moment can be described by a virtual bound state, having a reduced width (or an enhanced local density of states [54]). This gives rise to a behaviour like that expected of a "normal" Fermi gas (one-electron problem *), however with a degeneracy temperature of order T_K (many-body problem). The conjecture by Rivier and Zuckermann i.e. $kT_K = \hbar\tau_o^{-1}$ is substantiated qualitatively by the calculation of Schotte and Schotte. The latter authors find $kT_K = \Delta/1.85$, if one assumes $\Theta = T_K$ in the expression of the Curie-Weiss behaviour of the susceptibility for high temperatures $\chi = C/(T + \Theta) = C/(T + \Delta/1.85k)$.

In fig. 14 the results are shown of the fit, which was made by Schotte and Schotte to our data for the 0.19 at.% alloy. The fitting parameters Δ and μ_{eff} ($\Delta/k = 313$ K, $\mu_{eff} = 2.66\ \mu_B$) are in reasonable good agreement with the parameters of table 1.3 for this alloy (no. 2), remembering that the "correct" slope of the Curie-Weiss behaviour is only attained at temperatures above T_K. This is the first example where a theory can succesfully describe the behaviour of χ from $T = 0$ up to $T = T_K$.

The results of a comparison [35]) with the formula derived by Klein [56]), for temperatures $T << T_K$ (see fig. 11) are, for the 0.19 at.% alloy: $T_K = 250$ K; for 0.30 at.% alloy: $T_K = 200$ K. Comparison with an expression by Caroli et al. [57]) leads to a value $T_K = 283$ K, using $\Delta\chi(0)/c = 42 \times 10^{-4}$ (emu/mole V). This value for $\Delta\chi(0)/c$ has been derived from fig. 12 (cf. Creveling and Luo: 43×10^{-4}; Kume: 39×10^{-4})†.

---

*Lederer and Mills [55]) predicted this kind of behaviour for Pd-Ni alloys on the basis of LSF theory. The connection between this class of (isoelectronic) alloys with the ususal Kondo alloys (Cu-Fe) was, however, realized much later (see e.g. ref. 1b, p. 22, and chapter 4).

†The value quoted in ref. 32 (47×10^{-4} emu/mole V) is apparently incorrectly deduced from the data by Creveling and Luo and by Kume.

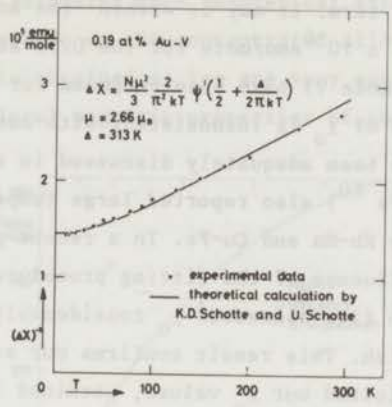

Fig. 14. A fit of our data to a theoretical expression of Schotte and Schotte (ref. 42). The values of the parameters of the resonant-level model obtained by the authors of ref. 42, are indicated; ψ' is the derivative of the di-gamma function. An explanation of the other symbols is given in the text.

In the foregoing discussion we have tacitly assumed that $\Delta\chi$ is totally due to temperature-dependent spin susceptibility. This assumption was made as the Curie-Weiss fits to the most dilute alloys showed χ_o to be equal to χ_{Au} (see table 1.3, case B). However, the Knight shift and relaxation time measurements on Au-V by Narath and Gossard [32]) indicated a positive contribution to the Knight shift. This positive contribution was ascribed by Narath and Gossard to a temperature-independent local susceptibility of orbital origin (analogous to the Van Vleck susceptibility). Using the value $H_{hfs}^{(orb)} = +0.19 \times 10^6$Oe[58]) they calculated $\chi_{orb} = +5.4 \times 10^{-4}$emu/mole V from $K_{orb} = +1.8\%$. The value of the positive contribution to the Knight shift K can also be deduced from the temperature dependence of K, assuming:

$$K(T) = K_o + K_d(T) = K_{orb} + \frac{A}{T + \Theta} \qquad (7)$$

In the limit $T \to \infty$ it turned out that $K(\infty) \equiv K_{orb} = +1.8\%$ [47]). This confirms the estimate in ref. 32. Although the magnitude of $H_{hfs}^{(orb)}$ is uncertain in the dilute alloy, (it should be between the value for pure V metal and the atomic value for V (0.19×10^6Oe $< H_{hfs}^{(orb)}$ *(alloy) $< 0.25 \times 10^6$Oe)[58]), this does not affect the value of χ_{orb} very much ($4.5 \times 10^{-4} < \chi_{orb} < 5.4 \times 10^{-4}$(emu/mole V)).

*This is the hyperfine field per spin (s = 1). Divide by two to get the hyperfine field per Bohr magneton.

From our measurements we cannot draw final conclusions about the presence of this temperature-independent term. It may be within the accuracy of the fits, as it corresponds to about 1 x 10^{-6} emu/mole for the 0.19 at.% alloy. Larger values of χ_o (≈ 15 x 10^{-4} emu/mole V) have been proposed for Au-V by Creveling and Luo [8]). This large value of χ_o is inconsistent with our data and with other experimental results, as has been adequately discussed in ref. 32. Barton and Claus [59]), Ekström and Meyers [60]) also reported large temperature-independent contributions in alloys like Rh-Mn and Cu-Fe. In a recent paper Claus [37]) demonstrated the important influence of the fitting procedure on χ_o. Expanding the temperature range of the fits decreased χ_o considerably and in most cases χ_o could be expected to vanish. This result confirms our statements in section 1.4.2. In fig. 15 we have plotted our χ_o values, obtained from the computer fits (case A), as a function of concentration. The solid line is the concentration dependence proposed by Creveling and Luo [8]). As can be seen the quality of the fit is not very good. The reason for this is the impossibility to describe the concentrated alloys with a simple Curie-Weiss term, as we have shown in section 4.2.

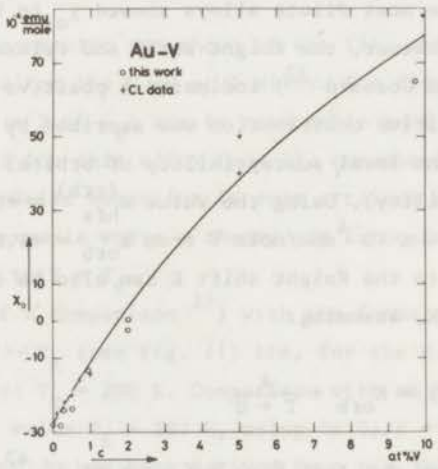

Fig. 15. Concentration dependence of the temperature-independent χ_o, resulting from the computerfits (see table 1.3). The solid line represents the behaviour suggested [8]) by Creveling and Luo (CL). Some data by CL are also plotted.

If we assume a temperature-independent contribution to the impurity susceptibility of 5 x 10^{-4} emu/mole V, our estimates of T_K become, e.g. {$\Delta\chi(0)/c$ = 37 x 10^{-4} emu/mole V} (Klein [56])) T_K = 230 K; (Caroli [57])) T_K = 320 K.

1.5.2. *Concentration dependence*. While the single magnetic-impurity problem ("Kondo effect") has attracted much theoretical attention in recent years, only few attacks have been made on the concentrated alloy (i.e. real alloy) problem [61,62,63]. The results obtained so far are very qualitative and can be summarized as follows: the local magnetic properties of an impurity can be enhanced

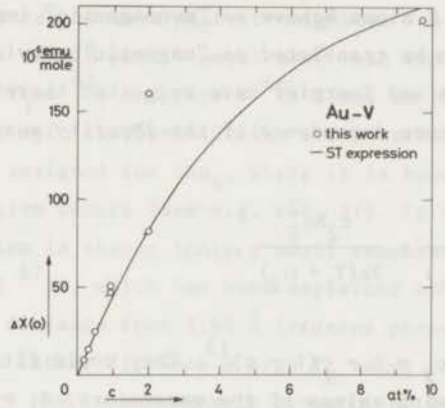

Fig. 16. Concentration dependence of $\Delta\chi$ at T = 0. Points marked (o) represent data for slowly cooled samples. The solid line represents the expression given by Souletie and Tournier (ST).

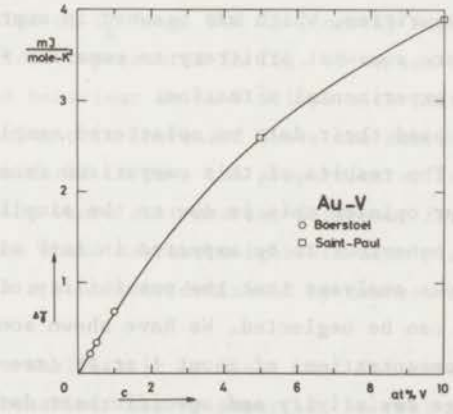

Fig. 17. Concentration dependence of the impurity contribution $\Delta\gamma$ ($\Delta\gamma = \Delta C/T$) to the electronic specific heat C_{el} ($C_{el} = \gamma T$). (o) values obtained from an analysis of Boerstoel's data (see ref. 73); ( ) values from Saint-Paul et al. [69].

or depressed by mutual interaction with other impurities, depending on the properties of the impurities and their relative positions.

For the case of Au-V alloys it has been assumed by several authors that

the local magnetic properties decrease with increasing concentration [3,8,32]. The concentration dependence of the incremental susceptibility (see fig. 16) clearly indicates a behaviour like this for large concentrations (c > 1 at.%). Also, the electronic contribution to the specific heat reflects a depression of the magnetic properties with increasing concentration (see fig. 17). This behaviour has been succesfully explained, at least qualitatively, by a model in which nearest-neighbour V atoms behave as "nonmagnetic" impurities [3,8,67]. "Nonmagnetic" behaviour can be translated as "magnetic"behaviour with a high Kondo temperature. Souletie and Tournier have suggested therefore the following expression for the temperature dependence of the impurity susceptibility of Au-V alloys [3]:

$$\chi(T) = \frac{c_1 N\mu_1^2}{3k(T + \Theta_1)} + \frac{c_2 N\mu_2^2}{3k(T + \Theta_2)} , \qquad (8)$$

where $c_1 = c(1 - c)^{12}$ and $c_2 = c - c(1 - c)^{12}$. They could fit some experimental results with the following values of the parameters: Θ_1 = 225 K, Θ_2 = 1120 K, assuming $\mu_1 = \mu_2 = 3.0\ \mu_B$.

In fig. 16 our data for $\Delta\chi(0)$ are compared with the expression (8) evaluated at T = 0 (see also fig. 5 of ref. 3). It is remarkable that the data for quenched samples deviate substantially, although for these samples a statistical distribution of the impurities, which was assumed in expression (8), might be expected. It is therefore somewhat arbitrary to consider formula (8) as an expression describing the experimental situation.

Creveling and Luo [8] used their data on splattered samples to compare with a statistical model. The results of this comparison (see fig. 13 in ref. 8) are inconclusive. In our opinion this is due to the simplicity of the models and the complexity of the behaviour to be expected in Au-V alloys. It has so far been assumed in previous analyses that the possibility of enhancing the local magnetic properties can be neglected. We have shown some evidence that this is not correct for concentrations of about 1 at.%V (see section 1.4.3). In this concentration range resistivity and specific-heat data also show an enhancement of the local magnetic properties [6,7]. (See, however, the remark about the specific-heat data in section 6). We propose a different explanation of this effect than Star and Boerstoel [6,7] suggested. Our explanation resolves a contradiction between their assumption of an extended spin polarization and the experimental evidence of its non-existence (see discussion in ref. 64). We assume that the local magnetic properties depend critically on the relative

distance between V atoms dissolved in Au. The local magnetic properties of a particular V atom can be characterized by a certain value of the Kondo temperature T_K (high values of T_K represent "nonmagnetic" behaviour, while low values correspond to "magnetic" behaviour).

In fig. 18 we have plotted the T_K values (on arbitrary scale) which can be assigned to V atoms at a certain distance (r) from a V atom at the origin (r = 0). The distances between nearest-neighbour V atoms in some ordered compounds of Au and V and in pure V metal have been indicated. High T_K values have been assigned for V_3Au [65]) and pure V [66]) since in these systems only weak temperature-dependent spin susceptibilities are observed. A very low T_K value (T_K = 0) has been assigned for VAu_4, where it is known that in the ordered phase ferro-magnetism occurs (see e.g. ref. 31). In the disordered state of VAu_4 ferro-magnetism is absent (only a small temperature-independent susceptibility is observed [67])), which has been explained by the reduction of the nearest-neighbour distance from 3.98 Å (ordered phase) to 2.85 Å (disordered phase). So for the latter distance a high T_K value can also be assumed. From the plot of fig. 18 the local magnetic properties, which can be expected for V atoms dissolved in Au, can be deduced. For nearest-neighbour (denoted n.n. in the plot) V atoms in Au, (r = 2.88 Å [68])), we would expect a very high T_K (e.g. 3000 K)("nonmagnetic"). For next-nearest neighbours (r = 4.07 Å [68])) we expect a low T_K (e.g. 30 K) ("magnetic"), while for isolated V atoms (r > 5 Å) an intermediate value of T_K (e.g. 300 K) ("nearly magnetic") is assumed. On the basis of the ideas represented in fig. 18 we can now understand qualitatively the observed behaviour in Au-V alloys with increasing concentration. When the concentration c is increased above the concentration c_o for which all V atoms can be considered to have the properties of isolated atoms, one goes over from a situation where next-nearest-neighbour interactions are important ($c \simeq c_1$) to a regime where nearest-neighbours also play a role ($c \simeq c_2$). Finally one ends up with a behaviour dominated by nearest-neighbour interactions ($c \simeq c_3$).

From the above analysis it is clear that for concentrations larger than c_o a very complex behaviour may be expected. We feel that the suggestion by Souletie and Tournier [3]), which can be represented by the dotdashed line in fig. 18, is still too simple to account for the observed concentration-dependent behaviour in Au-V alloys. With this in mind, an attempt to extract from the susceptibility data the contributions of different V atoms seems pretty hopeless, although the trend following from fig. 18 might be confirmed. Results of a two-term Curie-Weiss analysis of our data by Beck [70]) are consistent with

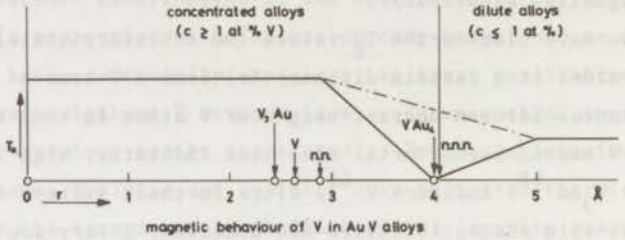

Fig. 18. Magnetic character of a V atom placed at a certain distance r from another V atom at the origin. The nearest-neighbour distances between V atoms in pure V metal, in ordered V_3Au and in ordered VAu_4 are indicated. The nearest-neighbour (n.n.) and next-nearest-neighbour distances (n.n.n.) in the gold lattice (Au-V alloys) are also marked. The scale for the Kondo temperature is arbitrary. The solid and dashed lines are explained in the text.

such a trend.

At low temperatures ($T < 8$ K) the properties of Au-V alloys are probably also influenced by small concentrations ($c \sim 10$ ppm) of strongly magnetic particles ($\mu \sim 10\ \mu_B$). The presence of these particles was suggested by the field dependence noted in section 1.4.2. We have analyzed [75]) the results for the samples 5b and 6b in cooperation with Prof. P.A. Beck (University of Illinois, Urbana, USA), who fitted our results to the following expression:

$$M \equiv M_{alloy} - M_{Au} = \chi_o H + c\mu B\{\mu, H/(T - \Theta)\} \qquad (9)$$

where χ_o is a temperature and field-independent susceptibility, c is the concentration and μ the magnetic moment of the particles, B is the Brillouin function with $g = 2$. Our data for $T < 8$ K and $H < 16$ kOe are shown, along with the fits, in fig. 19.

From the values of the parameters shown in table 1.4 the presence of strongly magnetic particles was deduced [75]). These particles were tentatively supposed to be small regions of ordered Au_4V.

By annealing the samples these regions could grow, resulting in more easily saturated particles. This explains the absence of field dependence in annealed samples as observed in ref. 69.

We have pointed out [75]) some interesting consequences of the analysis described above.

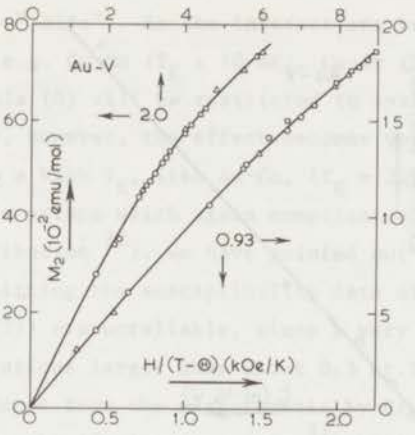

Fig. 19. $M_2(=M - \chi_o H)$ versus $H/(T - \Theta)$ for two quenched Au-V alloys. The full lines show the values calculated according to the best fits of eq. (9). The data have been obtained at three temperatures. For 0.93 at.%V: (o) T_1 = 4.13 K, ( ) T_2 = 2.68 K and ( ) T_3 = 2.15 K; for 2 at.%V: (o) T_1 = 4.07 K, ( ) T_2 = 3.04 K and ( ) T_3 = 2.11 K.

Table 1.4

Parameter values of best fits to eq.(1)

	0.93 at%V	2.0 at%V
c(ppm)	7.1	32.6
$\mu(\mu_B)$	9.47	5.57
Θ(K)	-5	-0.5
$\chi_o(10^{-6}$emu/mol)	37	93
RMSD(10^{-6}emu/mol)§	0.15	0.74

§RMSD = Root Mean Square Deviation

First of all, the extra contribution to the susceptibility at T = 0, $\Delta\chi$(o), turns out to be proportional with concentration up to 2 at.%V (see fig. 20). This result is similar to the behaviour of the specific heat, for which we demonstrated a variation of the electronic contribution proportional with concentration up to 1 at.%V [73]) (see fig. 17). (A recent measurement [76]) of the specific heat of an Au-V (2 at.%) alloy extended the range of proportionality to about 2 %V).

Secondly, the small concentration of the particles might explain the absence [73]) of observable effects in the specific heat, although it cannot be

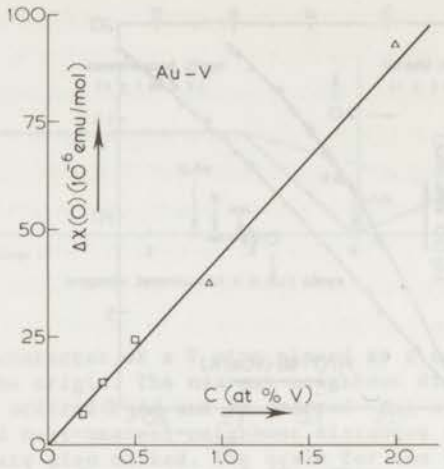

Fig. 20. Solute susceptibility at T = 0 versus solute concentration for some Au-V alloys (ref. 75).

excluded entirely, that these particles do contribute to the specific heat.

Finally, the effects observed in the resistivity at low temperatures [26]) can be attributed to the presence of the magnetic particles.

Although the interpretation of the field-dependent susceptibility offers a consistent explanation of the low temperature behaviour of several properties, it should be remarked that expression (9) is not adequate to describe the temperature dependence at higher temperatures, as noted in ref. 75.

This indicates the necessity of a complex model as discussed at the beginning of this section, if one tries to explain the experimental data over the whole temperature range.

I.6 Concluding remarks

We have presented some evidence that the temperature dependence of the susceptibility can be described by a simple power law for temperatures much less than T_K. This adds to the evidence [1b,2,34,48,50]) for a unified picture which appears to emerge for the low-temperature behaviour of Kondo alloys. At higher temperatures, $T \approx T_K$, the susceptibility shows a Curie-Weiss behaviour, which is commonly assumed to analyze the susceptibility results. The low-temperature deviation according to eq. (6) from the Curie-Weiss behaviour is opposite to the one which was observed in Cu-Fe [71]) and thought at that time

(1967) to be characteristic of the Kondo effect. It is now clear that deviations of this kind, which have often been observed e.g. refs. 59, 60 and 37 are due to interactions (e.g. "pairs"). As the interactions become more pronounced in systems with low T_K, e.g. Cu-Mn ($T_K \simeq 10$ mK), Cu-Cr ($T_K \simeq 2$ K), experimental verification of formula (6) will be restricted to systems with relatively high T_K*. In these systems, however, the effect becomes very small (e.g. Al-Mn [48])). In other systems with a high T_K, like Au-Co, ($T_K = 225$ K), a strong tendency to form small clusters exists which again complicates the determination of the single-impurity contribution [72]). We have pointed out that many physical conclusions drawn from fitting the susceptibility data of Au-V to a single Curie-Weiss term (formula (2)) are unreliable, since a very complex behaviour can be expected for concentrations larger than about 0.3 at.%V. In particular the high value for χ_o deduced from the measurements by Creveling and Luo [8]) is a spurious result due to the fitting procedure [37]). Fitting the susceptibility data to two Curie-Weiss terms [60]) or generally speaking fitting with more than three free parameters is also questionable due to the limited accuracy of the susceptibility measurements.

Finally, we have proposed an explanation for the concentration-dependent behaviour observed in the resistivity [6]), the specific heat [7]) (the deviation reported for the specific heat of Au-V alloys, however, is most probably due to a change in the lattice contribution [69,73])) and the magnetic susceptibility (this work) in the range of about 1 at.%V. This explanation fits into the model used to explain other properties (Mössbauer effect [31])), Knight shift [32]), susceptibility [8])) and therefore resolves the contradiction between the explanation put forward in refs. 6 and 7 and the Knight-shift data [32]).

*The flattening-off of χ at very low temperatures for Cu-Mn and Cu-Fe should not be mistaken as evidence for eq. (6), since it is due to impurity-impurity interactions (see e.g. ref. 39).

APPENDIX

Magnetic susceptibility of Au-V alloys *

Temperature (K)	Concentration (at.%V)								
	0	0.2	0.3	0.5	1.0	$1.0^{s.c.}$	2.0	$2.0^{s.c.}$	$10.0^{s.c.}$
	197.0	196.7	196.5	196.2	195.5	195.5	194.0	194.0	182.3
2	-27.6	-20.7	-13.0	- 3.0	+20.9	+18.6	+115	+51.9	+170
4	-27.7	-20.8	13.1	3.5	19.4	17.7	101	48.6	164
7	-27.8	-20.9	13.3	3.9	17.6	17.0	84.0	47.0	157
10	-27.9	-20.9	13.5	4.3	16.1	15.6	76.0	45.3	151
14	-28.0	-21.0	13.6	4.8	14.4	14.6	69.4	43.5	144
16	-28.0	-21.1	13.8	4.9	13.8	14.2	67.2	42.8	143
18	-28.1	-21.2	13.9	5.1	13.2	13.8	65.0	42.0	140
20		-21.2	14.0	5.3	12.8	13.4	62.9	41.3	138
30		-21.4	14.4	6.0	10.8	11.6	55.4	38.2	132
40		-21.6	14.9	6.7	9.2	10.1	50.0	35.6	127
50		-21.8	15.3	7.2	7.8	8.8	46.0	33.3	122
60		21.9	15.6	7.7	6.7	7.7	42.5	31.4	118
77.5		22.2	16.0	8.3	5.0	6.1	38.0	28.5	112
90		22.4	16.3	8.9	3.9	4.4	35.3	26.8	109
100		22.6	16.5	9.3	+ 3.0	2.7	33.4	25.6	106
125		22.9	17.0	10.2	+ 1.3	+ 1.3	29.3	22.8	102
150		23.2	17.4	11.0	- 0.2	+ 0.1	26.0	20.4	97.5
175		23.5	17.9	11.6	- 1.6	- 1.2	23.4	18.4	94.1
200		23.7	18.3	12.3	- 2.7	- 3.8	21.0	16.6	91.5
250		24.2	19.0	13.4	- 4.7	- 3.1	17.2	13.6	86.7
295	-28.1	-24.4	-19.5	-14.4	- 6.1	- 4.4	+14.6	+11.6	+84.5

* In units of 10^{-6} emu/mole. The data listed in this table have been obtained from smooth curves (figs. 4, 5 and 6) representing the measurements. For each alloy the nominal concentration and the molecular weight is indicated above the respective column; s.c. = slowly cooled sample.

REFERENCES CHAPTER 1

1) For a recent review of some relevant experiments, see
   a) Heeger, A.J., Solid State Physics, F. Seitz, D. Turnbull and H.Ehrenreich, eds., Academic Press (New York, 1969), vol. 23, p. 283.
   b) Van Dam, J.E. and Van der Berg, G.J., Phys. Status solidi (a) 3 (1970) 11.
2) a) Star, W.M., Boerstoel, B.M. and Van Baarle, C., J. appl. Phys. 41 (1970) 1152.
   b) Star, W.M., thesis Leiden, 1971; Physica 58 (1972) 585.
3) Souletie, J. and Tournier, R., J. Physique 32 (1971) C1-172.
4) Tholence, J.L. and Tournier, R., Phys. Rev. Letters 25 (1970) 867.
5) Daybell, M.D. and Steyert, W.A., Phys. Rev. Letters 18 (1967) 398.
6) Star, W.M. and Boerstoel, B.M., Phys. Letters 29A (1969) 26.
7) Boerstoel, B.M. and Star, W.M., Phys. Letters 29A (1969) 97.
8) Creveling, L. and Luo, H.L., Phys. Rev. 176 (1968) 614.
9) Hurd, C.M., Rev. sci. Instr. 37 (1966) 515.
10) Gerritsen, A.N. and Damon, D.H., Rev. sci. Instr. 33 (1962) 301.
11) Bates, L.F., Modern Magnetism, Cambridge University Press (New York, 1951).
12) Hoare, F.E. and Walling, J.C., Proc. Phys. Soc. B64 (1951) 337.
13) Hoare, F.E., Kouvelites, J.S., Matthews, J.C. and Preston, J., Proc. Phys. Soc. B67 (1954) 728.
14) Hurd, C.M., J. Phys. Chem. Solids 27 (1966) 1371.
15) Weiss, W.D. and Kohlhaas, R., Z. angew. Phys. 23 (1967) 175.
16) Foner, S., Doclo, R. and McNiff Jr., E.J., J. appl. Phys. 39 (1968) 551.
17) Budworth, D.W., Hoare, F.E. and Preston, J., Proc. Roy. Soc. A257 (1960) 250.
18) Hurd, C.M., Cryogenics 1 (1966) 264.
19) Henry, W.G. and Rogers, J.L., Phil. Mag. 1 (1956) 223.
20) Heyding, R.D., Taylor, J.B. and Hair, M.L., Rev. sci. Instr. 32 (1961) 161.
21) Hill, G.J., J. sci. Instr. (J. Phys. E) 2 (1968) 52.
22) Brickwedde, F.G., Van Dijk, H., Durieux, M., Clement, J.R. and Logan, J.K., J. Res. Nat. Bur. Stand. 64A (1960) 1.
23) Durieux, M., Van Dijk, H., Ter Harmsel, H. and Van Rijn, C., Temperature, its Measurement and Control in Science and Industry, Reinhold (New York, 1963), vol. 3, p. 383.
24) Henning, F. and Otto, J., Phys. Z. 37 (1936) 633.

25) Berman, R., Brock, J.C.F. and Huntley, D.J., Cryogenics 4 (1964) 233.

26) Rosenbaum, R.L., Rev. sci. Instr. 39 (1968) 890.

27) Van Rijn, C., private communication.

28) Nix, F.C. and MacNair, D., Phys. Rev. 60 (1941) 597.

29) Kume, K., J. Phys. Soc. Japan 23 (1967) 1226; Phys. Letters 24A (1967) 743.

30) Vogt, E. and Gerstenberg, D., Ann. Physik 4 (1959) 145.

31) Cohen, R.L., Wernick, J.H. and West, K.W., Phys. Rev. 188 (1969) 684.

32) Narath, A. and Gossard, A.C., Phys. Rev. 183 (1969) 391.

33) Heeger, A.J., Welsh, L.B., Jensen, M.A. and Gladstone, G., Phys. Rev. 172 (1968) 302.

34) Star, W.M., Physica 58 (1972) 623.

35) Van Dam, J.E. and Gubbens, P.C.M., Phys. Letters 34A (1971) 185.

36) Sakamoto, N., Yamaguchi, Y., Waki, S. and Ogawa, S., Proc. 12th int. Conf. low Temp. Phys., Kyoto 1970, E. Kanda, ed., Academic Press (Japan, 1971) p. 739.

37) Claus, H., Phys. Rev., B5 (1972) 1134.

38) Edelstein, A.S., Solid State Commun. 8 (1970) 1849.

39) Hirschkoff, E.C., Shanabarger, M.R., Symko, O.G. and Wheatly, J.C., Phys. Letters 34A (1971) 341 and J. low Temp. Phys. 5 (1971) 545.

40) Fischer, K., Phys. Status solidi (b) 46 (1971) 11.

41) Dworin, L., Phys. Rev. Letters 26 (1971) 1372; and to be published.

42) Schotte, K.D. and Schotte, U., Phys. Rev. B4 (1971) 2228.

43) Yuval, G. and Anderson, P.W., Phys. Rev. B1 (1970) 1522; Anderson, P.W., Yuval, G. and Hamann, D., Phys. Rev. B1 (1970) 4464; Anderson, P.W., Proc. 12th int. Conf. low Temp. Phys. Kyoto 1970, E. Kanda, ed., Academic Press (Japan, 1971) p. 657.

44) For a discussion of the s-d model see the review papers by Kondo, J., Solid State Physics, F. Seitz, D. Turnbull and H. Ehrenreich, eds., Academic Press (New York, 1969) vol. 3, p. 183 and Fischer, K., Springer Tracts in Modern Physics, G. Höhler, ed., Springer Verlag (Berlin, 1970) vol. 54, p. 1.

45) Anderson, P.W., Phys. Rev. 164 (1967) 352.

46) Van den Berg, G.J., Proc. 12th int. Conf. low Temp. Phys., Kyoto 1970, E. Kanda, ed., Academic Press (Japan, 1971) p. 671.

47) Narath, A., Solid State Comm. 10 (1972) 521.

48) Hedgcock, F.T. and Li, P.T., Phys. Rev. B2 (1970) 1342.

49a) Guertin, R.P., Oliveira, Jr., N.F. and Foner, S., Phys. Letters 36A (1971) 289.

49b) Knapp, G.S., J. appl. Phys. 38 (1967) 1267.
50) Triplett, B.B. and Phillips, N.E., Phys. Rev. Letters 27 (1971) 1001.
51) De Vroede, E., private communication.
52) Narath, A., Proc. 12th int. Conf. low Temp. Phys., Kyoto 1970, E. Kanda, ed., Academic Press (Japan, 1971) p. 675.
53) Rivier, N. and Zuckermann, M.J., Phys. Rev. Letters 21 (1968) 904.
54) This idea is already quoted in ref. 1a (p. 316) as a private communication from Suhl.
55) Lederer, P. and Mills, D.L., Phys. Rev. Letters 20 (1968) 1036.
56) Klein, A.P., Phys. Rev. 172 (1968) 520.
57) Caroli, B., Lederer, P. and Saint-James, D., Phys. Rev. Letters 23 (1969) 700.
58) Yafet, Y. and Jaccarino, V., Phys. Rev. 133 (1964) A1630.
59) Barton, E.E. and Claus, H., Phys. Rev. B1 (1970) 3741.
60) Ekström, H.E. and Meyers, H.P., Phys. kondens. Mat. 14 (1972) 265.
61) Nagaoka, Y., J. Phys. Chem. Solids 27 (1966) 1139.
62) Kim, D.J., Phys. Rev. B1 (1970) 3725.
63) Bennemann, K.H. and Garland, J.W., J. Physique 32 (1971) C1-750.
64) Hüfner, S., Z. Phys. 247 (1971) 46.
65) Bardos, D.I., Waterstrat, R.M., Rowland, T.J. and Darby, Jr., J.B., J. low Temp. Phys. 3 (1970) 509.
66) Kohlhaas, R. and Weiss, W.D., Z. angew. Phys. 28 (1969) 16.
67) Claus, H., Sinha, A.K. and Beck, P.A., Phys. Letters 26A (1967) 38.
68) Pearson, W.B., A Handbook of Lattice Spacings and Structures of Metals and Alloys, Pergamon Press (Oxford, 1967).
69) Saint-Paul, M., Souletie, J., Thoulouze, D. and Tissier, B., J. low Temp. Phys. 7 (1972) 129.
70) Beck, P.A., private communication.
71) Hurd, C.M., Phys. Rev. Letters 18 (1967) 1127.
72) Lecoanet, B. and Tournier, R., Proc. 12th int. Conf. low Temp. Phys., Kyoto 1970, E. Kanda, ed., Academic Press (Japan, 1971) p. 735.
73) Van Dam, J.E., Phys. Letters 38A (1972) 19.
74) Kazama, S., Kume, K. and Mizuno, K., Phys. Letters 38A (1972) 483.
75) Van Dam, J.E. and Beck, P.A., Phys. Letters 40A (1972) 183.
76) Pikart, M.F. and Verbeek, B.H., private communication.
77) Van Dam, J.E., Gubbens, P.C.M. and Van den Berg, G.J., Physica 61 (1972) 389.

CHAPTER 2

SPECIFIC HEAT OF DILUTE Pd-Ni ALLOYS

Abstract

The specific heat of some dilute (c < 2.2 at%Ni) Pd-Ni alloys has been measured in the temperature range from 1.3 to 25 K. From these data the temperature dependence of the effective Debye temperature is obtained. The results show a positive T^5-contribution to the specific heat, which we ascribe to local spin fluctuations. From a comparison with specific-heat data for a Pd-Cu and a Pd-Ag alloy we also conclude that the anomalous behaviour of $\Theta_{eff}(T)$ for pure Pd is not of direct electronic origin. An explanation in terms of the lattice contribution is discussed.

From our data we have also deduced the accurate concentration dependence of the coefficient (γ) of the linear term in the specific heat. Combination with earlier specific-heat results indicates a critical concentration for the occurrence of (ferro)magnetic ordering of about 2.7 at%Ni.

We have observed the influence of a magnetic field of about 20 kOe only in the two most concentrated alloys we have investigated.

2.1 Introduction

As was pointed out in the general introduction the behaviour of pure Pd shows all kinds of anomalous effects. One of the anomalies will be discussed in this chapter, i.e. the temperature dependence of the effective Debye temperature (Θ_{eff}). This anomaly was reported in detail by Boerstoel et al. [1]), substantiating earlier results by Veal and Rayne [2]). Contrary to most metals, pure Pd shows only a shallow minimum (about 2%) in the $\Theta(T)$ vs. T curve (see fig. 2.1). Shoemaker and Rayne [3]) suggested this anomaly to be due to a contribution of paramagnons, which would decrease the effective lattice specific heat and consequently increase the effective Debye temperature. To check this explanation of the anomaly in pure Pd, we have studied the behaviour of $\Theta(T)$ of dilute (c < 2.2 at%Ni) Pd-Ni alloys because in these alloys the contributions due to (local) paramagnons are increased [4]). For Pd-Ni alloys one would therefore expect a variation of Θ with temperature as shown e.g. in fig. 2.1 (curve c).

Our results which are presented in section 2.4.1. are not in agreement

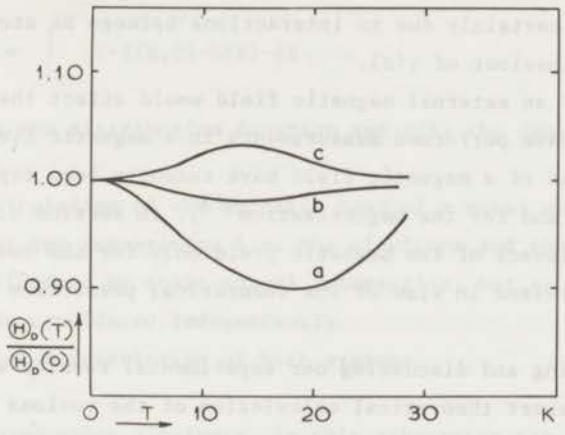

Fig. 2.1. Qualitative plot of the temperature dependence of the normalized Debye temperature. The curves correspond to: (a) the usual behaviour of a pure metal, (b) pure Pd and (c) the hypothetical behaviour of Pd-Ni alloys.

with the expected behaviour as sketched in fig. 2.1. The implications of our results for the explanation of the anomaly in pure Pd are also discussed in section 2.4.1. From this discussion and the behaviour of $\Theta(T)$ in a Pd-Cu [5]) and a Pd-Ag [6]) alloy we conclude that the anomaly is not due to a direct electronic contribution. A tentative explanation in terms of the lattice contribution is suggested.

Although the principal aim of our investigation was to obtain the behaviour of the lattice specific heat, we have devoted some discussion to the electronic contribution, in particular the concentration dependence of the coefficient (γ) of the linear term (section 2.4.2). Due to a high accuracy (about 0.5 %) of our measurements and the extended temperature range (1.3 to 25 K) we have determined γ as a function of concentration more accurately than in previous measurements [7,8]). Our result for $\gamma(c)$ shows a striking resemblance with the concentration dependence of the coefficient of the local-paramagnon contribution to the resistivity of Pd-Ni alloys as recently reported by Tari and Coles [9]).

The concentration dependence of the coefficient (β) of the T^3 term for the specific heat in Pd-Ni alloys is shown to be slightly deviating from a linear variation. The large decrease of β with increasing concentration has been explained previously, assuming negative contribution of electronic origin [7,8,10])(local paramagnons or localized spin fluctuations). The local exchange enhancement model [8,10]) predicts a linear variation of β with concentration

in qualitative agreement with experiments [7,8]). The deviation we have observed for c ≥ 1 at.%Ni is certainly due to interactions between Ni atoms as is also apparent from the behaviour of γ(c).

To establish if an external magnetic field would affect the specific heat of Pd-Ni alloys we have performed measurements in a magnetic field (about 20 kOe) also. Influences of a magnetic field have recently been reported for the resisitivity [11,12]) and for the magnetization [13]). In section 2.4.4. our results , which show an influence of the magnetic field only for the two most concentrated alloys, are discussed in view of the theoretical prediction by Doniach [14]) and Schulz [15]).

Before presenting and discussing our experimental results we outline in the next section a short theoretical calculation of the various contributions to the specific heat of a metal, with emphasis on the lattice contribution.

2.2 Theory

The specific heat of a substance is defined as the quantity of heat required to raise the temperature of a mole of the substance by a one degree. As the specific heat depends upon the temperature and upon external circumstances one can define more generally:

$$C_{x,y,..} = \lim_{\Delta T \to o} \left(\frac{\Delta Q}{\Delta T}\right)_{x,y,..} \qquad (2.1)$$

where ΔQ is the amount of heat giving rise to the temperature change ΔT. In most experiments only the specific heat at constant pressure (C_p) or at constant colume (C_v) is of importance. For solids one can even neglect the difference * between C_p and C_v at low temperatures (T < 30 K), because the thermal expansion is very small ($C_p - C_v = \beta^2 KVT$; β is the coefficient of cubical expansion, K is the isothermal bulk modulus, V is the molar volume and T is the temperature). So we can restrict ourselves to the calculation of C_v.

The expression 2.1 reduces in this case to

$$C_v = \lim_{\Delta T \to o} \left(\frac{\Delta Q}{\Delta T}\right)_v = \left(\frac{\Delta E}{\Delta T}\right)_v \qquad (2.2)$$

where E is the internal energy of the substance.

If we consider the substance to consist of "particles" (e.g. electrons, phonons), each with an energy E, we can write for the average energy of the

---

* e.g. for Pd at T = 30 K, $C_p - C_v / C_p$ = 0.03% (see ref. 16).

the substance:

$$\bar{E}(T) = \int_0^\infty E \cdot f(E,T) \cdot N(E) \cdot dE \qquad (2.3)$$

where f(E,T) is the distribution function and n(E) the density of (energy) states function.

For the calculation of the specific heat of a metal we can consider the metal to consist of two sub-systems i.e. the electrons and the phonons. Both sub-systems are influenced by their mutual interaction, but as a first approximation they can be considered independently.

We will give a description of both systems.

2.2.1 *The conduction electrons.* In this sub-system the "particles" are electrons, for which f(E,T) is equal to the Fermi-Dirac function, $f(E,T) = \{\exp((E - \zeta)/kT) + 1\}^{-1}$. Substituting the F-D function into expression 2.3 one can calculate the contribution of the conduction electrons to be [19])

$$C_{el} = \{ \frac{2}{3} \pi^2 N k^2 N(E_F) \} T = \gamma T \qquad (2.4)$$

k is Boltzmann's constant, N is Avogadro's number, and z is the number of electrons per atom; E_F is the Fermi energy (which is defined as the maximum possible energy at T = 0) and $N(E_F)$ is the density of states per atom, per unit energy and per spin direction. If γ is expressed in the following units: in J $mol^{-1}K^{-2}$, one can calculate the corresponding density of states at the Fermi level by the following numerical relation, $N(E_F)$ in states per eV per atom

$$N(E_F) = 0.212\ \gamma \qquad (2.5)$$

From (2.4) it is clear that we need only the density of states at the Fermi energy to calculate C_{el}. This is only valid for $T << T_F$, when $\frac{df(E)}{dE}$ vanishes except in the neighbourhood of $E = E_F$.

The simplest model to calculate the energy spectrum of electrons and hence the density of states is the free electron model. In this model

$$N(E_F) = \frac{3}{4} \frac{z}{E_F} = \frac{3}{4} \frac{z}{kT_F} \qquad (2.6)$$

or alternatively, $(n = zN/V_{mol})$,

$$N(E_F) = \frac{1}{2} \frac{m}{\pi^2 \hbar^2} (3\pi^2 N)^{1/3} V_{at} \qquad (2.7)$$

Substitution of (2.6) and (2.7) into expression (2.4) gives

$$C_{el} = \tfrac{1}{2}\pi^2 k \, Nz \, (\frac{T}{T_F}) = \frac{\pi k^2}{3h^2} (\frac{3N}{\pi})^{1/3} m \, V_{mol} \qquad (2.8)$$

The free electron model gives only a good description of the most simple metals like the alkalis. For the energy spectrum of all the other metals one has to take account of the bandstructure, which is caused by the periodic potential of the lattice. Also the correlation and exchange interactions between the electrons have to be considered. Formally the influence of these interactions upon the specific heat can be incorporated into expression (2.4) by introducing an effective density of states $N_{eff}(E_F)$ which is enhanced over the free electron value by a factor D:

$$N_{eff}(E_F) = DN(E_F) = \frac{N(E_F)}{1 - N(E_F)I} \qquad (2.9)$$

where I represents the interactions. Alternatively, one can introduce an effective Fermi temperature (T_F^*) or an effective mass (m^*) into eq. 2.8.

2.2.2 *The phonons.* The "particles" of the lattice subsystem are the phonons (quantum units of the lattice vibrations). For phonons f(E,T) is equal to the Bose-Einstein function

$$f(E,T) = \{ \exp(\hbar\omega/kT) - 1 \}^{-1} \qquad (2.10)$$

where $\hbar\omega$ is the energy of a phonon with (circular) frequency ω. (We will omit the adjective circular in the following). To calculate the lattice specific heat we need the density of states function for the phonons, $G(\omega)$. Due to the different behaviour of the B-E function compared to the F-D function we need $G(\omega)$ for all values of ω.

In order to obtain $G(\omega)$ we have to assume a model for the lattice vibrations. Historically one of the two models, which were suggested in 1912, has been much in favour because of its simplicity and its success in explaining the experimental data then available. We are referring to the work by Debye [20].

Although the other model, put forward by Born and von Kármán [21], is based on a more realistic description of the lattice, its complexity and its failure to describe the experiment as well as the Debye model, were apparently reasons to ignore this model for many years. However, in 1934 Blackman used the Born-von Kármán model again to calculate, numerically, $G(\omega)$ for a two-dimensional network of atoms [22b]. His calculations for a three-dimensional [22b] lattice showed the two-dimensional model to be changed only slightly. The result for $G(\omega)$ showed two distinct peaks, quite different from the Debye model. Only for very low ω values both spectra are similar, which explained the success of the Debye model at low temperatures. For larger frequencies Blackman's calculations showed $G(\omega)$ to increase stronger than in the Debye model. This behaviour explained [23] the deviations from the Debye model observed at that time.

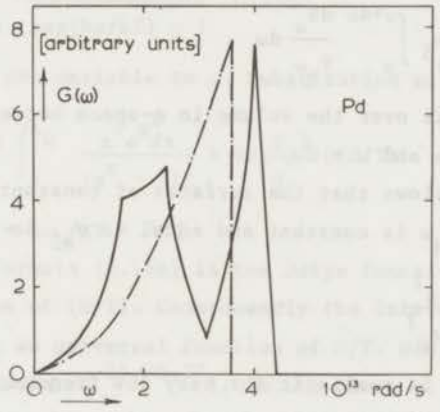

Fig. 2.2. An impression of the phonon density of states for pure Pd (after ref. 44). The dot-dashed line corresponds to the Debye model.

Before giving a more detailed description of realistic calculations of $G(\omega)$ we first introduce the Debye model since with this model the lattice specific heat can be characterized with only one parameter, the Debye temperature (Θ). It is convenient to express the actual lattice specific heat in terms of an effective Debye temperature (Θ_{eff}). The temperature dependence of this Θ_{eff} shows directly the deviations from the Debye model. Therefore it is still usual to discuss the actual behaviour of the lattice specific heat on the basis of Θ_{eff} vs. T curves.

The Debye model

In this model the lattice is considered to be an elastic isotropic continuum. The low frequency vibrations of a continuum are acoustic waves of

frequency ω and wave vector q, related to each other by the velocity of sound v_s:

$$\omega = v_s q \tag{2.11}$$

For the determination of $G(\omega)$ we have to count the number of modes (characterized by q) per unit frequency range. As the density of q-points in q-space is $\frac{V}{(2\pi)^3}$, where V is the (molar) volume, we have: [24,25])

$$G(\omega)d\omega = \frac{V}{(2\pi)^3}\int_{\omega}^{\omega+d\omega} d^3q = \frac{V}{(2\omega)^3}\int_{\omega}^{\omega+d\omega} dS_{\omega}.dq \tag{2.12}$$

or with $\nabla_q \omega = |\frac{d\omega}{dq}|$,

$$G(\omega)d\omega = \frac{V}{(2\pi)^3}\int_{\omega}^{\omega+d\omega} \frac{dS_{\omega}}{\nabla_q \omega} d\omega \tag{2.13}$$

where the integration is over the volume in q-space between two surfaces (S_{ω}) of constant frequency ω and $\omega + d\omega$.

From (2.11) it follows that the surfaces of constant ω are spheres of radius ω/v_s and that $\nabla_q \omega$ is constant and equal to v_s. So we finally obtain

$$G(\omega) = \frac{V}{2\pi^2}\frac{\omega^2}{v_s^3} \tag{2.14}$$

Although relation 2.11 is realistic for very low frequencies (temperatures), Debye assumed this relation to hold also for higher frequencies. However, to take into account to some extent the discrete character of the lattice Debye introduced an upper limit to the possible frequencies. This maximum frequency, the Debye frequency ω_D, is chosen in such a way that the total number of modes is equal to 3N (N is the total number of atoms). The value of ω_D can thus be calculated from the condition

$$\int_0^{\omega_D} G(\omega)d\omega = 3N \tag{2.15}$$

It turns out that

$$\omega_D^3 = \frac{9N}{V} 2\pi^2 v_s^3 \tag{2.16}$$

Substituting this expression for v_s into (2.14) we get the final expression for $G(\omega)$ in the Debye model:

$$G(\omega) = \frac{9N}{\omega_D^3}\,\omega^2 \qquad \text{if } \omega \le \omega_D$$
$$= 0 \qquad \text{if } \omega > \omega_D \tag{2.17}$$

This is a parabola cut off at $\omega = \omega_D$ (see fig. 2.2).

We can now calculate the lattice specific heat. First, substitute f(E,T) and G(E) into the general expression (eq. 2.3) for the internal energy. Secondly, differentiate this expression to the temperature. According to eq. 2.2 we obtain C_v in this way. The expression for C_v reads

$$C_v = \frac{\hbar^2}{kT^2}\int_0^\infty \frac{\omega^2 \exp(\hbar\omega/kT)}{\exp(\hbar\omega/kT) - 1}\, G(\omega)d\omega \tag{2.18a}$$

where we have changed the variable to ω. Substitution of $G(\omega)$ from (2.17) gives

$$C_v = 9R\left(\frac{T}{\Theta}\right)^3 \int_0^{x_D} \frac{x^4 e^x dx}{(e^x - 1)^2} = 9R\left(\frac{T}{\Theta}\right)^3 D(\Theta/T) \tag{2.18b}$$

with $x = \hbar\omega/kT$ and $x_D = \hbar\omega_D/kT = \Theta/T$.

The integral in formula (2.18b) is the Debye function $D(\Theta/T)$, which depends only on the value of (Θ/T). Consequently the lattice specific heat in the Debye approximation is an universal function of Θ/T. $D(\Theta/T)$ has been calculated numerically and tabulated [25,26,27]. In the limit of high and low temperatures we get a simple expression for C_v:

i. $T >> \Theta$ $(x \to o)$

The integrand in the integral of (2.18b) can be replaced by x^2; which results in

$$C_v = 3R \tag{2.19}$$

This is indeed equal to the classical result for a system of N atoms, each having 6 degrees of freedom.

ii. $T << \Theta$ $(x_D \to \infty)$

For low temperatures the upper limit becomes indistinguishable from infinity, which means independent of temperature. The integral can be evaluated

exactly and is equal to $4\pi^4/15$. Substitution gives

$$C_V = \frac{12\pi^4 R}{5\Theta^3} T^3 \equiv \beta T^3 \qquad (2.20)$$

with

$$\beta = 1943.7/\Theta^3 \text{ (J/mol K}^4\text{), if } \Theta \text{ is expressed in Kelvin} \qquad (2.21)$$

This is the well known T^3 law observed in most substances at sufficiently low temperatures.

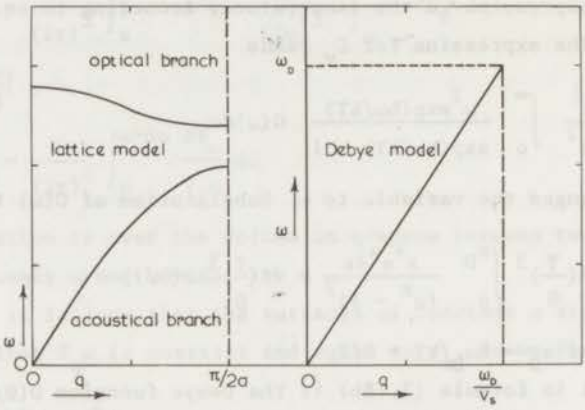

Fig. 2.3. Phonon dispersion relations for the diatomic (one-dimensional) lattice model and the Debye model.

Born-von Kármán model

In this model the discrete nature of the lattice is taken into account by considering the vibrations of the individual atoms. It is assumed that the forces upon the atoms are proportional to the displacements (harmonic approximation). As a linear diatomic chain, consisting of atoms with masses m and M, already shows the prominent features of the three-dimensional lattice, we will discuss only this simple case in some detail [25]).

One dimensional (diatomic) lattice

If the atoms of mass m occupy even numbered positions (x_{2n}) and the atoms with mass M odd positions (x_{2n+1}), we can set up the equations of motion. Taking into account only interactions between nearest neighbours we get:

$$m\ddot{x}_{2n} = \alpha(x_{2n+1} - 2x_{2n} + x_{2n-1})$$

$$M\ddot{x}_{2n+1} = \alpha(x_{2n+2} - 2x_{2n+1} + x_{2n})$$

where α is the force constant.

We can write the solutions of this set of equations as travelling waves:

$$x_{2n} = \xi \exp i \{ \omega t + 2nqa \}$$
$$x_{2n+1} = \eta \exp i \{ \omega t + (2n+1)qa \} \tag{2.23}$$

where a is the lattice spacing. Substituting these values into (2.22) we get equations of motion for ξ and η (ξ and η are the so-called normal coordinates)

$$-\omega^2 m\xi = \alpha\eta(e^{iqa} + e^{-iqa}) - 2\alpha\xi$$
$$-\omega^2 M = \alpha\xi(e^{iqa} + e^{-iqa}) - 2\alpha\eta \tag{2.24}$$

These two coupled equations have non-zero solutions for ξ and η only if the determinant of the coefficients vanishes:

$$\begin{vmatrix} 2\alpha - m\omega^2 & -2\alpha\cos qa \\ -2\alpha\cos qa & 2\alpha - M\omega^2 \end{vmatrix} = 0 \tag{2.25}$$

Eq. (2.25) restricts the possible values of the frequencies. The roots of this so-called "secular equation" give ω as a function of q. Symbolically we can write for (2.25)

$$|\alpha_{ij} - \delta_{ij} M\omega^2| = 0 \tag{2.26}$$

We note that this equation is solved for certain values of ω^2. (This general result is of importance in the determination of a power series development of $G(\omega)$). The solution of (2.25) gives two values for ω^2:

$$\omega^2_{1,2} = \alpha\left(\frac{1}{M} + \frac{1}{m}\right) \pm \alpha \left\{\left(\frac{1}{M} + \frac{1}{m}\right)^2 - \frac{4\sin^2 qa}{Mm}\right\}^{\frac{1}{2}} \tag{2.27}$$

The two roots for ω^2 correspond to the acoustical and the optical branch of the dispersion relation $\omega(q)$ (see fig. 2.3). All the possible solutions, which amount to the number of atoms, are contained in the interval $0 \leq q \leq \pi/2a$, so we need only to consider this part of q-space (called the first Brillouin zone in the three-dimensional case). For comparison we have sketched also the

behaviour of (q) in the Debye model according to (2.11). From fig. 2.3 we can note that in the Born-von Kármán model two special features show up:

1) the appearance of new vibrational modes (the optical modes)
2) the dependence of the group velocity $\nabla_q \omega$ (=dω/dq) on q

These two features have important consequences for the density of states G(ω).

From eq. 2.13 we can deduce that G(ω) will become infinite if ω increases to a value for which $\nabla_q \omega = 0$, i.e. for $q = \pi/2a$. For still higher values of ω there is a gap in G(ω) until we reach the optical branch where for the same reason singularities occur at $q = \pi/2a$ and $q = 0$.

Three-dimensional lattice

Blackman was the first to calculate G(ω) using the Born-von Kármán model. In two consecutive papers (22a, 22b) he deduced G(ω) for the one-dimensional diatomic chain (see above), a two-dimensional network and a three-dimensional lattice. He showed that the essential features of the linear diatomic lattice are only qualitatively changed for two and three dimensions. The singularities in G(ω) for the one-dimensional lattice become two broadened peaks in G(ω) and the gap between the singularities disappears also if we only consider atoms of the same mass. The broadening of the singularities is caused by the averaging over all q-directions (In three dimensions we have in general three acoustic branches, corresponding to the possibility of longitudinal and transversal waves). However, at certain symmetry-points (called critical points) still singularities (called van Hove singularities [28]) can occur, which show up as kinks in G(ω) vs. ω. Computer calculations of G(ω) do indeed reveal these fine structures (see e.g. fig. 2.2).

The actual determination of G(ω) is a matter of many tedious calculations for which large electronic computers are a great help. We will only sketch the method first used by Blackman [22,23]: the root sampling method (A discussion of other methods is given in refs. 29, 30) Using a known set of force constants, which are obtained from fitting experimental ω(q)-curves to e.g. a Born-von Kármán model, the secular equation is solved for a number of q-points uniformly distributed over the Brillouin zone. The function G(ω) is then approximated by a normalized histogram. (A serious disadvantage of this method is the possibility to overlook singularities in the actual G(ω).) From this short description of the root sampling method it is clear that the accuracy of G(ω) is determined by the number of q-points at which the frequencies are calculated.

The use of large electronic computers has therefore greatly improved the calculations of $G(\omega)$. An extension of the root sampling method by Gilat and Dolling [31]) gives almost the exact spectrum for $G(\omega)$ [32].

Having determined $G(\omega)$ numerically one has to calculate C_v also numerically. The frequency range is divided into a large number of intervals. The mean frequencies $< \omega_i >$ of the intervals are weighted according to the value of $G(<\omega_i>)$ and substituted in the expression (2.18a). The contributions of all the intervals are summed in order to obtain C_v. This procedure is equivalent to the summation of weighted contributions of a large number of independent oscillators. It is clear from this kind of calculation that a model in which only oscillators of one frequency are present (Einstein model) is a too simple picture [33]) of a lattice.

We will now focus our attention upon the low-temperature lattice specific heat.

Low temperature lattice specific heat; deviations from the Debye model.

For temperatures sufficiently lower than the Debye temperature (say $T \leq 0.1\ \Theta$) we see from fig. 2.2 that the main difference between the Born-von Kármán model and the Debye model is a stronger increase of $G(\omega)$ with increasing ω in the case of the Born-von Kármán model. This is a direct consequence of the dispersion relation $\omega(q)$, which results in a decreasing group velocity $d\omega/dq$ (see fig. 2.3) and hence from (2.13) in an increasing $G(\omega)$.

We can develop $G(\omega)$ at low frequencies in a power series [24])

$$G(\omega) = a_1\omega^2 + a_2\omega^4 + a_3\omega^6 + \cdots\cdots \qquad (2.28)$$

We have only even powers because $G(\omega)$ is an even function in ω since the secular equation is solved for ω^2 (see 2.26). There is no constant term in (2.28) as we know that in the acoustic limit $q \to o$ and $\omega \to o$. Thus $G(\omega)$, which is proportional to q^2 (2.13), is zero for $\omega = o$.

When we substitute expression (2.28) into (2.18a) we get also a power series for C_v:

$$C_v = \beta T^3 + \delta T^5 + \varepsilon T^7 + \cdots\cdots \qquad (2.29)$$

Comparison with the expression for the Debye model at low temperatures (2.20) shows that C_v according to the Born-von Kármán model will in general be larger than C_v (Debye) because $a_2 > o$ and hence $\delta > o$.

To demonstrate this difference as a function of temperature one calculates an effective Debye temperature (Θ_{eff}) from a fit of C_v at each temperature to (2.18). From the qualitative arguments given before we conclude that Θ_{eff} will in general initially decrease with temperature. This behaviour was for the first time explained as "normal" by Blackman [23]). In the past few years some exceptions to this normal behaviour have been observed, notable Al [34]) and Au [35,1]). In these cases Θ_{eff} increases initially with temperature, which corresponds to $\delta < o$ and $a_2 < o$. At present a behaviour like this is not understood.

2.2.3 *Electron-phonon interaction.* The electron-phonon interaction, which we have neglected so far, is of fundamental importance to understand some physical properties e.g. electrical resistivity, thermal conductivity. It can lead to spectacular changes in these properties, like the occurrence of superconductivity.

As far as the specific heat is concerned one tries to describe the electron-phonon interaction (V_{ph}) by its effect on the electrons and phonons separately. The corrected ("renormalized") electrons and phonons can again be treated independently, because the corrections are small for most metals.

Renormalization of the electrons.

The effect of the phonons on the electrons is only important in a small energy range (of order $k\Theta$) around the Fermi energy, as shown by Midgal [36]). This effect results in a "mass-enhancement" or equivalently in an enhanced density-of-states $N(E_F)$. It is customary to write, analogous to (2.9)

$$N(E_F) = \frac{N_o(E_F)}{1 - N_o(E_F)V_{ph}} \equiv (1 + \lambda_{ph})\, N_o(E_F) \tag{2.30}$$

where $N_o(E_F)$ is the "bare" density of states (i.e. without interactions) and $\lambda_{ph} = \frac{N_o(E_F)V_{ph}}{1 - N_o(E_F)V_{ph}}$. Substitution of (2.30) in (2.4) gives

$$C_{el} = \frac{2}{3}\pi^2 k^2 (1 + \lambda_{ph})\, N_o(E_F) T \tag{2.31}$$

The value of V_{ph} can be deduced from a comparison between the measured and the calculated specific heat, using for the latter a value for $\eta(E_F)$ obtained from bandcalculations ($N(E_F) = N_o(E_F)$),

$$\frac{\gamma_{exp}}{\gamma_{calc}} = 1 + \lambda_{ph} \tag{2.32}$$

For most metals λ_{ph} is about 0.1.

Renormalization of the phonons.

To take account of the presence of the (conduction) electrons in the calculation of the phonon spectrum one has developed a lot of models (see ref. 30). Qualitatively the influence can be considered as a decrease of the frequencies of the phonons. This results from the screening of the lattice potential by the electrons and the large bulk modulus, which can be ascribed to the electron gas.

In the acoustic limit ($\omega \to o$ and $q \to o$) the electron-phonon interaction leads to a renormalized velocity of sound. The effect can thus be described by a change in the coefficient β of the T^3 term into β^1:

$$C_L = \beta^1 T^3 \tag{2.33}$$

The changes in β , calculated e.g. by de Launay for Al and Cu, are about 5%. For $\omega, q \neq o$ one can expect anomalies in the dispersion relation because of van Hove singularities in the electron spectrum. For certain values of q (q depends on the topology of the Fermi surface, since $q \pm k = 2k_F$) the screening becomes very small thereby allowing the phonon frequency to become very large. When these singularities have a detectable effect on the measured phonon spectra one can expect the necessity to include many neighbours in a fit to a Born-von Kármán model, accounting for the presence of long range forces.

2.2.4 *Electron-paramagnon interaction.* In some metals (notably Pd and Pt) the interactions between the conduction electrons, which have a strong d-character and therefore form a narrow band, are very large. This results for example in a high magnetic susceptibility which is enhanced by the so-called Stoner factor S:

$$\chi = \frac{\chi_o}{1 - N_o I} = S\chi_o \tag{2.34}$$

where I represents the electron-electron interaction, which is due to exchange interaction. If $N_o I = 1$ the susceptibility becomes infinite corresponding with a ferromagnetic transition. For pure Pd $N_o I = 0.9$ [37]) indicating a nearly ferromagnetic behaviour. In pure Pd we can therefore describe the susceptibility to arise from long lived itinerant spin fluctuations or virtual spin

waves, which in a quasi-particle picture are called "paramagnons". These particles behave in many respects like phonons (e.g. $\omega_{sf} \propto q$; boson distribution function). It is therefore not surprising that the influence of the paramagnons upon the electronic specific heat can be described also by a "mass-enhancement".

Besides this contribution one could also expect a $T^3 \ln(T/T_S)$ term, where T_S is the characteristic temperature of the paramagnons. For a nearly ferromagnetic metal we have, consequently [4])

$$C_{el} = (\frac{m}{m}^*) \gamma_o T + AT^3 \ln(T/T_S) \qquad (2.35)$$

The value of $\frac{m}{m}^*$ for Pd and Pt is about 1.6 [37]).

The second term in (2.35) has not been observed experimentally [7,8]). This can be due to a high value of T_S ($T_S \simeq 400$ K) which renders a distinction between a $T^3 \ln(T/T_S)$ term and a T^3 term experimentally impossible. There has also been a theoretical suggestion that the $T^3 \ln(T/T_S)$ term can be supressed when the mean free path of the electrons is small [38]).

The enhancement factor S can be varied by alloying. It is known that most elements decrease S (e.g. Ag, Cu) while some elements increase S (e.g. Rh, Ni, Fe). In the case of Fe the increase is so large as to cause ferromagnetic behaviour. We will only be concerned here with the paramagnetic alloys.

For the explanation of the behaviour of the nearly ferromagnetic alloys two models have been developed, the "uniform exchange-enhancement" model and the "local exchange-enhancement" model (see ref. 4).

Experimental data on Pd-Ni have shown the applicability of the latter model to this alloys system [5]).

The "local exchange-enhancement" model developed by Lederer and Mills [10]) gives the following expression for the extra electronic specific heat [8])

$$\Delta C_{el} = c\{ \Delta\gamma T + AT^3 \ln(T/T_{s,o}) - BT^3/T^2_{s,loc} \} \qquad (2.36)$$

where c is the concentration of the impurities, $T_{s,o}$ is the spin fluctuation temperature of the host and $T_{s,loc}$ is the local spin fluctuation temperature.

It should be emphasized that (2.36) is only valid for dilute alloys (i.e. no interactions between the impurities are considered).

2.3 Experimental technique; sample preparation.

We have measured the specific heat from 1.3 - 25 K using a set-up which has been described previously [39,40]. Some details have been added, like an automatic switch with switches off the heating current when the recorder, used to monitor the temperature rise, reaches a pre-set value at the end of the scale [41]. We can now use the set-up in a semi-automatic operation.

The samples have been prepared in Al_2O_3-crucibles by melting in an induction furnace (A.D.Little) under a flow of pure Argon gas. The samples were melted twice (each time for about 30 minutes), the second time after turning the sample upside down. After solidification the samples were slowly cooled down to room temperature. Although the induction furnace prevents gravitational segregation we have annealed the samples to ensure a good homogeneity in the large samples, which are in the form of cylinders (20 x 15 mm). The annealing was performed in vacuo (10^{-5} torr) in a radiation furnace. Before annealing the samples were heavily etched in aqua regia, after annealing the samples were quenched in water.

The samples have been prepared by consecutively adding Ni to the first sample (0.5 at.%Ni).

The determination of the Ni concentration was carried out by Dr. Kragten and co-workers from the Natuurkundig Laboratorium, University of Amsterdam. The results of this analysis, which was performed by atomic-absorption spectrophotometry, are shown in table 2.1. There is a good agreement between the average and the nominal concentrations, showing the accuracy of the preparation The small differences in concentration between top and bottom of the samples indicate a fairly homogeneous solution of Ni in Pd.

TABLE 2.1

SAMPLE DATA OF Pd-Ni ALLOYS

SAMPLE	lab. no.	analyzed conc(at%)		average conc(at%)	annealing time,temp	mass (g)
Pd-Ni 0.5 %	7039			0.50	48h;1000°C	43.158
Pd-Ni 1.0 %	7069	t* 1.09 b 1.00		1.05	60h;1000°C	39.713
Pd-Ni 1.5 %	7155			1.50	64h;1000°C	35.772
Pd-Ni 1.85%	7188	t 1.88 b 1.90	1.81¶	1.85	51h;1000°C	34.972
Pd-Ni 2.2 %	7207	t 2.18 b 2.13	2.12¶	2.15	48h;1000°C	33.533

*t = top; b = bottom; ¶ = middle.

The starting materials were obtained from Johnson-Matthey, London. Pd was in the form of sponge (JM S 8750) and Ni in the form of sheet (JM 7806). The purity of these elements was 99.999%. In particular the Fe content of the Pd was very low (∿ 1 ppm) as specified by Johnson-Matthey and evident from its susceptibility (see chapter 3).

2.4 Experimental results and discussion.

We will now present our results for the specific heat of dilute (c < 2.2 at.%Ni) Pd-Ni alloys focussing our attention upon the temperature dependence of the effective Debye temperature (section 2.4.1), the concentration dependence of γ (section 2.4.2), the concentration dependence of β (section 2.4.3) and the field dependence of γ and β (section 2.4.4). In each sub-section a discussion of the results will be given.

2.4.1 *Temperature dependence of the effective Debye temperature.* In order to derive the values of the effective Debye temperature (see also section 2.2.2) we have to calculate the lattice specific heat (C_L) from the measured total specific heat. To obtain C_L we have fitted out data by computer with a least-squares program to the following expression (see (2.4) and (2.29)):

$$\frac{C}{T} = \sum_{i=1}^{6} C(i)\, T^{2i-2} \qquad (2.37)$$

The same fitting procedure was performed by Boerstoel et al. [1]) for pure Pd and is found to give a good representation of the experimental data in the range from 1.3 to 25 K (see also section 2.4.2). The coefficients and r.m.s.-values of the fits are given in the appendix to this chapter. Using these coefficients in expression (2.37) the total specific heat was calculated at one degree intervals from 1 - 25 K. At each temperature the lattice contribution C_L was derived by subtracting the electronic contribution, assumed to be equal to C(1)T. By comparing $C_L(T)$ with the Debye function [27]) we have calculated the effective Debye temperature (Θ_{eff}). The results are shown in table 2.2 and in figs. 2.4 and 2.5.

From the figures it is evident that the behaviour of $\Theta_{eff}(T)$ is quite different from our expectations (see fig. 2.1, curve c). Instead of decreasing, the "depth" of the minimum in the Θ_{eff} vs. T curve increases with Ni concentration. For a more clear representation and comparison with other metals we have plotted the normalized effective Debye temperature, $\Theta_{eff}(T)/\Theta_{eff}(o)$, as a function of temperature in fig. 2.6. The normalized Θ_{eff} for Pd-Ni alloys

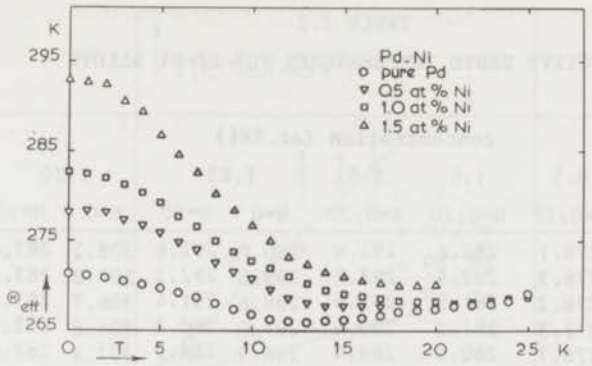

Fig. 2.4. Experimental temperature dependence of the effective Debye temperature (Θ_{eff}) for pure Pd (after ref. 1) and three Pd-Ni alloys.

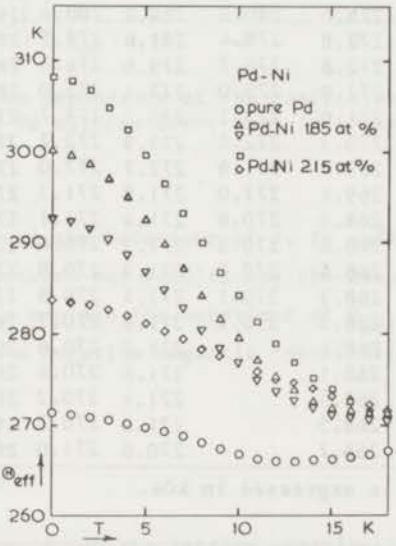

Fig. 2.5. Temperature dependence of Θ_{eff} for pure Pd and two Pd-Ni alloys. Note the field dependence for these alloys. (Δ) Pd-Ni 1.85 at.%, H=0 and (∇) H=20 kOe; ( ) Pd-Ni 2.15 at.%, H=0 and ( ) H=20 kOe.

does indeed become smaller with increasing Ni concentration.

Discussion

As we have pointed out in the previous section, the temperature dependence of Θ_{eff} is due to higher order terms in the specific heat (T^5, T^7, etc.). A decrease in the normalized Θ_{eff} is caused by an increase in the T^5 term. In fig. 2.7 the concentration dependence of δ is shown (δ ≡ c(3)). We note that δ increases with Ni concentration, while we expected δ to decrease or even

TABLE 2.2

EFFECTIVE DEBYE TEMPERATURES FOR Pd-Ni ALLOYS

T	concentration (at.%Ni)							
(K)	0	0.5	1.0	1.5	1.85		2.20	
	H=0	*H=0;27	H=0;20	H=0;20	H=0	H=20	H=0	H=20
0	271.3	278.1	282.6	293.0	300.0	292.6	308.2	283.6
1	271.1	278.3	282.4	292.7	299.6	292.3	307.8	283.5
2	270.8	278.2	281.9	292.4	298.6	291.4	306.7	283.2
3	270.5	277.3	281.2	290.6	297.0	290.3	304.8	282.7
4	270.1	276.7	280.3	289.4	294.9	288.7	302.4	282.0
5	269.7	275.8	279.2	286.8	292.5	286.8	299.6	281.2
6	269.2	274.7	277.6	284.6	289.8	284.8	296.5	280.3
7	268.7	274.0	276.6	282.6	287.1	282.8	293.3	279.5
8	268.0	272.5	275.0	280.2	284.2	280.4	290.0	278.4
9	267.3	271.5	273.8	278.4	281.6	278.5	286.8	277.8
10	266.7	270.7	272.8	276.7	279.6	276.9	284.3	276.9
11	266.2	269.5	272.0	275.0	277.1	275.0	281.4	275.9
12	266.0	268.6	271.0	273.2	275.3	273.7	279.0	275.2
13	265.9	268.1	270.3	272.4	273.9	272.7	276.9	274.6
14	266.1	267.7	269.5	271.6	272.7	272.0	275.2	274.0
15	266.2	267.7	269.1	271.0	271.8	271.3	274.0	273.3
16	266.4	267.8	268.9	270.6	271.4	271.1	272.6	272.8
17	266.7	267.7	268.6	270.3	271.3	270.6	271.6	272.2
18	267.1	266.6	268.4	270.0	271.3	270.8	270.8	271.5
19	267.4		268.3	270.1	271.4	270.8	270.0	270.7
20	267.7		268.3	270.2	271.6	270.7	269.3	269.7
21	267.9		268.1		271.7	270.6	268.4	268.6
22	268.1		268.1		271.6	270.4	267.4	267.2
23	268.3		268.3		271.4	270.2	266.1	265.8
24	268.6		268.5		271.0	270.3	264.7	264.5
25	268.9		268.7		270.6	271.0	263.1	263.5

*the magnetic field is expressed in kOe.

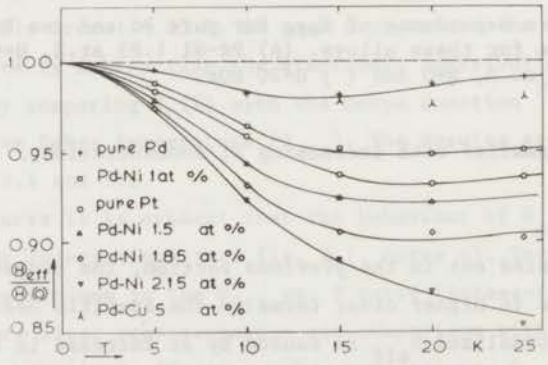

Fig. 2.6. Temperature dependence of the normalized Θ_{eff}. Note the similarity between pure Pd and the Pd-Cu 5 at.% alloy.

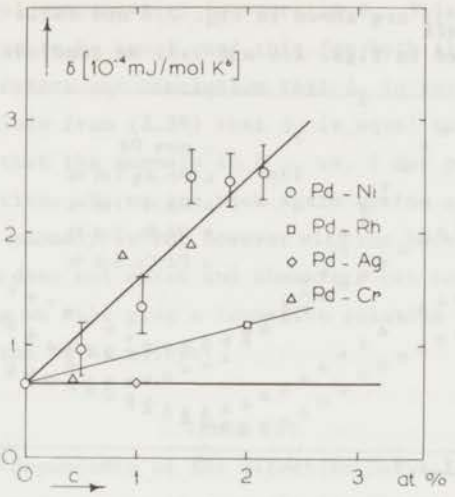

Fig. 2.7. Concentration dependence of the coefficient (δ) of the T^5 term in the specific heat of some Pd alloys. Error bars indicate the estimated accuracy.

to become negative.

We will now discuss the behaviour of δ, to understand the consequences of the disagreement between our results and the assumptions on which the expectations were based. To explain the behaviour of $\Theta_{eff}(T)$ in pure Pd it was suggested that there was a negative magnetic contribution to the specific heat, so we can write

$$\delta = \delta_1 - \delta_2 \tag{2.38}$$

with $\delta_1 > o$ and $\delta_2 > o$. δ_1 is the lattice contribution to the T^5 term and δ_2 is the assumed magnetic contribution to the T^5 term. From the experimental result for pure Pd [1]) we know that δ is positive but small. The suggestion by Veal and Rayne [2]) means that this small δ is caused by a relatively large δ_2 ($\delta_2 \leq \delta_1$).

Upon alloying with Ni we expect the magnetic contribution and therefore δ_2 to increase. If δ_1 remains constant or changes only slightly with alloying, δ would become smaller and eventually negative. This does not happen, however. We observe an increase in δ with alloying, which can only be reconciled with an increasing δ_2 when δ_1 increases very much with Ni concentration. This latter possibility is however very unlikely. In order to exclude this possibility with more certainty we have analyzed the specific heat data for a Pd-Ag [5])

(1 at.%Ag) and a Pd-Cu [6]) (5 at.%Cu) alloy in the same way as the Pd-Ni alloys.

The results for Θ_{eff} are shown in fig. 2.8 and table 2.3 while the normalized $\Theta_{eff}(T)$ is plotted in figs. 2.6 and 2.9. We conclude from these figures

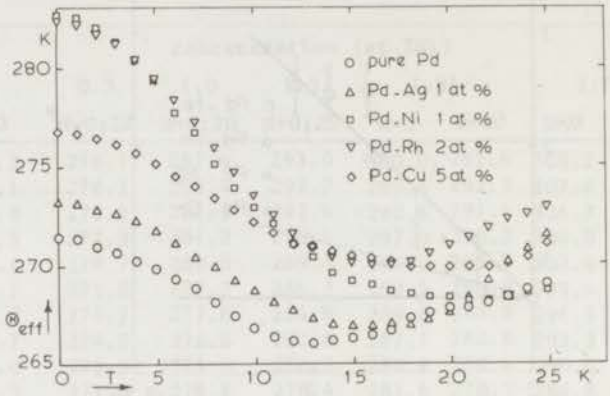

Fig. 2.8. Temperature dependence of Θ_{eff} for some Pd alloys. The data for Pd-Rh and Pd-Ag are from ref. 6; those for Pd-Cu from ref. 5.

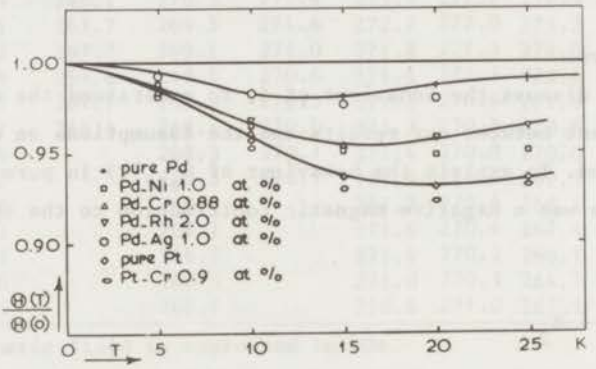

Fig. 2.9. Temperature dependence of the normalized Θ_{eff} of some Pd alloys and a Pt alloy. Data for pure Pt are from ref. 1, for Pd-Cr and Pt-Cr from Boerstoel et al. (see ref. 46) and Zwart [48]).

that in both alloys the temperature dependence of Θ_{eff} is not different from pure Pd. From fig. 2.7 we also conclude that δ in Pd-Ag (also in Pd-Cu) is equal to the pure Pd value. This indicates that δ_2 in pure Pd is very small and that δ_1 does not vary upon alloying up to Cu concentrations of 5 at.%. We come to this conclusion because if $\delta_2 \neq 0$ in pure Pd we would have $\delta = \delta_1 - \delta_2$ constant in both the Pd-Ag and Pd-Cu alloy. The δ_2 term can be expected to decrease appreciably in the Pd-Cu (5 at.%Cu) alloy as $N_o(E_F)$ and hence S (see 2.34) decreases (the decrease in $N_o(E_F)$ can be deduced from the decrease in

the linear term of the specific heat). Keeping a constant δ while δ_2 decreases would require an equal compensating increase in δ_1. This is rather unlikely as $\frac{d\delta_1}{dc}$ and $\frac{d\delta_2}{dc}$ would have to be equal, and this for both alloy systems Pd-Ag and Pd-Cu. We repeat therefore our conclusion that δ_2 in pure Pd is very small. Consequently we conclude from (2.38) that δ_1 is equal to δ and therefore also small. This implies that the anomaly in Θ_{eff} vs. T for pure Pd is due to the behaviour of the lattice. So we are back again at the starting point, having still to explain the anomaly in Pd, however with the knowledge that the supposed magnetic contribution does not exist and therefore can not solve this problem.

In the following we will give a tentative solution to the behaviour of Θ_{eff} of pure Pd and the Pd-Ni alloys.

TABLE 2.3

Temperature dependence of the effective Debye temperature (in K) for some non-magnetic Pd-alloys

T(K)	Pd-Ag 1 at%		Pd-Cu 5 at%		Pd-Rh 2 at%
0	273.1	0	276.6	0	282.3
1	273.0	1	276.5	1	282.0
2	272.7	2	276.3	2	281.6
3	272.5	3	276.0	3	281.1
4	272.1	4	275.6	4	280.3
5	271.6	5	275.1	5	279.3
6	271.0	6	274.5	6	278.2
7	270.3	7	273.9	7	277.0
8	269.8	8	273.3	8	275.8
9	269.1	9	272.7	9	274.6
10	268.6	10	272.1	10	273.4
11	268.0	11	271.6	11	272.4
12	267.6	12	271.2	12	271.5
13	267.2	13	270.8	13	270.8
14	266.9	14	270.5	14	270.3
15	266.8	15	270.3	15	270.0
16	266.8	16	270.1	16	269.9
17	266.9	17	270.0	17	269.9
18	267.0	18	269.9	18	270.1
19	267.2	19	269.8	19	270.5
20	267.5	20	269.8	20	270.9
21	268.3	21	269.8	21	271.3
22	269.2	22	269.8	22	271.8
23	270.1	23	270.0	23	272.3
24	271.7	24	270.3	24	272.5
25	273.5	25	271.0	25	272.9

Explanation for pure Pd.

The lattice dynamics of pure Pd has been studied experimentally by Miiler

and Brockhouse [42,43]), using inelastic neutron scattering to determine the dispersion relations $\omega(q)$ in the major symmetry directions of a single crystal of Pd. Their results exhibit an "anomalous wiggle" in one of the branches of the phonon spectrum (the $[o\zeta\zeta]$ T_1 branch) about the line representing the velocity of sound. This anomaly turned out to be strongly temperature dependent [43]). We suggest that this anomaly could be responsible for the anomalous behaviour of $\Theta_{eff}(T)$. To check this suggestion we have calculated Θ_{eff} from the lattice specific heat, which was computed by Miiller and Brockhouse. The results are shown in fig. 2.10. Two features are very interesting, first of all Θ_{eff} is nearly independent of temperature and secondly the absolute value of Θ_{eff} is in good agreement with the values derived from the specific heat measured by Boerstoel [1]). These are remarkable results as the calculation of C_L by Miiller and Brockhouse was performed with a density of states $G(\omega)$ in which the anomaly in the $[o\zeta\zeta]$ T_1 branch was included (model MP2). To investigate the influence of the anomaly on the lattice specific heat C_L they also calculated $G(\omega)$ and C_L excluding the "anomalous wiggle" (model MP2*). The change in $G(\omega)$

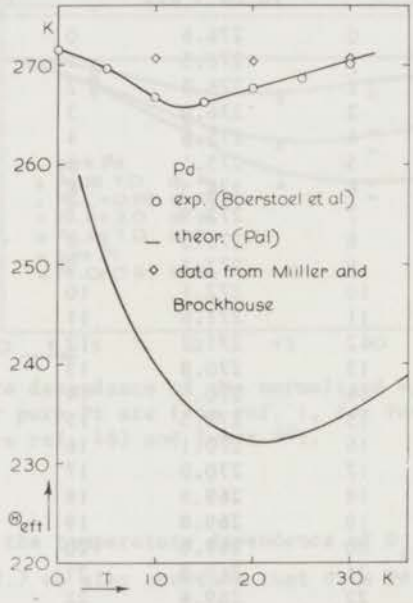

Fig. 2.10. Comparison between experimental and theoretical temperature dependence of Θ_{eff} for pure Pd. Data are obtained from Boerstoel et al. [1]), et al. [43]) and Pal [44]).

was only slight and C_L at high temperatures ($T \geq 80$ K) was not affected. But at low temperatures C_L changed, e.g. at T = 80 K with 0.1%, at T = 40 K with 1% and at T = 20 K with 5%. The authors did not report in their paper [43]) if

this change was positive. When this change turns out to be positive the corresponding Θ_{eff} would decrease resulting in a "normal" variation of Θ_{eff} with temperature.

In this respect the calculation by Pal [44] (see fig. 2.10) is interesting. We note that this calculation does not explain the shallow minimum observed in Pd. Although in the model used by Pal the influence of the conduction electrons is taken into account, Pal's results do not fit the wiggle in the [ζζ0] T_1 branch as is clear from his fig. 1, ref. 44. This might be the reason why the variation with temperature of Θ_{eff} calculated by Pall resembles the "normal" behaviour.

The above arguments do favour our suggestion, but are not sufficient to prove that it is correct. In any case it is significant that the inclusion of the "anomalous wiggle" in the Born-von Kármán analysis of the data by Miller and Brockhouse requires eight nearest-neighbour force constants. This indicates, as noted by Miller and Brockhouse, the presence of weak long range forces which become more important at low temperatures. These long range forces are intimately connected with the presence of the conduction electrons. As the interaction between the conduction electrons in Pd is very strong because of their d-character, one could imagine that in Pd the influence of these long range forces is large. Qualitatively this leads to a behaviour of the lattice as a continuum, which results in the behaviour as expected from a Debye model, i.e. $\Theta_{eff} = \Theta =$ constant.

Another check of our suggestion can be made by calculating C_L and $\Theta_{eff}(T)$ for Pt. The lattice dynamics of Pt has also been measured by Dutton and Brockhouse [45] and an anomaly in the [ζζ0] T_1 branch, similar to that observed in Pd, has been reported. If our suggestion is correct the anomaly in Pt should influence the lattice specific heat to a lesser extent than in Pd, since $\Theta_{eff}(T)$ for Pt is almost "normal".

Explanation for Pd-Ni alloys.

In the explanation of the Θ_{eff} vs. T curves for the Pd-Ni alloys we limit ourselves also to a discussion of the T^5 term.

As in the case of Pd we start with the hypothesis that the coefficient δ is composed of two contributions: one from the lattice (δ_1) and one from the electrons (δ_2). So

$$\delta = \delta_1 + \delta_2 \qquad (2.39)$$

where $\delta_1 > o$ and $\delta_2 > o$.
(As we have argued above δ_2 is very small for pure Pd.) The observed increase of δ with Ni concentration is caused by an increase in δ_1 or an extra term (δ_2) or by an increase in both δ_1 and δ_2. From the results for Pd-Ag and Pd-Cu we conclude that δ_1 does not change appreciably with alloying for concentrations less than 5 at.%. So the only possibility to explain the increase in δ is to assume a magnetic contribution to the T^5 term (δ_2) in Pd-Ni alloys. (The assumption of a negative δ_2 would be consistent with the data only if δ_1 would increase strongly with Ni concentration, which is not the case.)

The assumption of a T^5 contribution which is of electronic origin (electron-paramagnon interaction) is consistent with the large electronic contribution to the T^3 term (see section 2.4.3). Another indication is the field dependence of Θ_{eff} which is clear from fig. 2.5.

We have analyzed the specific-heat data for the system Pd-Cr [46], Pt-Cr [47] and Pd-Rh [6], to see if in these alloys magnetic contributions to the T^3 and T^5 term occurred. The results are given below.

Pd-Cr and Pt-Cr.

The values of Θ_{eff} calculated for Pd-Cr from computer fits (the coefficients are given in the appendix) of the data to expression (2.37) are shown in fig. 2.11 and are tabulated in table 2.3. Except for the Pd-Cr 0.43 at.% alloy we note a behaviour of Θ_{eff} different from pure Pd. The normalized $\Theta_{eff}(T)$ (see fig. 2.9) shows that Pd-Cr alloys behave qualitatively the same as Pd-Ni alloys. This is also apparent in fig. 2.7 where we have plotted the values of δ for Pd-Cr. In section 2.4.3 we will see that the same holds true for the variation of β with concentration. This indicates clearly that also in Pd-Cr (for $c > 0.5$ at.%Cr) magnetic contributions to the T^3 and T^5 term exist. It is very interesting in this respect that for the Pd-Cr 0.43 at.% alloy these contributions appear to be absent. From other studies [46] we know that Pd-Cr in the single-impurity limit behaves non-magnetically at low temperatures (see also chapter 4). This explains the absence for the 0.43 at.% alloy of magnetic contributions and the variation of Θ_{eff}, which is very much the same as for Pd-Ag. For concentrations higher than about 0.5 at.% interactions between the Cr-impurities lead to a magnetic behaviour as demonstrated quite directly by the susceptibility data [47] (see chapter 4).

The results for a Pt-Cr 0.91 at.% alloy [48], shown in fig. 2.12 and tabulated in table 2.3, reveal only a slight change in the behaviour of $\Theta_{eff}(T)$ (see also fig. 2.9). This small change compared to the effects observed in

TABLE 2.4

Temperature dependence of the effective Debye temperature (in K) for some Pd-Cr alloys and a Pt-Cr alloy

	Pd-Cr			Pt-Cr
T	0.43 at%	0.88 at%	1.5 at%	0.91 at%
0	271.8	282.0	291.6	240.0
1	271.7	281.7	291.1	239.7
2	271.6	281.3	290.6	239.3
3	271.2	279.8	289.7	238.5
4	270.8	279.2	288.2	237.5
5	270.4	277.8	285.8	235.9
6	269.9	276.1	284.2	234.7
7	269.3	274.4	282.7	233.1
8	268.7	273.3	280.5	231.7
9	268.3	272.2	279.0	230.2
10	267.7	271.3	277.8	228.8
11	267.2	270.6	276.4	227.4
12	266.9	270.0	275.0	226.0
13	266.5	269.4	274.3	224.9
14	266.4	269.2	273.6	223.9
15	266.3	269.1	273.5	223.1
16	266.6	268.9	273.1	222.4
17	266.7	268.8	273.0	222.2
18	267.0	268.7	272.7	221.8
19	267.3		272.1	221.5
20	267.7		272.6	221.6
21	268.1		272.6	221.6
22	268.5		271.9	221.8
23	268.9		271.4	222.2
24	269.2		271.7	222.8
25	269.4		272.0	223.7

Pd-Cr can be understood qualitatively as the magnetic character of Pt-Cr is less pronounced [46]) (see also chapter 4).

The results of our analysis of the specific heat of Pd-Cr and Pr-Cr, as far as the concentration dependence of the linear term is concerned, will be discussed in chapter 4.

Pd-Rh.

Our analysis is of the specific-heat data [6]) for a Pd-Rh (2 at.%Rh) alloy gives quite interesting results (see fig. 2.8). It turns out that $\Theta_{eff}(T)$ varies in about the same way as a Pd-Ni 1 at.% alloy and a Pd-Cr 0.88 at.% alloy, see fig. 2.9. From the explanation of the Pd-Ni and Pd-Cr behaviour we

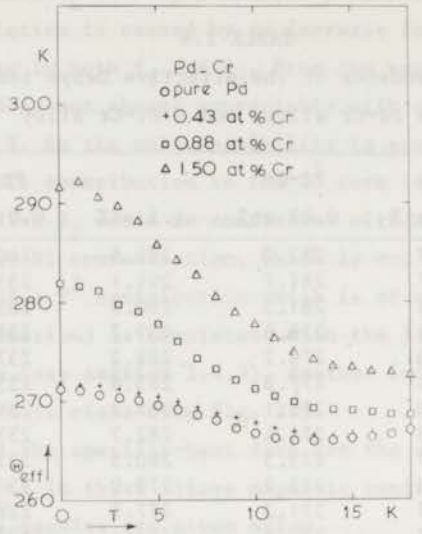

Fig. 2.11. Temperature dependence of Θ_{eff} for pure Pd and some Pd-Cr alloys.

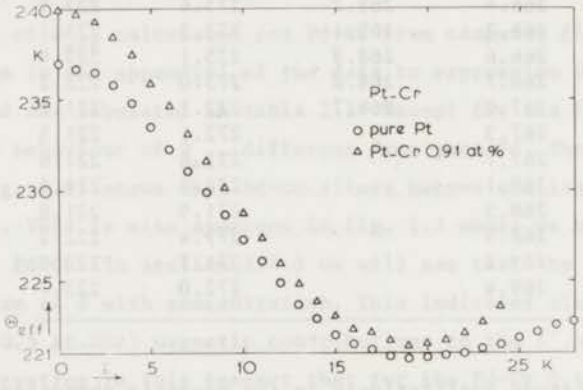

Fig. 2.12. Temperature dependence of Θ_{eff} for Pt and a Pt-Cr 0.91 at.% alloy. Data are from Zwart [48] (see also ref. 46).

conclude that also for Pd-Rh a magnetic contribution is present, although this contribution is smaller (see fig. 2.7). As we will see in section 2.4.3 there is also a contribution to the T^3 term, which is consistent with the observed variation of $\Theta_{eff}(T)$.

2.4.2 *Concentration dependence of γ, the coefficient of the linear term in the specific heat as a function of temperature.* Before considering the concentration dependence of γ *we discuss the data analysis,* which we have performed to obtain γ (and β) from our specific-heat results.

It has been and still is customary to derive γ and β values from a plot of C/T vs. T^2 assuming a linear relationship between these quantities. Although at sufficiently low temperatures (e.g. $T < 0.01\ \Theta_D$) this relationship is expected to hold, deviations occur at higher temperatures. It depends on the accuracy of the measurements whether one can observe these deviations. Especially when the temperature range of the measurements is limited (e.g. from 1.3 - 4.2 K) these deviations could be considered still to belong to the T^3-region. In this way systematic errors can be made, γ being too low and β too high . As the accuracy of the specific-heat measurements has been improved over the last twenty years almost an order of magnitude, this trend in γ and β has been evident, as was shown for some pure metals recently by Boerstoel et al. [1]). We have used the advantage of our extended temperature range (1.3 - 25 K) to investigate possible systematic errors introduced by a particular way of analyzing the data.

We have performed computer fits of our data to the general expression for the specific heat (eq. 2.37) in three different temperature ranges:

a) from 1.3 to 4.2 K with m = 2;

b) from 1.3 to 7 K with m = 3;

c) from 1.3 to 25 K with m = 6.

By varying m it turned out that the best fits were obtained for all alloys for the values of m indicated in each temperature range.

TABLE 2.5

Concentration dependence of the coefficient γ

conc. (at%)	γ (average)	range a, m=2		range b, m=3		range c, m=6	
		H=0	H=20	H=0	H=20	H=0	H=20
0*	9.45					9.45	
0.50	10.29	10.26	10.31	10.27	10.31	10.29	10.30
1.05¶	11.09	11.09	11.19	11.10	11.21	11.05	11.03
1.05	11.09	11.09	11.10	11.10	11.11	11.08	11.11
1.50	12.05	12.03	12.07	12.04	12.07	12.05	12.06
1.85	12.90	12.90	(12.68)	12.92	(12.68)	12.87	(12.68)
2.15	13.75	13.80	(-)	13.75	(13.14)	13.72	(13.14)

*this value is obtained from ref. 1

¶these data are more reliable

values for γ are in (mJ/mol-K^2); for H in (kOe)

The results for γ of these best fits are listed in table 2.5. As one can note the differences in γ between the various fits are not systematic and within the experimental accuracy (0.4%). The average value (the γ values for c = 1.85 and 2.15 at.% are only averaged over H = 0 values, since γ is field-dependent) is tabulated in the second column of table 2.5 and shown in fig. 2.13, in which the previously determined values [7,8]) are also indicated. The agreement between all the γ values is good. Taken separately, our measurements show

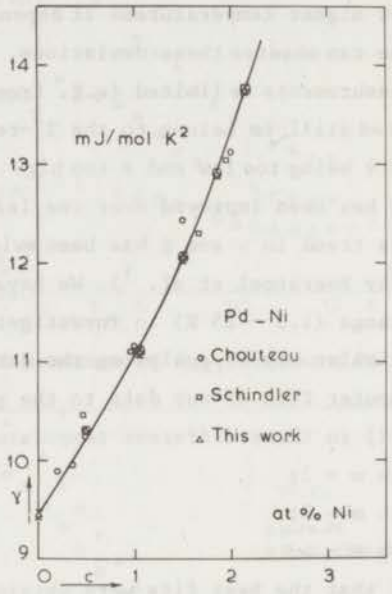

Fig. 2.13. Concentration dependence of the coefficient of the linear term (γ) of the specific heat of some Pd-Ni alloys. Previous results obtained by Schindler et al. [7]) and Chouteau et al. [8]) are also shown.

a more consistent behaviour of γ, which enables an accurate determination of $\gamma(c)$. We first consider the dilute region (c < 0.5 at.%Ni).

The linear term in the specific heat of Pd-Ni alloys is very large. It is clearly enhanced due to (magnetic) interactions.

In the dilute region the increase in γ is of comparable magnitude as for dilute Pd-Cr alloys [46]) (see table 2.6 in which $(d\gamma/dc)$ per mol of impurity is tabulated for some magnetic and non-magnetic Pd-based alloys).

According to eq. 2.36 we can calculate (see ref. 49) the local spin fluctuation temperature T_{sf}, expressing $(d\gamma/dc)$ as follows,

$$\frac{d\gamma}{dc} = \frac{\pi R}{T_{sf}} \qquad (2.40)$$

TABLE 2.6

$d\gamma/dc$ values for some Pd alloys

alloy	$d\gamma/dc$ ($mJ/molK^2$-mol)	ref.
Pd-Ni	+150	this work
Pd-Cr	+100	46
Pd-Rh	+ 26	6
Pd-Ag	- 28	6
Pd-Cu	- 29	5

where R is the molar gas constant: 8.314 (J/mol K), and $(d\gamma/dc)$ is expressed in ($J/mol\ K^2$-mol).

We have omitted the factor (21 + 1) in eq. 2.40 as the case of strong Hund's rule coupling applies to Pd-Ni alloys [50].

Substitution of the $(d\gamma/dc)$ value derived from the initial slope in fig. 2.13 ($d\gamma/dc = 150 \times 10^{-3}$ ($J/mol\ K^2$-mol Ni) we derive T_{sf} = 170 K. This value is rather high compared with estimates, see table 2.6, deduced from the temperature dependence of the resistivity [51,52]) and of the T^3 term in the specific heat [8]) (see also next subsection).

TABLE 2.7

Values for T_{sf} deduced from different properties for Pd-Ni

property	T_{sf}(K)	ref.
$\rho(T)$	76	51
$d(\rho)/d(T^2)$	23	52
$d\beta/dc$	20	8
$d\beta/dc$	30	this work
$d\gamma/dc$	170	this work

The disagreement between the T_{sf} values derived from $(d\gamma/dc)$ and from the other properties can be partially resolved by taking into account the change in $(d\gamma/dc)$ due to a change in the density of states. A recent calculation [53]) shows $N(E_F)$ to decrease with increasing Ni concentration. This results in a larger value of $(d\gamma/dc)$ due to the magnetic contribution and consequently to a smaller T_{sf}. It is difficult to estimate $(d\gamma/dc)$ corrected for the change in $N(E_F)$, but it will not increase more than a factor two, as can be expected for Pd-Cr [46]). The difference might indicate a quantitative difference between the behaviour of the resistivity and the specific heat. We are not aware of any

theoretical justification for this suggestion, however.

For concentrations larger than about 0.5 at.%Ni the behaviour of $\gamma(c)$ is non-linear as reported previously [7,8]. Our results (see fig. 2.13) confirm these observations. The concentration dependence of γ indicates that the interactions between the Ni impurities increase their contribution to γ. One can therefore describe the effect of these interactions as a decrease of the local spin fluctuation temperature with increasing concentration. It is known from several different experiments that by increasing the concentration beyond a certain concentration c_o these interactions give rise to a ferromagnetic ordered state [4]. At the critical concentration (c_o) T_{sf} can be considered to be zero or the local susceptibility to be infinite [54]. For Pd-Ni c_o is approximately equal to 2 at.%. When $c > c_o$ the ordering temperature, T_c, rises strongly to values which compare to those obtained for other magnetic alloys [70] (e.g. Pd-Co [71]) of the same concentration (see fig. 2.14).

The precise value of the critical concentration is the subject of current interest as theoretical calculations can now predict values for c_o, fitting the experimental data to certain models.

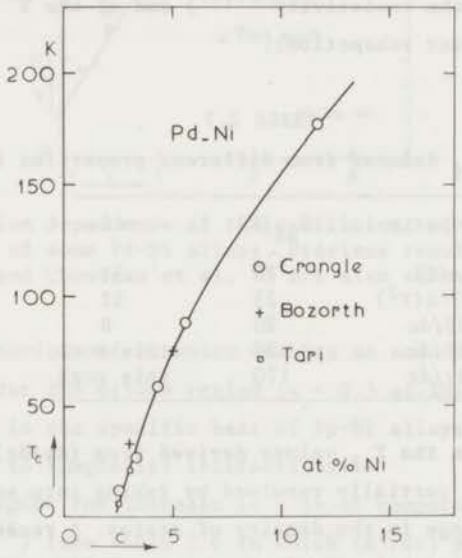

Fig. 2.14. Variation with concentration of the ferromagnetic ordering temperature (T_c) of some Pd-Ni alloys. Data are collected from Tari et al. [9], Bozorth et al. [55] and Crangle et al. [57].

The value of c_o can be obtained from the variation of T_c, from susceptibility data in the paramagnetic regime and from the concentration dependence

of the resistivity and the specific heat. We will discuss these different determinations in the following.

a. From the *variation of* T_c, determined by magnetization measurements [55, 57], a value of about 2.5 at.% was deduced for c_o (see fig. 2.14).

b. *Susceptibility data* in the paramagnetic regime [7,56,58] can be extrapolated to $\chi^{-1}(c_o) = 0$. We have plotted the available data in fig. 2.15. As one can notice the data from different authors are not very consistent. Especially the results by Williams (quoted in ref. 7) are systematically different. We have therefore extrapolated (by smooth curve fitting) each set of measurements separately. The extrapolation of the results from Chouteau et al. [56] is inaccurate because the data for c > 1.5 at.% deviate considerably from a smooth curve. The extrapolation of these results gives a higher value for c_o than the other extrapolations. This may be a real difference since Chouteau et al. deduced their susceptibility data from measurements at very low temperatures (T << 1 K), where Fe-contamination is easily saturated. This could result in systematically smaller values of χ, as compared with the other data, representing perhaps better χ_{alloy} (at least for c < 1.5 at.%). However, the field dependence of the magnetization reported by the same authors [13] in a later publication can also provide an explanation for the deviations at higher concentrations.

Taking into account the uncertainty of the extrapolations we deduce from fig. 2.16

$$c_o = (2.6 \pm 0.1) \text{ at.\%}$$

A theoretical analysis of these susceptibility data has recently also been reported by Harris and Zuckermann [59]. These authors have calculated the susceptibility of Pd-Ni alloys using an analog of the coherent potential approximation (CPA) [60]. The local-exchange potentials ($I_{A,B}$) are substituted for the ordinary potentials ($V_{A,B}$) which are assumed to be equal at A and B sites in the alloy. The CPA enables one to calculate some properties (those connected with the density of states at the Fermi level) for arbitrary concentrations A and B. In this way results are not restricted to dilute alloys.

From fits of their model-calculation to the data by Fawcett et al. [58] the value c_o = 2.5 at.%Ni is derived by Harris and Zuckermann; their fit to data of Williams (referred to in ref. 57) gives c_o = 2.3 at.%Ni. The latter fit is worse than the former, as can be judged from fig. 2 and fig. 3 in ref. 59. In both fits, however, the initial slope $n = \left(\frac{1}{\chi}\frac{d\chi}{dc}\right)_{c=0}$ is smaller (60 and

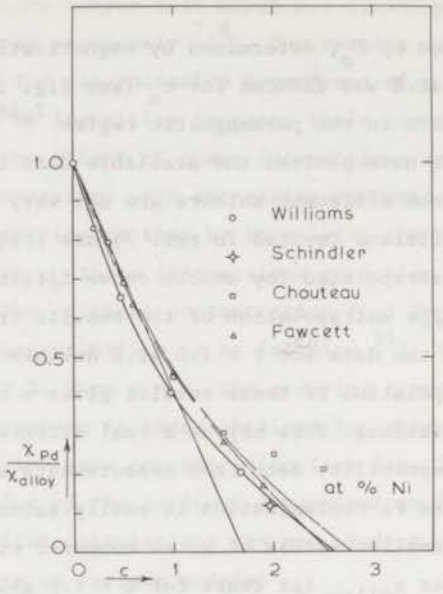

Fig. 2.15. Concentration dependence of the inverse susceptibility (normalized to the value for pure Pd) of Pd-Ni alloys. Data are obtained from Chouteau et al. [56], Schindler et al. [7] and Fawcett et al. [58]. Data by Williams are reported in ref. 7.

70) than the value (η = 87) consistent with Chouteau's results, to which no fit was reported.

An extension of the above calculation was performed by Levin et al. [53], including a possible difference in normal potential scattering ($V_A \neq V_B$). These authors also tried to fit the susceptibility data for Pd-Ni alloys. However, they assumed c_o to be equal to 2.2 at.% instead of calculating its value. Although the inclusion of normal potential scattering should be an improvement of the model, according to normalized atom calculations [61], it turned out that a better agreement with experiment was obtained in the weak scattering limit of their model, which agrees with the fit by Harris and Zuckermann [59]. The discrepancy between the fit by Levin et al. can probably not be removed by choosing a different value of c_o.

A totally different theoretical approach to the calculation of c_o was reported by Edwards et al. [62]. These authors discuss the magnetic properties of strongly paramagnetic dilute alloys on the basis of the generalized Landau theory of phase transitions. Inclusion of the spatial dependence of the coefficient of M^2 and taking into account the term involving the gradient of the

magnetization M in the expansion of the free energy, one can apply this theory to Pd-Ni alloys. Restricting the calculation, as a first approach, to dilute paramagnetic alloys an expression is derived for $\chi(c)$. Fitting the slope $d\chi(c)/dc$ to the value of Chouteau et al. [56]) the parameter which determines c_o was obtained.

To calculate $\chi(c)$ for interacting Ni impurities ($c > 0.5$ at.%Ni) a simplified model is introduced. The concentration for which a sudden transition to a ferromagnetic state occurs is calculated to be

$$c_o = 1.80 \text{ at.\%}$$

It is remarkable that this value is almost equal to the value obtained by a straightforward linear extrapolation of the dilute region (see fig. 2.15).

c. The critical concentration has recently been derived by Tari and Coles [9]) from *resistivity measurements*. Analogous to the T term in the specific heat, the localized spin fluctuations give rise to a T^2 term in the resistivity [51,63]). When $c > 0.5$ at.%Ni the coefficient A of the T^2 term increases strongly with concentration. However, Tari and Coles observed that for $c \simeq c_o$ the resistivity cannot be described by a T^2 term in the temperature range below 4.2 K. Therefore they fitted their results to the following expression

$$\rho(T,c) = \rho(o,c) + A(c)T^n \qquad (2.41)$$

where n varied from 2.0 to 1.40 for $c = 5.83$ to 2.25 at.%Ni; being lowest at $c = c_o$ and increasing for c below and above c_o.

When the A values derived from these fits are plotted versus the concentration a pronounced peak in A(c), almost symmetric around $c = c_o$, is obtained. In this way Tari and Coles claim a very accurate determination of c_o, which has the value

$$c_o = (2.32 \pm 0.03) \text{at.\%Ni}$$

This value is rather low compared to our analysis of the susceptibility data and the fit [59]) to the data by Fawcett. Only the results by Williams, including a uncertain data point [7]) for c = 1.95 at.%, extrapolate to $c_o = 2.3$ [59]).

The peak in A(c) was also obtained by Leger and Muir [64]). Their data are limited however to concentrations above 3 at.%Ni, so no accurate determination of c_o is possible from these measurements.

d. In order to determine c_o from γ *versus concentration*, we have plotted our results ($c < 2.2$ at.%Ni) and those of Chouteau et al. [8]) ($c > 2.5$ at.Ni) in fig. 2.16. From the combination of these results we note that $\gamma(c)$ is also

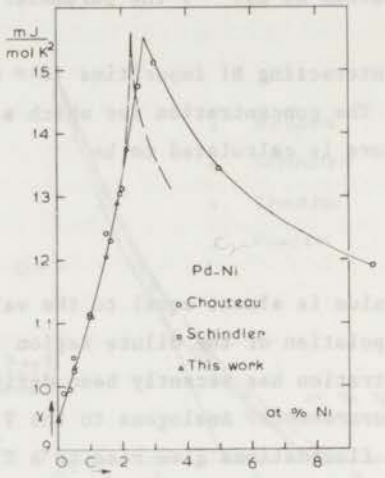

Fig. 2.16. Concentration dependence of γ for Pd-Ni alloys. Notice the peak at 2.7 at.%. The dashed line is a hypothetical curve corresponding to a critical concentration of 2.3 at.%, which was reported in ref. 9.

peaked, although at a considerably higher concentration than the one deduced by Tari and Coles. We estimate from fig. 2.17

$$c_o = (2.7 \pm 0.1) \text{ at.\%Ni}$$

This value compares favourably with the other determinations, giving c_o = 2.6 ± 0.1 at.%Ni.

In order to obtain c_o = 2.3 at.%Ni from $\gamma(c)$, the peak in $\gamma(c)$ should lie between the data point for the highest concentration we measured and the data point for c = 2.5 at.%Ni from ref. 8. This could be the case only if the data points taken from ref. 8 are somehow consistently too large. This seems improbable, although not impossible. So, before speculating about the possibility of a different behaviour of ρ, χ and c, further accurate specific-heat measurements on Pd-Ni alloys are necessary in the concentration range 2.2 - 5 at.%Ni to determine c_o with great certainty from $\gamma(c)$.

TABLE 2.8

Values for β derived from fits of the data to eq. 2.37

concentration(at%)	range a, m=2		range b, m=3		range c, m=6		average value	Θ (K)
	H=0	H=20	H=0	H=20	H=0	H=20		
0†	10.2				9.73		9.7	272
0.50	9.51	9.04	9.28	8.95	9.04	8.94	9.1	277.5
1.05	8.57	7.77	8.27	7.00	8.68	8.69	8.6	282.5
1.05*	8.77	8.86	8.61	8.71	8.70	8.53		
1.50	8.20	7.88	7.97	7.63	7.53	7.64	7.7	293.5
1.85	7.09	(7.99)	6.44	(7.61)	7.20	(7.76)	7.2	300
2.15	5.86	-	6.71	(8.63)	6.64	(8.52)	6.6	308

† data from ref. 1

* these values are more reliable

values for β are expressed in (10^{-2}mJ/mol-K^4); H is given in kOe; the accuracy in β is about 2%

2.4.3. *Concentration dependence of β, the coefficient of the T^3 term in the specific heat as a function of temperature.* The values of β, obtained with the data analysis described in section 2.4.2, are listed in table 2.8. Comparing the values determined in the different temperature ranges we note a slight trend: the values in range a ($1.3 < T < 4.2$ K) being systematically higher than those in range b or c. However, the differences are in general within the error of β (about 2%). We have adopted the values in the range c in most cases as the most probable values for β, designated "average value" in table 2.8. (For c = 0.5 and 1.5 the average of the values in the ranges b and c was adopted.) In the last column of table 2.7 the Debye temperatures, calculated according to eq. 2.21 from β, are tabulated.

We have plotted the average values of β as a function of concentration in fig. 2.17. One can notice a slight non-linear behaviour of β(c), qualitatively similar to γ(c) (see preceding subsection). This non-linearity was not reported in earlier measurements by Chouteau et al. [8]). This is certainly due to the inaccuracy (about 6%) of their data for β, as can be noted from fig. 2.18. Besides the discrepancy in the absolute values of β (the large difference in β for pure Pd was already noted in ref. 1), the values for $(d\beta/dc)$ are also not in agreement. We obtain for $\beta^{-1}(d\beta/dc)_{c=0}$ a value of (-12 ± 1), while Chouteau et al. [8]) give a value of (-20 ± 5).

Although our value for $-\beta^{-1}(d\beta/dc)$ is smaller than that obtained by the authors in ref. 8, it is still much larger than for non-magnetic alloys

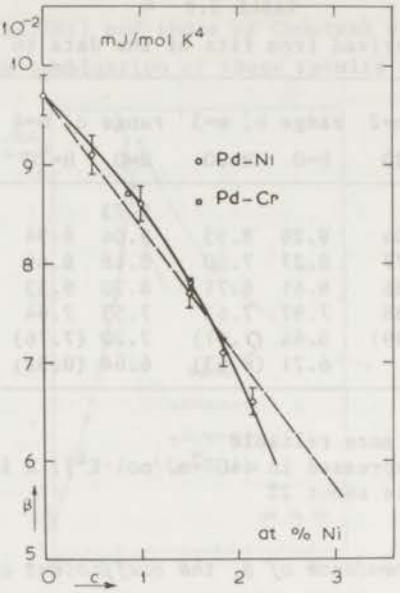

Fig. 2.17. Concentration dependence of the coefficient (β) of the T^3 term of the specific heat of some Pd-Ni alloys. Note the similarity between Pd-Ni and Pd-Cr alloys. Error bars indicate the estimated accuracy (about 2%). The dashed line shows a linear fit to the data; the slope of this line results in $\beta^{-1}(d\beta/dc) = -13$.

(cf. Pd-Cu: $-\beta^{-1}(d\beta/dc) = +1$). Therefore the attribution of the change in β to a contribution from localized spin fluctuations (see eq. 2.36) is still correct. Omitting the $T^3 \ln T$ term (which will be justified at the end of this subsection) we can write [8,49]

$$\frac{\Delta C}{cT} = \Delta\gamma \{ 1 - \frac{4\pi^2}{5} (\frac{T}{T_{sf}})^2 \} \qquad (2.42)$$

From eq. 2.42 we can calculate T_{sf}, substituting the experimental values for $(d\gamma/dc)$ and $(d\beta/dc)$ into

$$T_{sf}^2 = -\frac{4\pi^2}{5} (\frac{d\gamma}{dc})(\frac{d\beta}{dc})^{-1} \qquad (2.43)$$

With our results, $(d\beta/dc) = -12$ (mJ/mol K^4-mol) and $(d\gamma/dc) = +150$ (mJ/mol K^2-mol), we obtain $T_{sf} \simeq 30$ K. This value was already quoted in table 2.7, where it was compared to other determinations of T_{sf} (e.g. 20 K [8]) also from $d\beta/dc$).

The large difference in β-values between our results and those of Chouteau et al. [8]) is difficult to understand, especially while the values for γ do

agree. Perhaps the limited temperature range (0.4 < T < 3 K) combined with experimental accuracy could lead to a too high value for β as discussed in the

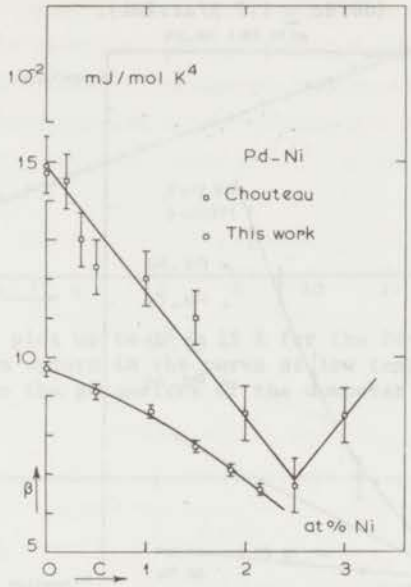

Fig. 2.18.Concentration dependence of the coefficient β; comparison of the present results with previous data by Chouteau et al. [8]).

section about data analysis. However, the value reported [8]) for β of pure Cu is only 3% larger than the accepted value [72]). So this probably systematic error cannot explain the large disagreement (about 50%) between the values for pure Pd (and the Pd-Ni alloys). It is remarkable that for about 2 at.% the values for β are in reasonable agreement (see fig. 2.18). As the data for β of pure Pd by Chouteau et al. [8]) are certainly incorrect (see ref. 1 for a discussion) we believe our β values for Pd-Ni alloys also to be correct, since they extrapolate to the correct value for Pd.

In fig. 2.18 we have also plotted the results of our analysis of Pd-Cr alloys. It is remarkable that β-values for Pd-Cr alloys are almost identical to the ones for Pd-Ni. The similarity between these systems will be discussed in the next chapter.

Debye temperature of Pd-Ni, Pd-Rh and Pd-Ag.

In fig. 2.19 the variation with concentration of the Debye temperature for Pd-Ni alloys is shown.

This variation ($d\theta/dc \simeq 11$ K/at.%Ni) also clearly indicates the presence

of extra (magnetic) contributions to the T^3 term, since for non-magnetic alloys one would expect approximately a linear variation between the Debye temperatures of Pd [1]) and Ni [65,7]) ($d\Theta/dc \simeq 1.7$ K/at.%Ni).

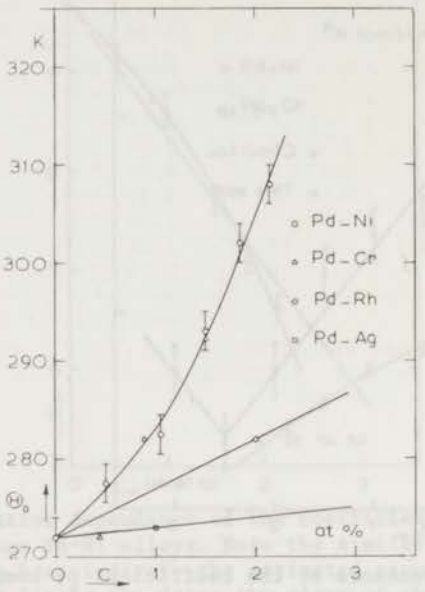

Fig. 2.19. Variation with concentration of the Debye temperature (Θ_D) for some Pd alloys (see table 2.3, 2.4 and 2.8).

We have also included in fig. 2.19 data for a Pd-Rh and a Pd-Ag alloy [6]). The variation of Θ for Pd-Ag is that expected for a non-magnetic alloy, while for Pd-Rh ($d\Theta/dc$) is in between the values for Pd-Ag and Pd-Ni. The same behaviour was apparent from $\gamma(c)$. This lends support to the suggestion (see next chapter) that dilute Pd-Rh alloys are also on the verge of becoming magnetic, alhtough to a lesser extent than Pd-Ni alloys. (If we calculate T_{sf} for Pd-Rh according to eq. 2.43 we get $T_{sf} = 40$ K).

Absence of the $T^3 ln(T/T_s)$ term.

As was already remarked in section 2.2.4, previous measurements of the specific heat of pure Pd and Pd-Ni alloys did not show a $T^3 \ln(T/T_s)$ term, which was predicted theoretically (for a review see ref. 4).

We have also considered the possibility of a $T^3 \ln(T/T_s)$ term by including this term in the power series expansion (eq. 2.36). Analysis of the parameters resulting from these fits (see appendix) learned that these fits resulted in unrealistic changes in the coefficient of the T^3 term. Also plots of C/T vs T^2

did not show an upturn at low temperatures. As this upturn can be expected to

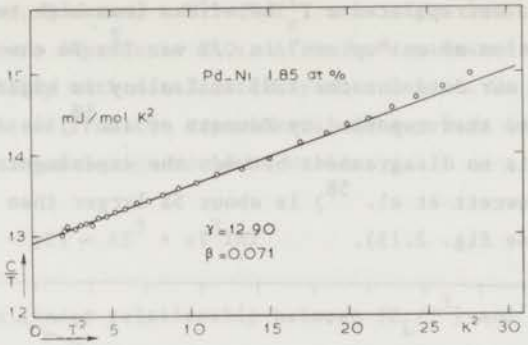

Fig. 2.20.C/T vs. T^2 plot up to $T^2 \sim 25$ K for the Pd-Ni 1.85 at.% alloy. There is no evidence for an upturn in the curve at low temperatures. The values for γ and β correspond to the parameters of the computer fit (see tables 2.5 and 2.8)

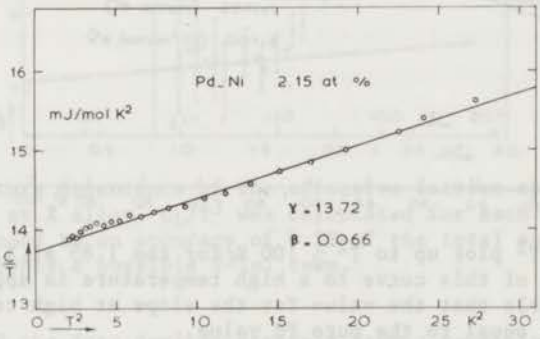

Fig. 2.21.C/T vs. T^2 plot up to $T^2 \sim 25$ K for the Pd-Ni 2.15 at.% alloy. Also for this alloy there is no turnup at low temperatures. The values for γ and β correspond to the parameters of the computer fit in range c (see table 2.5 and 2.8).

be largest for concentrations near the critical one, we show only C/T vs. T^2 plots for the 1.85 at.% and the 2.15 at.% alloy (figs. 2.20 and 2.21). (The results for the 1.85 at.% alloy are representative for the experimental accuracy. In the case of the 2.15 at.% alloy the accuracy was less, due to some problems with the recorder during the measurements.) As can be seen from these figures no upturn in C/T vs. T^2 is present. So our measurements substantiate the earlier conclusions [7,8]) about the absence of a $T^3 \ln(T/T_s)$ term in the specific heat and disagree with the suggestion by Fawcett et al. [58]). In our analysis the low temperature range is considered to be the T^3-region, while

the deviation from this law occurs at higher temperatures (due to a T^5 term etc.). Fawcett et al. extrapolated a T^3 behaviour from high temperatures which leads to the observation of an "upturn" in C/T vs. T^2. To check this procedure, we have also plotted our data for the 1.85 at.% alloy to higher temperatures. A behaviour similar to that reported by Fawcett et al. [58]) is apparent from fig. 2.22. So there is no disagreement between the experimental data, although the value for γ by Fawcett et al. [58]) is about 5% larger than we would expect for c = 1.89 at.% (see fig. 2.13).

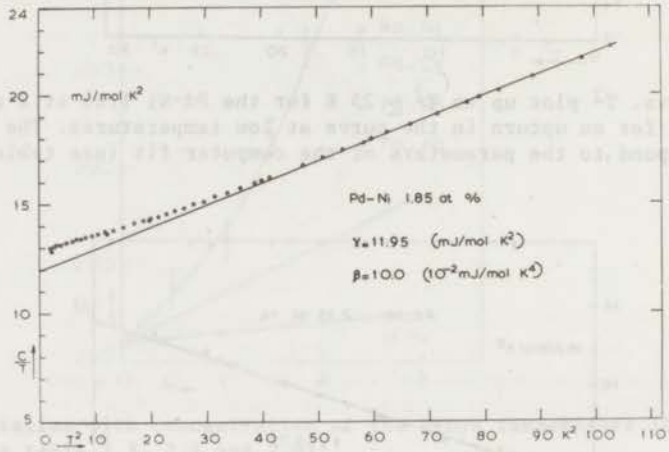

Fig. 2.22. C/T vs. T^2 plot up to $T^2 \sim 100$ K for the 1.85 at.% alloy. A gradual change in the slope of this curve to a high temperature is apparent from this plot. It is remarkable that the value for the slope at high temperatures ($T \gtrsim 7$ K) is almost equal to the pure Pd value.

It is remarkable that the slope of C/T vs. T^2 at high temperatures ($T \simeq$ 10 K) is almost equal to the value obtained for pure Pd ($\beta = 9.7 \times 10^{-2}$ mJ/mol K^4). This turned out to be also the case for the 2.15 at.% alloy. This return to the value of Pd can be noted also in the Θ_{eff} vs. T curves (see fig. 2.4 and 2.5). From fig. 2.22 one gets the impression that an extra contribution is present in the addition to a background represented by the straight line. From this point of view [66]) it is clear that the enhancement of γ at T = 0 in the Pd-Ni alloys results at low temperatures in a negative contribution to the T^3 term. At higher temperatures a positive contribution (T^5 term, see section 2.4.1) has to compensate the negative T^3 term in order to regain the value of pure Pd. The electronic character of the contributions to the T^3 and the T^5 term is evident in this picture, which can also be formulated as a temperature dependence of γ. The latter point of view is implicit

in eq. 2.42. In our analysis we have assumed that the higher order term in (2.42) is a T^5 term. However, a $T^3 \ln(T/T_s)$ term might in principle also describe the temperature dependence of γ. As we have measured up to 25 K we can check this possibility with more certainty than before. We have plotted (C_L/T^3) versus lnT, calculated from the experimental data points (see fig. 2.23).

If the following relation would be valid:

$$C_L \equiv (C - \gamma T) = \beta T^3 + \varepsilon T^3 \ln T \qquad (2.43)$$

one could expect a linear relationship between (C_L/T^3) and lnT. As can be

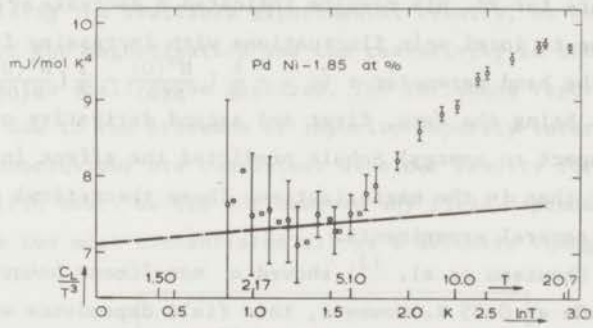

Fig. 2.23. Temperature dependence of the effective lattice specific heat (C_L) of the Pd-Ni 1.85 at.% alloy. C_L/T^3 was calculated for each data point. The error bars correspond to an accuracy of 0.5% of the total specific heat. The dashed line represents a possible $T^3 \ln T$ term.

noted in fig. 2.23 the data deviate strongly from a possible linear variation represented by the dot-dashed line (We have drawn this line assuming $\beta = 7.1 \times 10^{-2}$ (mJ/mol K^4), see table 2.8). We conclude therefore that the $T^3 \ln(T/T_s)$ term is not observed in Pd-Ni alloys, at least not for $T \geq 5$ K.

Although the temperature dependence of γ fits into the picture of a gradual disappearance of the local spin fluctuations with increasing temperature, it is not clear to us at the moment how the temperature independent contribution to γ could be explained. This contribution, obtained from extrapolation of the "background" specific heat (see fig. 2.22), is too large, $\Delta\gamma = 2.5$ (mJ/mol K^2), to be accounted for by a change in the density of states with alloying (see Pd-Cu).

2.4.4. *Field dependence of the specific heat.* In the preceding sections we have shown that γ as well as β contain contributions from localized spin fluctuations. It is interesting to see whether an external magnetic field can

influence these contributions to the specific heat as a strong influence of the magnetic field on the magnetization of Pd-Ni alloys, even in the dilute limit, was predicted by Doniach [14]). This author argued that the large local exchange enhancement on the Ni site was strongly field dependent. Depending on the position of the Fermi level with respect to the peak in the density of states this would result in a more or less decrease of the magnetization with increasing field. The mechanism introduced by Doniach would also affect the specific heat and the resistivity. A calculation of the latter property was performed by Schulz [15]). This author extended the model by Doniach to include the dynamical behaviour of the local susceptibility and also introduced a more realistic bandstructure for Pd. His results indicated a decrease or an increase of the resistivity due to local spin fluctuations with increasing field, depending on the sign of the band parameter σ ($\sigma \simeq -\frac{1}{6}\{\frac{N''(0)}{N(0)} - \frac{3}{2}(\frac{N'(0)}{N(0)})^2\}$, N(0), N'(0) and N''(0) being the zero, first and second derivative of the density of states with respect to energy.) Schulz predicted the effect in the resistivity to be stronger than in the magnetization. These theoretical predictions have been checked in several experiments.

Measurements by Chouteau et al. [13]) showed a *non-linear behaviour of M(H)* for fields up to 80 kOe at 0.05 K. However, this field dependence was only observed for c > 0.5 at.%. From a remark by Foner [67]) it is clear that the same holds for fields up to 200 kOe at 4.2 kOe. He suggested the reported field dependences at higher concentrations (c > 0.5 at.%) to be due to impurity-impurity interactions.

The influence of a magnetic field on the resistivity caused by the scattering of the conduction electrons by the localized spin fluctuations was determined by Purwins et al. [12]) and Schindler and La Roy [11]). The first authors fitted their data (H < 50 kOe) to the model of Schulz [15]), including a small shift of the Fermi level with concentration. The free parameter of these fits is $\sigma(c)$, which turns out to have a value in reasonable agreement with the band-calculations of Andersen [37]). The main result shows a decrease of the coefficient A of the T^2 term in $\rho(T)$ with increasing field. This effect becomes more pronounced for increasing concentration. Both features can be understood semi-quantitatively by the model of Doniach and Schulz. However, it was noted that the field dependence of A occurred only for concentrations above the dilute limit ($c \simeq 0.5$ at.%). Also the field dependence of A could be fitted only for fields larger than about 10 kOe Another interesting behaviour showed up in their measurements, i.e. the common value of A reached the high field (H = 50 kOe) limit for all concentrations. Purwins et al. [12]) suggested this value

to be characteristic for the dilute limit, the extra change at lower fields and higher concentrations (c > 0.5 at.%) being due to impurity-impurity interactions. As an interesting consequence of this suggestion they proposed the possibility of suppressing ferromagnetic ordering in alloys of a concentration slightly larger than the critical one by applying a sufficiently large magnetic field. Up to now no measurements have been performed to investigate this possibility. As in the resistivity T_c is barely visible [9]) this effect could probably be observed more clearly in the specific heat or the Mössbauer effect.

The measurements by Schindler and La Roy [11]) in fields, which ranged up to 93 kOe are in good agreement with the data by Purwins et al. [12]).

Summarizing the available experimental results, we conclude that the field dependence of the magnetization and the resistivity in the dilute limit (c < 0.5 at.%) is too small to be observed. The influence reported for c > 0.5 at.% is probably due to the presence of impurity-impurity interactions.

These conclusions are consistent with our results for the field dependence of the specific heat. We did not observe any field dependence for c ≤ 1.5 at.%. Only for the two most concentrated alloys a definite change could be detected.

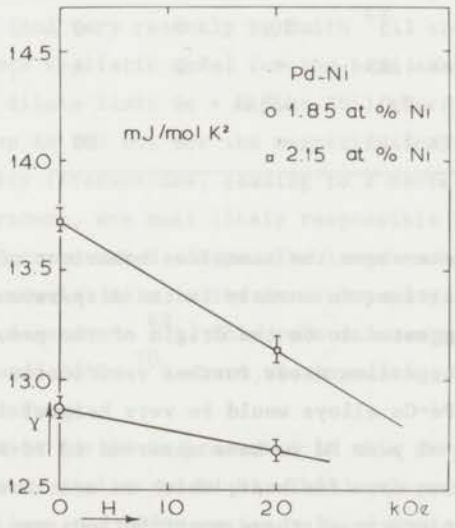

Fig. 2.24.Field dependence of the coefficient γ for the 1.85 at.% and the 2.15 at.% alloy (see table 2.5).

In fig. 2.24 we have plotted the variation of γ with the applied magnetic field. The change in γ increases with concentration as was observed for the changes in the magnetization and the resistivity. The change in β (see table 2.7) also follows this pattern and is a direct evidence for a magnetic contribution to

the T^3 term.

In table 2.9 we give the experimentally observed changes in the coefficients A (T^2 term in the resistivity), γ and β for a field of 20 kOe. The changes in the specific heat are lower than those in the resistivity. This explains why we did not observe any field dependence in the alloys with 1.0 and 1.5 at.%Ni.

TABLE 2.9

Variation of the resistivity and the specific heat with magnetic field. Changes are indicated when an external magnetic field of 20 kOe is applied.

ref.	alloy (at%)	$\Delta A/A$ (%)	$\Delta\gamma/\gamma$ (%)	$\Delta\beta/\beta$ (%)
11;12	0.2	0	-	-
12	0.50	6	0	0
11	0.54	10	-	-
12	1.0	10	0	0
12	1.5	20	0	0
this work	1.85	-	2	8
11;12	2.0	46;44	-	-
this work	2.15	-	4	20

2.5 Conclusions.

In this chapter we have shown the anomalous behaviour of Θ_{eff} of pure Pd to be a property of the lattice. An anomaly in the dispersion relation of the lattice waves in Pd is suggested to be the origin of the peculiar temperature variation of Θ_{eff}. This suggestion needs further verification. Neutron diffraction measurements on Pd-Cu alloys would be very helpful in this respect.

Contrary to the case of pure Pd we have observed in Pd-Ni alloys extra contributions to the lattice specific heat, which we attributed to local spin fluctuations. The magnetic origin of these contributions was demonstrated by measurements in a magnetic field and by comparison with a non-magnetic Pd-Cu alloy.

The determination of the critical concentration c_o, above which Pd-Ni alloys behave ferromagnetically is still controversial. The value we have deduced from the concentration dependence of the linear term in the specific heat (c_o = 2.7 ± 0.1 at.%Ni) is significantly higher than the value obtained

recently from the variation of the resistivity with concentration (c_o = 2.32 ± 0.03 at.%).

Further accurate measurements of the specific heat are needed to settle the question whether this disagreement is true or not. We do not regard the value(s) of c_o deduced from the susceptibility data sufficiently reliable to favour any value between 2.3 at.% and 2.7 at.%. Mössbauer's experiments on samples in the concentration range 1.5 - 3.5 at.% could give an independent determination of c_o. The reported value [68]) of about 1.95 at.% does not fit into the range consistent with resistivity, susceptibility and specific-heat data and therefore warrants new measurements. With experiments performed in high magnetic fields one could possibly induce an ordered state for $c \leq c_o$ as also suggested by Smith [69]).

We have noticed a large difference between the values of T_{sf} calculated from ($d\gamma/dc$) and from ($d\beta/dc$). This indicates most likely a numerical error in formula 2.42.

The magnetic field dependence of the specific heat turned out to be rather small compared with the effects observed in the resistivity. The field dependence is in general much smaller than predicted originally by Doniach. (Calculations by Schulz (and very recently by Smith [69])) showed a smaller field dependence when a more realistic model for the band shape of Pd is used). This explains why in the dilute limit (c < 0.5 at.%Ni) there is no observable field dependence (e.g. up to 200 kOe for the magnetization). At higher concentrations inter-impurity interactions, leading to a decrease of the (local) spin fluctuation temperature, are most likely responsible for the observed field-dependence in the concentrated alloys. The large exchange enhancement in the host (Pd) plays a crucial role in the inter-impurity interactions and therefore in the field dependence [69]). This role is even more prominent in alloys like Pd-Mn, Pd-Fe and Pd-Co [70]) where the impurities have much lower spin fluctuation temperatures.

From the results for Pd-Cr presented in this chapter we conclude this system to behave very similar to Pd-Ni. This analogous behaviour is of importance since we believe the Pd-Cr system to be a Kondo alloy (like Cu-Fe), as shown in ref. 46. A consequence of the similarity between Pd-Cr and Pd-Ni is the description of a Kondo system in terms of localized spin fluctuations. This will be discussed in the next chapter.

APPENDIX CHAPTER 2

Parameters of computerfits of the specific heat data to eq.2.37.

Pd-Ni 0.5 at% H=0	Pd-Ni 0.5 at% H=0	Pd-Ni 0.5 at% H=27 KG	Pd-Ni 0.5 at% H=27 KG	Pd-Ni 1 at% H=0
C(1) = 1.0289 E+01	C(1) = 1.0221 E+01	C(1) = 1.0307 E+01	C(1) = 1.0303 E+01	C(1) = 1.1052 E+01
C(2) = 9.0424 E-02	C(2) = 1.1716 E-01	C(2) = 8.9426 E-02	C(2) = 9.1506 E-02	C(2) = 8.8650 E-02
C(3) = 7.3234 E-05	C(3) = 3.6380 E-04	C(3) = 1.1951 E-04	C(3) = 1.5214 E-04	C(3) = 1.2472 E-04
C(4) = 2.8820 E-07	C(4) =-1.3197 E-06	C(4) =-3.2898 E-07	C(4) =-5.5514 E-07	C(4) =-4.0080 E-07
C(5) =-2.9977 E-09	C(5) = 1.7636 E-09	C(5) =-1.0639 E-10	C(5) = 7.2041 E-10	C(5) = 5.6602 E-10
C(6) = 5.4464 E-12	†C(6) =-1.8739 E-02	C(6) = 1.1561 E-12	†C(6) =-1.6237 E-03	C(6) =-3.0915 E-13
RMSFD = 1.7 E-03	RMSFD = 1.4 E-03	RMSFD = 1.7 E-03	RMSFD = 1.7 E-03	RMSD = 5.0 E-02

Pd-Ni 1 at% H=22.5 kOe	Pd-Ni 1 at% H=0	Pd-Ni 1 at% H=0	Pd-Ni 1 at% H=20	Pd-Ni 1 at% H=20
C(1) = 1.1030 E+01	C(1) = 1.1087 E+01	C(1) = 1.1127 E+01	C(1) = 1.1111 E+01	C(1) = 1.1111 E+01
C(2) = 8.6890 E-02	C(2) = 8.7003 E-02	C(2) = 7.3929 E-02	C(2) = 8.5324 E-02	C(2) = 8.5287 E-02
C(3) = 1.4221 E-04	C(3) = 1.1599 E-04	C(3) = 3.5861 E-05	C(3) = 1.5148 E-04	C(3) = 1.3450 E-04
C(4) =-5.3863 E-07	C(4) =-3.7153 E-07	C(4) =-9.6025 E-08	C(4) =-5.7096 E-07	C(4) =-4.2792 E-07
C(5) = 8.7382 E-10	C(5) = 5.4533 E-10	C(5) = 5.5855 E-11	C(5) = 9.1925 E-10	C(5) = 4.4937 E-10
C(6) =-5.3984 E-13	C(6) =-3.2492 E-13	†C(6) = 8.0127 E-03	C(6) =-5.1030 E-13	†C(6) = 2.8186 E-04
RMSD = 7.75 E-02	RMSD = 3.93 E-02	RMSFD = 2.0 E-03	RMSD = 4.66 E-02	RMSFD = 2.3 E-03

Pd-Ni 1.5 at% H=0	Pd-Ni 1.5 at% H=20 kOe	Pd-Ni 1.8 at% H=0	Pd-Ni 1.8 at% H=20 kOe	Pd-Ni 2.2 at% H=0
C(1) = 1.2057 E+01	C(1) = 1.2063 E+01	C(1) = 1.2866 E+01	C(1) = 1.2679 E+01	C(1) = 1.3725 E+01
C(2) = 7.5348 E-02	C(2) = 7.6463 E-02	C(2) = 7.2047 E-02	C(2) = 7.7642 E-02	C(2) = 6.6396 E-02
C(3) = 2.7510 E-04	C(3) = 2.2587 E-04	C(3) = 2.4565 E-04	C(3) = 2.0876 E-04	C(3) = 2.5333 E-04
C(4) =-1.3294 E-06	C(4) =-8.4555 E-07	C(4) =-8.5413 E-07	C(4) =-8.0290 E-07	C(4) =-7.9719 E-07
C(5) = 2.9996 E-09	C(5) = 1.3627 E-09	C(5) = 1.2512 E-09	C(5) = 1.3557 E-09	C(5) = 1.1728 E-09
C(6) =-2.6052 E-12	C(6) =-8.0019 E-13	C(6) =-6.6141 E-13	C(6) =-8.4787 E-13	C(6) =-6.2268 E-13
RMSFD = 2.2 E-03	RMSFD = 2.7 E-03	RMSFD = 3.5 E-03	RMSFD = 2.2 E-03	RMSFD = 4.3 E-03

† this is the coefficient of the $T^3 \ln T$ term.

Pd-Ni 2.2 at% H=0	Pd-Ni 2.2 at% H=20 kOe	Pd-Ni 2.2 at% H=20 kOe	Pd-Cr 0.43 at% H=0	Pd-Cr 0.88 at% H=0
C(1) = 1.3956 E+01	C(1) = 1.3145 E+01	C(1) = 1.3243 E+01	C(1) = 9.8620 E+00	C(1) = 1.0430 E+01
C(2) =-1.5418 E-02	C(2) = 8.5180 E-02	C(2) = 5.8495 E-02	C(2) = 9.6799 E-02	C(2) = 8.6699 E-02
C(3) =-2.3468 E-04	C(3) = 9.7020 E-05	C(3) =-3.5240 E-05	C(3) = 6.7832 E-05	C(3) = 1.7606 E-04
C(4) = 6.9536 E-07	C(4) =-3.8022 E-07	C(4) = 7.4864 E-09	C(4) =-2.4895 E-07	C(4) =-9.0530 E-07
C(5) =-1.0798 E-09	C(5) = 7.6877 E-10	C(5) = 1.7867 E-10	C(5) = 3.2751 E-10	C(5) = 2.0971 E-09
C(6) = 6.2525 E-13	C(6) =-5.2912 E-13	C(6) =-1.9046 E-13	C(6) =-1.5802 E-13	C(6) =-1.8214 E-12
†C(7) = 5.0426 E-02	RMSFD = 2.3 E-03	†C(7) = 1.5542 E-02	RMSFD = 2.1 E-03	RMSFD = 1.7 E-03
RMSFD = 2.2 E-03		RMSFD = 2.2 E-03		

Pd-Cr 1.5 at% H=0	Pd-Cr 1.5 at% H=21.7 kOe	Pt-Cr 0.91 at% H=0	Pt-Cr 0.91 at% H=20	Pd-Ag 1 at% H=0
C(1) = 1.14750 E+01	C(1) = 1.1479 E+01	C(1) = 7.0590 E+00	C(1) = 7.1159 E+00	C(1) = 9.1725 E+00
C(2) = 7.83953 E-02	C(2) = 7.7361 E-02	C(2) = 1.4074 E-01	C(2) = 1.3984 E-01	C(2) = 9.5452 E-02
C(3) = 1.89937 E-04	C(3) = 1.9398 E-04	C(3) = 2.8475 E-04	C(3) = 2.9013 E-04	C(3) = 6.8511 E-05
C(4) =-7.85185 E-07	C(4) =-7.4057 E-07	C(4) =-7.6618 E-07	C(4) =-7.6881 E-07	C(4) =-2.2589 E-07
C(5) = 1.41273 E-09	C(5) = 1.2495 E-09	C(5) = 8.7291 E-10	C(5) = 8.4605 E-10	C(5) = 3.0001 E-10
C(6) =-9.18339 E-13	C(6) =-7.7785 E-13	C(6) =-4.4554 E-13	C(6) =-3.9193 E-13	C(6) =-1.8990 E-13
RMSFD = 3.2 E-03	RMSFD = 2.1 E-03	RMSFD = 2.6 E-03	RMSFD = 2.2 E-03	RMSFD = 2.6 E-03

Pd-Rh 2 at% H=0	Pd-Cu 5 at% H=0
C(1) = 9.9699 E+00	C(1) = 7.9790 E+00
C(2) = 8.6423 E-02	C(2) = 9.1884 E-02
C(3) = 1.2064 E-04	C(3) = 6.6822 E-05
C(4) =-3.8764 E-07	C(4) =-2.5164 E-07
C(5) = 4.6792 E-10	C(5) = 4.4158 E-10
C(6) =-1.9940 E-13	C(6) =-2.9849 E-13
RMSFD = 3.0 E-03	RMSFD = 2.6 E-03

† this is the coefficient of the $T^3 \ln T$ term.

REFERENCES CHAPTER 2

1. Boerstoel, B.M., Zwart, J.J. and Hansen, J., Physica 54 (1971) 442.
2. Veal, B.W. and Rayne, J.A., Phys. Rev. 135 (1964) A 442.
3. Shoemake, G.E. and Rayne, J.A., Phys. Letters 26 A (1968) 222. The suggestion about a possible paramagnon contribution was communicated to these authors by Doniach.
4. Schindler, A.I., Naval Research Laboratory Report 7057, Washington, D.C., 1970.
5. Pikart, M.F., private communication.
6. Nieuwenhuys, G.J., private communication.
7. Schindler, A.I. and Mackliet, C.A., Phys. Rev. Letters 20 (1968) 15.
8. Chouteau, G., Fourneaux, R., Tournier, R. and Lederer, P., Phys. Rev. Letters 21 (1968) 1082.
9. Tari, A. and Coles, B.R., J. Phys. F: Metal Physics 1 (1971) L 69.
10. Lederer, P. and Mills, D.L., Phys. Rev. Letters 20 (1968) 1036.
11. Schindler, A.I. and La Roy, B.C., Solid State Commun. 9 (1971) 1817.
12. Purwins, H.G., Schulz, H. and Sierro, J., Int. J. Magnetism 2 (1972) 153.
13. Chouteau, G., Manhes, B. and Tournier, R., Proc. Int. Low Temp. Conf. (LT11), St. Andrews, 1968, p. 1316.
14. Doniach, S., J. Phys. Chem. Solids 29 (1968) 2169.
15. Schulz, H., Z. Physik 242 (1971) 381.
16. (C_p-C_v) for Pd was calculated using the values for β and K reported in refs. 17 and 18.
17. White, G.K. and Pawlowicz, A.T., J. Low Temp. Physics 2 (1970) 631.
18. Gschneider, K.A., in Solid State Physics series, ed. Seitz, F. and Turnbull, D. (Academic Press, New York) vol. 16 (1964) p. 275.
19. Mott, N.F. and Jones, H., "The theory of the properties of metals and alloys" (Dover Publications, New York) 1958, p. 175 vv.
20. Debye, P., Ann. Physik 39 (1912) 789.
21. Born, M. and von Kármán, T., Physik Z. 13 (1912) 297.

22a. Blackman, M., Proc. Roy. Soc. A 148 (1934) 365.

22b. Blackman, M., Proc. Roy. Soc. A 148 (1934) 384.

23. Blackman, M., Proc. Roy. Soc. A 149 (1935) 117.
24. de Launay, J., in Solid State Physics series, ed. Seitz, F. and Turnbull, D. (Academic Press, New York) vol. 2, 1956, p. 219.

25. Gopal, E.S.R., "Specific heats at low temperatures" (Heywood Books, London) 1966.
26. Beattie, J.A., J. Math. and Phys. 6 (1926/27) 1.
27. Landolt-Börnstein, physikalisch-chemische Tabellen (Springer, Berlin) ed. 6, vol. 2 (1961), part 4, p. 736 and ed. 5, Suppl. 1 (1927), p. 702.
28. van Hove, L., Phys. Rev. 89 (1953) 1189.
29. Maradudin, A.A., Montroll, E.W. and Weiss, G.H., "Theory of lattice dynamics in the harmonic approximation", Suppl. 3 to Solid State Physics series, ed. Seitz, F. and Turnbull, D. (Academic Press, New York) 1963.
30. Joshi, S.K. and Rajagopal, A.K., in Solid State Physics series, ed. Seitz, F. and Turnbull, D. (Academic Press, New York) vol 22 (1968) p. 159.
31. Gilat, G. and Dolling, G., Phys. Letters 8 (1964) 304.
32. Gilat, G. and Raubenheimer, L.J., Phys. Rev. 144 (1966) 390.
33. Einstein, A., Ann. Physik 22 (1907) 180.
34. Berg, W.T., Phys. Rev. 167 (1968) 583.
35. Martin, D.L., Phys. Rev. 141 (1966) 576.
36. Migdal, A.B., Sov. Phys. JETP 7 (1958) 996.
37. Andersen, O.K., Phys. Rev. B2 (1970) 883.
38. Fulde, P. and Luther, A., Phys. Rev. 170 (1968) 570.
39. Boerstoel, B.M., van Dissel, W.J.J. and Jacobs, M.B.M., Physica 38 (1968) 287.
40. Boerstoel, B.M., thesis Leiden, 1970.
41. Zwart, J.J., internal report, 1972.
42. Miiller,A.P. and Brockhouse, B.N., Phys. Rev. Letters 20 (1968) 798.
43. Miiller,A.P. and Brockhouse, B.N., Canad. J. Phys. 49 (1971) 704.
44. Pal, S., J. Phys. F: Metal Physics 1 (1971) 588.
45. Dutton, D.H., Brockhouse, B.N. and Miiller, A.P., Canad. J. Phys., to be published.
46. Star, W.M., de Vroede, E. and van Baarle, C., Physica 59 (1972) 128.
47. Star, W.M., Boerstoel, B.M., van Dam, J.E. and van Baarle, C., Proc. Int. Low Temp. Conf. (LT11), St. Andrews, 1968, p. 1280.
48. this analysis was performed by J.J. Zwart.
49. Saint-Paul, M., Souletie, J., Thoulouze, D. and Tissier, B., J. Low Temp. Phys. 7 (1972) 129.
50. Caroli, B., Lederer, P. and Saint-James, D., Phys. Rev. Letters 23 (1969) 700.
51. Kaiser, B. and Doniach, S., Int. J. Magnetism 1 (1970) 11.

52. Purwins, H.G., Talmor, Y., Sierro, J. and Hedgcock, F.T., Solid State Commun. 11 (1972) 361.
53. Levin, K., Bass, R. and Bennemann, K.H., Phys. Rev., B6 (1972) 1865.
54. Kim, D.J., Phys. Rev. B1 (1970) 3725.
55. Bozorth, R.M., Davis, D.D. and Wernick, J.H., J. Phys. Soc. Japan, Suppl. B-1 (1962) 112.
56. Chouteau, G., Fourneaux, R., Gobrecht, K. and Tournier, R., Phys. Rev. Letters 20 (1968) 193.
57. Crangle, J. and Scott, W.R., J. Appl. Phys. 36 (1965) 921.
58. Fawcett, E., Bucher, E., Brinkman, W.F. and Maita, J.P., Phys. Rev. Letters 21 (1968) 1183.
59. Harris, R. and Zuckermann, M.J., Phys. Rev. B5 (1972) 101.
60. Soven, P., Phys. Rev. 156 (1967) 809; Phys. Rev. 178 (1969) 1136.
61. Hodges, L., Watson, R.E. and Ehrenreich, H., Phys. Rev. B5 (1972) 3953.
62. Edwards, D.M., Mathon, J. and Wohlfarth, P., preprint.
63. Lederer, P. and Mills, D.L., Phys. Rev. 165 (1968) 837.
64. Leger, M.G. and Muir, W.B., Phys. Stat. Sol. (b) 49 (1972) 659.
65. Rayne, J.A. and Kemp, W.R.G., Phil. Mag. 1 (1956) 918.
66. this point of view was suggested by Dr. P. de Châtel (University of Amsterdam); see also Beal-Monod, M.T., Solid State Commun. 11 (1972) 683.
67. Foner, S., Proc. Int. Low Temp. Conf. (LT11), St. Andrews, 1968, discussion remark p. 1328.
68. Ferrando, W.A., Segnan, R. and Schindler, A.I., Phys. Rev. B5 (1972) 4657.
69. Smith, G.B., J. Phys. F: Metal Physics 2 (1972) L 55.
70. Boerstoel, B.M., van Dam, J.E. and Nieuwenhuys, G.J., Proc. Nato Advanced Study Institute on "Magnetism-Current Topics", La Colle sur Loup, 1970, to be published.
71. Nieuwenhuys, G.J., Boerstoel, B.M., Zwart, J.J., Dokter, H.D. and van den Berg, G.J., Physica, 62 (1972) 278.
72. Osborne, D.W., Flotow, H.F. and Schreiner, F., Rev. Sci. Instr. 38 (1967) 159.

CHAPTER 3

THE PURE Pd PROBLEM

Abstract

The temperature dependence of the susceptibility of pure Pd shows an anomalous behaviour. We discuss various suggestions which have been put forward to explain this behaviour. Recent calculations by Andersen are compared with our results. No satisfactory quantitative agreement with this calculation can be obtained. The properties of Pd-Rh and Pd-Ag alloys are reviewed in connection with the calculated electronic density of states of pure Pd. The enhancement of the electronic specific heat, evaluated from recent data, is shown to vary only slightly for for alloys up to 2 at.%Rh or Ag. Comparison between the observed variation of γ and the calculated variation of $N(E_F)$ indicates a deviation from rigid-band behaviour. It is suggested that the large enhancement of the susceptibility in Pd-Rh alloys is also due to deviations from rigid-band behaviour. Finally we compare our results with previously obtained data to discuss the differences in the absolute values of the susceptibility of different Pd samples.

3.1 Introduction.

The properties of pure Pd have been studied quite extensively during the last twenty years. We will focus our attention on the (magnetic) susceptibility in order to understand the data presented in chapter 4.

The susceptibility of pure Pd has one of the largest values among the elements. This is caused partly by the presence of a narrow band of d electrons with a high density of states at the Fermi level. In addition the electrons interact strongly, which gives rise to an exchange-enhancement of the susceptibility. As a first approximation the susceptibility of the interacting electrons can be written as follows:

$$\chi = \frac{\chi_p}{1 - N(E_F)I} \qquad (3.1)$$

where χ_p is the Pauli susceptibility of the non-interacting electrons,

$\chi_p = 2\mu_B^2 N(E_F)$; $N(E_F)$ is the electronic density of states (per spin direction) at the Fermi energy and I is a constant, accounting for the exchange interaction between the electrons. From expression 3.1 it is immediately clear that for $N(E_F)I \simeq 1$ the susceptibility can become very large. It turns out that for Pd the value of $N(E_F)I$ is about 0.9, so $\chi \simeq 10\ \chi_p$.

It also follows from eq. 3.1 that small variations in the value of $N(E_F)I$, e.g. caused by alloying or variation of the temperature, result in drastic changes of χ. An increase of about 5% in $N(E_F)I$ leads to a rise in χ of 100%! Therefore a very accurate knowledge of $N(E_F)I$ is essential for an accurate calculation of χ.

A few years ago accurate bandstructure calculations have become available [2,3]) which predict the variation of χ with temperature and magnetic field and upon alloying with the neighbouring elements Rh and Ag. We will show that a quantitative explanation of the experimental data is still not possible. This might be due to inadequate assumptions about I, which is considered to be wavevector independent and constant with changing temperature. However the influence of scattering by lattice defects, vacancies etc. can also give rise to discrepancies between theory and experiment. In alloys the use of the rigid band approximation to calculate $N(E_F)$ might not be appropriate, causing discrepancies between theory and experiment. (In the rigid band model the form of the band is assumed to be constant ("rigid"), so $N(E_F)$ for the alloy is only determined by the number of electrons per atom). Recently developed techniques to calculate $N(E_F)$ for alloys in a self-consistent way (e.g. the coherent potential approximation,CPA) might improve the situation [4]). An attempt [5]) to apply the CPA method to Pd alloys (Pd-Rh, Pd-Ni, Pd-Pt) shows some interesting results but being based on an oversimplified model of the d band is unable to make unequivocal predictions.

Apart from the large value and the strong temperature dependence, the susceptibility as a function of temperature also shows a broad maximum at about 85 K. This maximum was first observed by Hoare and Matthews [6]) and has been detected in all later investigations. To explain this phenomenon several mechanisms have been suggested. In the next sections we will present our results and discuss the various suggestions put forward to explain $\chi(T)$ for Pd. We also compare our data with some recent theoretical calculations.

3.2. Experimental results.

We have measured the susceptibility of three different pure Pd samples from 2 - 300 K with the apparatus described in chapter 1. The samples were

obtained by melting very pure (5N) material (sponge (S), or wire (W)) from Johnson Matthey in a high-frequency induction furnace using Al_2O_3 crucibles. The samples were cut from rolled melts prepared for resistivity specimens or they consisted of pieces of the wire used as resistivity sample. In table 3.1 the sample characteristics are given.

TABLE 3.1

DATA FOR PURE Pd SAMPLES

sample	KOL lab.no.	form	heat treatment (h) ; (^{o}C)	RRR	Fe content (ppm)
JM W2103	6815	chips	3 ; 1000	12†	4
JM W1774	6816	wire	7 ; 550	6†	4
JM S8750	6992	chip	11 ; 700	150†	< 1

†after W.M. Star, priv. commun.

The residual resistivity ratio (RRR = ρ(293 K)/ρ(1.2 K)) was determined of wire obtained from the same melt as the susceptibility samples. After drawing, the resistivity samples were annealed at 800 ^{o}C or 600 ^{o}C to remove strains (for a full description of the heat treatment of the resistivity samples see ref. 18).

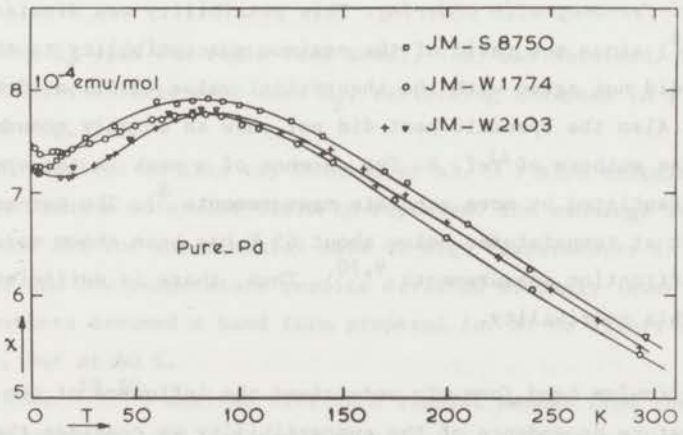

Fig. 3.1. Susceptibility vs. temperature for three different pure Pd samples. Data marked (▽) were taken on 16-5-68, while those designated (+) were obtained on 21-1-70.

The results of our measurements are shown in fig. 3.1. Smoothed values are listed in the appendix. All samples show a maximum in the $\chi(T)$ curve around 90 K. The absolute values are not equal, the differences of 5% being outside the experimental error (0.5%). These differences have been noted earlier and will be discussed in section 3.4. We also note the slight increase in χ below about 20 K. This increase is now generally attributed to the presence of small amounts of magnetic impurities (mainly Fe). It is noteworthy that for the nominally purest sample (JM S8750) no detectable increase occurs. In the next section we will consider the temperature dependence of the susceptibility of pure Pd in more detail.

3.3. Anomalous temperature dependence of the susceptibility.

In order to explain the occurrence of a maximum in $\chi(T)$ of Pd the following mechanisms responsible for this anomaly have been suggested (the first three were already proposed in the pioneering paper by Hoare and Matthews [6]).

1. antiferromagnetic ordering
2. particular band form
3. thermal expansion
4. temperature dependent I
5. Fermi-liquid properties

We will discuss each suggestion separately.

3.3.1. *anti-ferromagnetic ordering.* This possibility was dismissed by Hoare and Matthews [6] since the ratio of the maximum susceptibility to the value at T = 0 (0.95) did not agree with the theoretical value (0.67) as derived by van Vleck [7]. Also the specific heat did not show an anomaly around 85 K, as remarked by the authors of ref. 6. The absence of a peak in the specific heat has been substantiated by more accurate measurements [8]. The non-existence of magnetic order at temperatures below about 85 K has been shown more directly by neutron diffraction measurements [9,10]. Thus, there is sufficient evidence to rule out this possibility.

3.3.2. *particular band form.* To understand the influence of the band form on the temperature dependence of the susceptibility we consider the expression, valid for temperatures much below the Fermi temperature T_F [11].

$$\chi_p(T) = \chi_p(o)(1 + \frac{\pi^2}{6} \eta k^2 T^2) \qquad (3.2)$$

where $\eta = \{ (\frac{N''}{N}) - (\frac{N'}{N})^2 \}_{E_F}$; N, N' and N'' being the zero-th, first and second order derivatives with respect to energy of the density of states N, evaluated at E_F; k is the Boltzmann constant, T the temperature and $\chi_p(o)$ the Pauli susceptibility at T = 0. When N(E) varies strongly near $E = E_F$ the value of η can become large and positive. In this way the occurrence of a maximum can be qualitatively explained, if at high temperatures χ decreases with temperature (which is the case for Pd).

Before the actual density of states of Pd was calculated one *assumed* a particular band form and tried to fit the data for $\chi(T)$. In this category fall the calculations by Elcock et al. [12]), Rhodes [13]) and Shimizu et al. [14]). Rhodes and Shimizu et al. considered the existence of a small dent in the N(E) curve, just above E_F, over a range of about 0.02 eV. This extreme fine structure in N(E), which can nowadays be regarded as unphysical (see ref. 3), could be adjusted so as to reproduce the variation of χ of pure Pd with temperature.

A more realistic density of states was obtained by Shimizu et al. [14]) from the specific heat data on Pd-Rh [16]) and Pd-Ag [15,17]) alloys.

Assuming the coefficient (γ) of the electronic contribution to the specific heat to be representative of the density of states at E_F (ignoring possible spin fluctuation or phonon contributions), according to the expression (see chapter 2)

$$\gamma = \frac{2}{3} \pi^2 k^2 N(E_F) \qquad (3.3)$$

and calculating E_F with the rigid band model, N(E) was obtained. This density of states exhibits a large peak near E_F, reflecting the peak in γ at about 5 at.%Rh (see fig. 3.2).

With N(E) derived in this way Shimizu et al. [14]) also calculated $\chi(T)$, taking into account a molecular field to represent the exchange interaction. Although a good fit for experimental data at high temperatures (T > 300 K) was obtained, the low temperature results deviated strongly (even no maximum). When these authors assumed a band form proposed for Ni-Cu alloys a maximum was obtained, but at 60 K.

Doclo et al. [19,20]) derived N(E) in a similar manner from their susceptibility data using eq. 3.1 and assuming a certain value for the Stoner factor S, $S = (1 - N(E_F)I)^{-1}$, and the applicability of the rigid band model. Their result for N(E) shows a fine structure near E_F which is reminiscent of the earlier assumptions [14]). Using this N(E) Doclo et al. could reproduce $\chi(T)$ of Pd-Rh and Pd-Ag alloys, although systematic deviations of about 5%

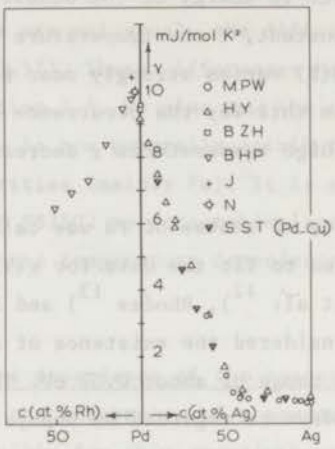

Fig. 3.2. Variation of γ with concentration for Pd-Rh and Pd-Ag alloys. Results for Pd-Cu are also shown for comparison. Data have been collected from the following references (in parentheses). MPW (68), HY (17), BZH (35), BHP (16), J (34), N (33) and SST (67).

occurred at high temperatures (T > 200 K).

Band structure calculations and the density of states.

The first band structure calculations for Pd were performed by Friedel et al. [21]) using the tight-binding approximation. Refining these calculations by taking into account spin-orbit coupling and the correct number of holes in the d band,(n_d = 0.36) as derived from de Haas-van Alphen experiments [22]), Allan et al. [23]) calculated χ(T). A maximum in χ was shown to occur due to the presence of van Hove singularities (see chapter 2) in the density of states in the neighbourhood of E_F. However, the maximum was located at 250 K instead of 85 K.

Mori [24]), using the band structure calculated by Friedel et al. [21]), also computed χ(T), but did not obtain a quantitative agreement either.

The first, and only, accurate band structure calculations were performed by Mueller et al. [2]) and by Andersen [3]). In both calculations the augmented plane wave (APW) method is used and relativistic effects are taken into account to calculate the energy levels. The density of states is however obtained differently. Mueller et al. used a refined sampling technique (see chapter 2), (1.000.000 points in k-space) to get a histogram for N(E). Andersen calculated N(E) from the volumes between constant energy surfaces around E_F in k-space. The latter method gives a more accurate description of the density of states

near E_F. It does not show any irregularities or discontinuities near E_F within say 0.02 eV. The recent calculations by Lipton and Jacobs [25]), whose results cannot be considered as accurate as those of Andersen, showed a small irregularity in N(E), right at E_F. This result can probably be considered as spurious, due to the method and accuracy of calculating N(E). Since the calculations of ref. 2 and 3 are essentially in agreement with each other we will only compare the experimental data with the calculation by Andersen.

Comparison of calculated density of states with some experimental data.

a. a temperature dependence of χ for Pd

From the N(E) vs. E curve Andersen derived values for the coefficient η in eq. 3.2 as a function of the location of the Fermi level. It turns out that η is very sensitive to the value of E_F, e.g. it can vary a factor 5 when E_F is changed by an amount corresponding to the addition of 3 at.%Rh, which change is within the accuracy of the calculation. So one can use the value of E_F within a certain range as a free parameter. As η was found to be positive, the initial rise in $\chi(T)$ with increasing temperature could be explained. The maximum in $\chi(T)$ was also obtained due to the presence of a van Hove singularity at 7 mRy ($\sim$ 0.1 eV) below E_F (corresponding to 6.6 at.%Rh).

In a recent calculation [26]) Andersen calculated $\chi(T)$ up to room temperature. His result, when E_F is chosen so as to correspond with 3 at.% in his

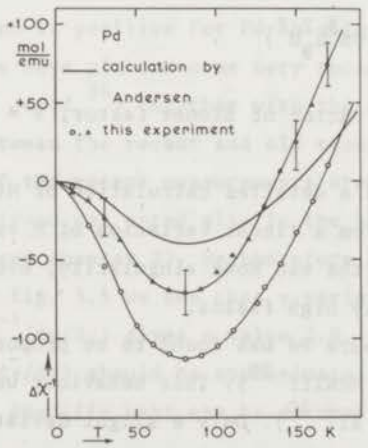

Fig. 3.3. $\Delta\chi^{-1}(\equiv \chi(T)^{-1} - \chi(o)^{-1})$ vs. temperature. The experimental points are for the JMS 8750 sample (o)(with $\chi(o) = 7.26 \times 10^{-4}$ emu/mol) and for the JMW 1774 sample (Δ) with $\chi(o) = 7.36 \times 10^{-4}$ emu/mol. For clarity the data points are connected by a smooth curve. Error bars correspond to 1% of $\chi(T)$.

original calculation, is sketched in fig.3.3 by the solid line without data points ($\Delta\chi^{-1} \equiv \chi^{-1}(T) - \chi^{-1}(o)$). For comparison we have also plotted our values of $\Delta(\chi^{-1})$ for two pure Pd samples. The value of $\chi(o)$ for the JMW 1774 sample was estimated to be 7.36×10^{-4}(emu/mol). It should be noted that the solid line connecting our experimental results is drawn smoothly through the data points and noes *not* represent the theoretical calculation by Andersen. The difference between our results will be discussed in the next section. These samples can be considered to be extreme cases, i.e. the data points for other samples will lie between the values indicated in fig. 3.3. As can be noted from this figure the calculated χ has a maximum at the correct temperature (T_{max}) but the value of χ at $T = T_{max}$ is too small, causing a large discrepancy at high temperatures. Shifting E_F can give a reasonable fit at high temperatures but in this case T_{max} is incorrect. So we conclude that the calculation can not give a satisfactory quantitative explanation of $\chi(T)$ over a large temperature range (0 - 300 K).

b. field dependence of the magnetization.

By measuring the magnetization in very high fields (> 100 kOe) one can also obtain information about the density of states near E_F. The field dependence of the susceptibility (non-linear field dependence of the magnetization) is given by an expression similar to eq. 3.2.

$$\chi(H) = \chi(o)(1 + \tfrac{1}{2}\nu S^3 \mu_B^2 H^2) \qquad (3.4)$$

where S is the enhancement factor or Stoner factor, $S = (1 - N(E_F)I)^{-1}$, and $\nu = \{ (\frac{N''}{N}) - 3(\frac{N'}{N})^2 \}_{E_F}$.

Andersen [28]) published a detailed calculation of M(H), predicting the occurrence of deviations from a linear variation of M vs. H and in some cases (Pd-Rh alloys with E_F near the van Hove singularity) even deviations which changed sign at sufficiently high fields.

The magnetization of pure Pd was found to be proportional to the field up to 150 kOe by Foner and McNiff [29]). This behaviour was also observed to about 300 kOe by Muller et al. [30]). Only a slight deviation for still higher fields (up to 350 kOe) could be detected by these authors.

For a Pd-Rh 5 at.% alloy Foner and McNiff [31]) observed a deviation from linearity in the M(H) curve. Their data, extending up to 200 kOe, indicated a decrease of the slope at increasing magnetic field.

The same type of deviation was reported by Gersdorf and Muller [32]) for a Pd-Rh 2 at.% alloy. In this case the deviation is much smaller and can be observed only above 200 kOe. No anomalous field dependence as predicted by Andersen [28]) was observed.

A reasonable fit to the magnetization data of pure Pd at "low" fields ($H < 200$ kOe) could be obtained by Andersen [26]) by shifting E_F to a value corresponding to 3 at.%Rh. With this choice of E_F also a fit to the magnetization data of the Pd-Rh 2 at.% alloy could be made for intermediate fields ($100 \text{ kOe} < H < 200 \text{ kOe}$). A serious discrepancy between the theoretical calculation [28]) and experiment [32]) is the absence of anomalies in M(H) which could be expected to arise, due to the van Hove singularity in the density of states. However, a direct comparison of N(E) calculated within a rigid-band model with experimental results for the magnetization of dilute Pd-Rh alloys is probably doomed to fail. This will be discussed in the next subsection.

c. alloy properties (Pd-Rh, Pd-Ag and Pd-Rh-Ag).

Knowing the density of states, N, as a function of energy one can calculate $\chi_p(o)$ and γ as function of concentration for Pd-Rh and Pd-Ag alloys. Assuming a rigid-band model Andersen [3]) has calculated N as a function of atomic concentration (see fig. 3.4). The variation of N around E_F is practically linear with concentration, as one can deduce from fig. 3.4. From the slope dN/dc and the value of N at $c = o$ we have calculated $N^{-1}(dN/dc)$ to be equal to 1.9. (We omit the sign, which is positive for Pd-Rh alloys and negative for Pd-Ag alloys). In fig. 3.5 we have plotted some very recent (unpublished) results by Nieuwenhuys [33]) and Junod [34]) together with the older results. There is a striking difference between the recent and old results in the case of Pd-Rh alloys. The γ values of the recent measurements are consistently higher (the β values lower). This trend was noted also in the history of γ and β values of some pure metals [35]) (see chapter 2). We therefore consider the recent data to be more reliable. From fig. 3.5 we see that γ varies almost linearly around $c = o$. Evaluation of $\gamma^{-1}(d\gamma/dc)$ gives a value 2.8.

The value of $\gamma^{-1}(d\gamma/dc)$ should be approximately equal to $N^{-1}(dN/dc)$ as the enhancement of the specific heat can be assumed to be only weakly concentration dependent.

The discrepancy between these values indicates most probably the breakdown of the rigid-band model. Andersen [26]) has also calculated values of $N^{-1}(dN/dc)$ assuming that only the density of states for the d band is changing upon

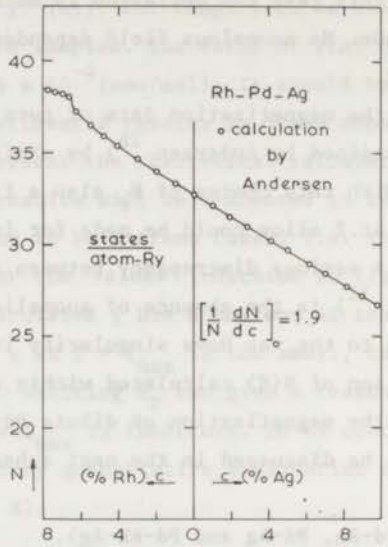

Fig. 3.4. Theoretical density of states vs concentration for Pd-Rh and Pd-Ag alloys (after ref. 3). The discontinuity for 6.6 at.%Rh corresponds to the van Hove singularity in N(E) at 0.9 mRy below E_F.

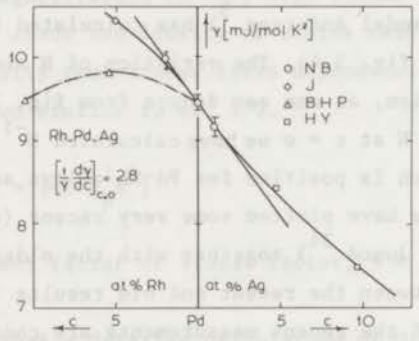

Fig. 3.5. γ vs. concentration for Pd-Rh and Pd-Ag alloys. The new results for Pd-Rh are from Nieuwenhuys (NB ref. 33) and from Junod (J, ref. 34). The other data are from ref. 16 (BHP) and ref. 17 (HY).

alloying (see fig. 3.6, upper curve). The value obtained for $N^{-1}(dN/dc)$ with this assumption is in remarkably good agreement with the value for $\gamma^{-1}(d\gamma/dc)$. From fig. 3.5 we also conclude that the maximum in $\gamma(c)$ does not occur for c = 5 at.%Rh but at higher concentration. New measurements are necessary to determine the correct concentration dependence of γ, which might be more in agreement with the variation of N, which peaks at 20%Rh according to Andersen[3]).

The concentration dependence of χ for Pd-Rh [16]) and Pd-Ag alloys [15]) is

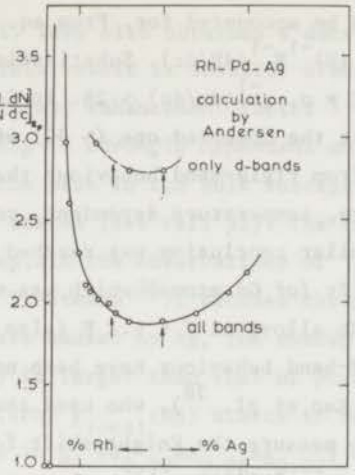

Fig. 3.6. $N^{-1}(dN/dc)$ versus concentration for Pd-Rh and Pd-Ag alloys. Arrows indicate the position of the Fermi level of pure Pd in the case of the original calculation, see ref. 3 (c = o), and for a shift of about 0.9 mRy (c = 3 at.%Rh).

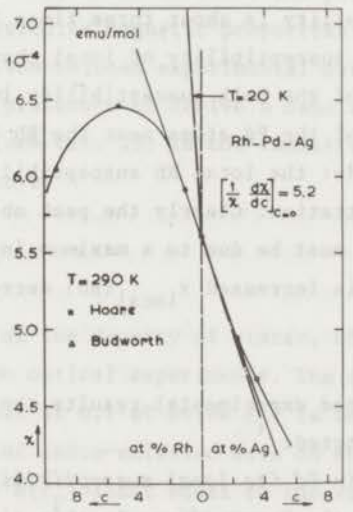

Fig. 3.7. χ versus concentration for Pd-Rh and Pd-Ag alloys at T = 290 K. The results at 20 K are normalized at the value for pure Pd at 290 K. Data were taken from ref. 15 and 16.

shown in fig. 3.7 for two temperatures, T = 20 K and T = 293 K. We see that for T = 20 K there is a discontinuous variation at c = o, while for T = 293 K the variation is almost linear. (This behaviour was already noted in ref. 36). The value of $\chi^{-1}(d\chi/dc)$ is 5.2, much larger than $N^{-1}(dN/dc)$. However, a direct comparison is not possible since $N^{-1}(dN/dc)$ was calculated for T = o. Also the

exchange enhancement has to be accounted for. From eq. 3.1 we have $\chi^{-1}(d\chi/dc) = (1 - IN)^{-1}\chi_p^{-1}(d\chi_p/dc) = (1 - IN)^{-1}N^{-1}(dN/dc)$. Substituting the value for $N^{-1}(dN/dc)$ we obtain, for T = o, $\chi^{-1}(d\chi/dc) \sim 28$. It is remarkable that for Pd-Rh this value is close to the observed one ($\sim$ 30) at T = 20 K.

Besides a deviation from rigid-band behaviour the difference between 20 K and 293 K indicates an extra, temperature dependent, contribution which is not contained in eq. 3.1. A similar conclusion was reached by Cottet and Peter [37]), while they observed a g-shift (of Gd atoms) which was not proportional to the host susceptibility of Pd-Rh alloys at T = 4.2 K (also not at room temperature). Large deviations from rigid-band behaviour have been noted in the measurement of the Knight shift of Rh. Rao et al. [38]), who used the perturbed angular correlation technique (PAC) to measure the Knight shift found a temperature dependence of the local Rh susceptibility, which they considered as an evidence for the presence of *local moments* on the Rh atoms. However, this interpretation was shown to be incorrect by NMR and nuclear relaxation time measurements reported by Narath and Weaver [39]). From the observed Knight shifts they concluded that the local Rh susceptibility is about three times larger than the local Pd susceptibility. This extra susceptibility of local character is however only 12% of the total increase of the bulk susceptibility in dilute Pd-Rh alloys, indicating a polarization of the Pd atoms near the Rh impurities. Another important observation was made: the local Rh susceptibility did not show any peak as function of concentration. Clearly the peak observed in the bulk susceptibility at about 5% Rh must be due to a maximum in the host polarization. When the Rh concentration is increased $\chi_{local}(Rh)$ decreases and for c > 40 at.% Rh, $\chi_{local}(Rh) \simeq \chi_{local}(Pd)$.

From the above described experimental results the following picture of Pd-Rh alloys can be constructed:
When an Rh atom is solved in Pd its local susceptibility is strongly enhanced, polarizing the Pd atoms in the surrounding. In this situation small changes with temperature in the local density of states at the Rh atom can explain the observed temperature dependence of the Knight shift, as suggested by Narath and Weaver [39]), and of the bulk susceptibility. The difference in $\chi(T)$ for Pd-Rh and Pd-Ag alloys as noted by Doclo et al. [20]), (T_{max} shifting rapidly to zero with increasing concentration in the case of Pd-Rh, while for Pd-Ag alloys T_{max} remains constant) can be understood also from the more or less "magnetic" character of the Rh atoms. Furthermore, the calculations by Levin et al. [5]) showed Rh in dilute Pd-Rh alloys to be near local moment formation,

analogous to dilute Pd-Ni. They also obtained a decrease for Pd-Rh alloys relative to $N(E_F)$ for Pd. This result is doubtful since it requires a strong variation of the specific-heat enhancement factor λ with concentration.
The local Rh susceptibility is strongly dependent on the surroundings. This is probably the reason for the peak in the bulk susceptibility at 5%Rh instead of a peak in the density of states (see ref. 32). The importance of the local environment might also explain the observations of "pseudo" Pd and "pseudo" Pd-Rh alloys by Hahn and Treutmann [36]. Because the positive Rh contribution is larger than the decrease caused by Ag, the susceptibility of "pseudo" Pd (e.g. $Pd_{0.98}Rh_{0.01}Ag_{0.01}$) is larger than that of pure Pd. However for larger concentrations ($c \geq 5$ at.%Rh) $\chi_{local}(Rh)$ starts to decrease, which explains why "pseudo" Pd-Rh alloys (e.g. $Pd_{0.90}Rh_{0.08}Ag_{0.02}$) show a smaller susceptibility than the corresponding Pd-Rh alloy (e.g. $Pd_{0.94}Rh_{0.06}$). To complete this picture data on "pseudo" Pd-Ag alloy would be interesting, since these would have to show a larger susceptibility than the corresponding Pd-Ag alloy. This is actually observed [36], which confirms the picture presented above.

In view of these particular magnetic properties of Pd-Rh alloys one cannot make a direct comparison between experimental data and the calculated density of states. Also the procedure to derive a density of states from the measured susceptibility (see ref. 20) is not consistent with the picture of Pd-Rh alloys described above.

d. optical properties.

A direct impression of the density of states, over a wide range of energies, can be obtained from optical experiments. The structure observed for Pd [40], especially the peak at 0.1 eV below E_F, is in general agreement with the calculated N(E). Recent photo-emission data on Rh by Pierce and Spicer [41] seem to imply a value for $N(E_F)$ about equal to the value for Pd. This is in disagreement with the calculations by Andersen [3], who obtained a lower value for Rh. (18.7 as compared to 32.7 states/atom). The value of $N(E_F)$ for Rh was recently confirmed by a bandstructure calculation of Christensen [42]. The disagreement between theory and experiment might be due to the sensitivity of the photo-emission results for certain parts in k-space (corresponding to transitions between parallel bands), which can give an incorrect impression of the density of states (see ref. 43). One set of the experiments, by Eggs and Ulmer [44], using soft X-ray spectroscopy, is in total disagreement with the calculated density of states. These experiments show a continuously decreasing

$N(E_F)$ from Rh to Pd, to Ag. The discrepancy may be due to the unique feature of these measurements, viz., that the data were taken at high temperature ($\sim$ 1000 K). Apparently the density of states near E_F is at these temperatures a continuous function of energy, the peak present at low temperatures being washed out.

As regards *alloy studies*, measurements on Pd-Ag alloys by Myers et al. [45, 46] showed a serious break down of the rigid-band model. In Ag-rich alloys the presence of virtual bound states on Pd has been clearly demonstrated. By increasing the concentration of Pd the width of these virtual bound states increases [46] and goes over into the width of the Pd band at still higher concentrations, as was demonstrated by Hüfner et al. [47].

The influence of disorder scattering introduced by alloying was pointed out by Norris and Myers [46]. This aspect will be considered in section 3.4.

To summarize the discussions of this section we conclude that even the most accurate bandstructure calculations available do not give a quantitative description of the temperature dependence of the susceptibility of Pd. The rigid-band model to calculate the properties of Pd-Rh and Pd-Ag alloys, during a long time considered as appropriate, is not valid which renders a direct comparison between alloy properties and band calculations impossible.

3.3.3. *Thermal expansion.* The thermal expansion of the lattice gives rise to a change in volume which has an effect on the density of states. This effect was found to be quite large in Pd by White and Pawlowicz [48], who suggested the volume derivative of the effective density of states $N_{eff} = N_o/(1 - N_o I)$ to be mainly due to a volume change of the exchange parameter I. This conclusion was based on the small pressure dependence of the cross sectional area of the Fermi surface [49]. We think the small pressure dependence of the Fermi surface areas is not necessarily evidence for a small change in $N_o(E_F)$. Because of the large value of $N_o(E_F)$ and the large first derivative dN_o/dE, a small change in E_F (and in Fermi-surface area) could correspond to a relatively large change in $N_o(E_F)$.

Very recently Das et al [50] have calculated the pressure dependence of the bandstructure of Pd. A change in the lattice constant (a) of 2% (corresponding to a pressure of 100 kbar) resulted in a change of $N_o(E_F)$ of 10%.

From the thermal expansion results [48] we estimate the lattice parameter to change by 0.02% from T = 0 to T = 80 K. Assuming Δa to be proportional to $\Delta N_o(E_F)$ we calculate a change in $N_o(E_F)$ of 0.1%. This corresponds to a change

in the susceptibility, between T = 0 and T = 80 K, of about 1%.

Although this effect is too small to account for the observed change in χ (5 - 10%) it is not negligible. Moreover Das et al. [50]) also predict a pressure dependence of the exchange constant I, which will add to the change in N_o since χ is determined by the product of N_o and I (see eq. 3.1). Unfortunately, so far there is no quantitative estimate of the change in I.

3.3.4. *Temperature dependent exchange constant I.* The possibility of a temperature dependent I was suggested by Eggs and Ulmer [44]) to explain the temperature dependence of the susceptibility of Pd-Rh alloys (see also ref. 36). Theoretical calculations by Edwards [51]) showed the possibility of a decrease of I with increasing temperature. Although we have discussed an explanation of the susceptibility of Pd-Rh alloys in section 3.3.2, the suggestion of a temperature dependent I cannot be disregarded. Both effects mentioned above can play a role and since no good quantitative calculations for I and I(T) exist we cannot rule out the influence on the susceptibility of a temperature dependent I. It is interesting to note that the early calculations [52]) for the mass-enhancement (λ) of the specific heat give much too large values for λ ($\lambda \sim 5$). In order to obtain a better agreement with the "experimental" value ($\lambda = 0.66$) one has to include interatomic exchange [53]) and to take the wave vector dependence of the exchange into account [54,55]). Especially the inclusion of interatomic exchange can lead to a temperature dependence via the thermal expansion of the lattice. Still the main contribution (90%) to I is of interatomic character, which is the reason why up to now the temperature dependence (and also concentration dependence) of I has been neglected in most calculations.

3.3.5. *Fermi liquid properties.* Recently an alternative explanation of the maximum in the susceptibility vs. temperature curve of Pd has been proposed by Misawa [56]). He considers the properties of a Fermi liquid and notes the occurrence of a $T^3 \ln T$ term in the specific heat as a correction to the leading term (which is proportional to T). By analogy this logarithmic term also appears in the expression for the susceptibility

$$\chi(T) = \chi(o) - aT^2 \ln(T/T_1) \qquad (3.5)$$

If $a > o$, a maximum in $\chi(T)$ is predicted at T_{max} ($T_{max} = e^{-\frac{1}{2}} T_1 \sim 0.6\ T_1$). For substances with large exchange enhancement (like He^3 and Pd) this maximum could be detected. Misawa obtained a good fit up to 100 K of the experimental

data from ref. 6 to expression 3.5 with T = 132 K. To extend the fit to higher temperatures he suggested to include a higher order term, so

$$\chi(T) = \chi(o) - aT^2\ln(T/T_1) + bT^4\ln(T/T_2) \qquad (3.6)$$

With expression 3.6 the susceptibility data for Pd could be described up to 300 K (T_1 = 132 K and T_2 = 142 K).

Recently, Jamieson and Manchester [57]) fitted their data from 20 K up to 80 K to eq. 3.5 with T_1 = 144 K. (The lowest temperature data were excluded since they are influenced by magnetic contamination, of order of a few ppm).

We have also fitted our data by computer by a least-squares procedure to eq. 3.5 and 3.6.

The results of these computer fits, i.e. the parameters $\chi(o)$, a, b, T_1 and T_2 are shown in table 3.2.

TABLE 3.2

PARAMETERS OF LEAST SQUARE FITS TO MISAWA'S THEORY

sample	$\chi(o)$ (10^{-4} emu/mol)	a (10^{-8} emu/mol K^2)	b (10^{-13} emu/mol K^4)	T_1 (K)	T_2 (K)	RMSFD (10^{-3})
a. fits to eq. 3.6 (20 - 300 K)						
JM S8750	7.29	2.42	-2.86	100	783	4.0
JM W2103	6.97	2.84	-3.55	101	746	3.8
JM W1774	7.26	2.26	-2.92	93	756	2.0
Jamieson	7.07	2.93	-3.40	102	794	5.0
Manuel	7.10	2.83	-3.36	102	774	4.2
Hoare	7.61	1.85	-2.19	94	787	3.3
b. fits to eq. 3.5 (20 - 80 K)						
JM S8750	7.25	2.66		117		4.2
JM W2103	7.01	1.77		156		1.6
JM W1774	7.31	1.44		131		1.6
Jamieson	7.12	1.87		150		2.0
Schinkel	7.09	1.91		148		

We have also included results for our fits to the data obtained by Hoare and Matthews [6]), Jamieson and Manchester [57]), Schinkel et al. [58]) and Manuel and St. Quinton [59]).

The fits are quite good as can be judged from the small values of the standard deviations (RMSFD = Root Mean Square of the Fractional Deviation). However, our fits to eq. 3.6 give values for T_1 which are systematically lower than the one obtained by Misawa (see above), while our value for T_2 is substantially higher (which causes our value for b in eq. 3.6 to be negative). Misawa fitted the normalized susceptibility χ_N($\chi_N = \chi/\chi(T = 0)$) instead of the actual susceptibility. Since the value of $\chi(T = 0)$ is uncertain (it is obtained by some extrapolation procedure) a fit to χ_N can give different results from a fit to χ. Misawa did not report the value of $\chi(T = 0)$ used in his fit, so we cannot check this procedure.

A comparison between the fit reported by Jamieson and Manchester [57]) and our fit to the same data shows a good agreement between the parameters.

Although the temperature dependence of the susceptibility of pure Pd can be described quite accurately by eq. 3.6, the significance of the fits is not clear to us. Especially the fit with five free parameters (case a) does not "prove" that the expression (3.6) is correct. The theoretical justification of (3.6) is based upon the existence of a $T^3 \ln T$ term in the specific heat of Fermi liquids. Since this term has not been detected in pure Pd (see chapter 2), the application of Misawa's theory to Pd might be doubtful. Further theoretical study is necessary to clarify this problem.

3.4. Influence of electron scattering on the susceptibility of pure Pd.

It has been noted by several authors that the absolute values of the susceptibility of different samples (i.e. from different suppliers or even different batches from the same supplier) are different. The differences are largest at low temperatures ($T \sim 20$ K) and at room temperature ($T \sim 293$ K).

Hoare and Matthews [6]) noticed a difference at 293 K of about 4% between their samples designated Pd II and Pd III. These authors attributed the difference to different strains in the samples.

Donzé [60]) reported a change in $\chi(T)$ at temperatures below 100 K when the same sample was quenched instead of annealed (at 950 °C for 75 min.); the value of χ at T = 293 K did not change. The larger concentration of vacancies in the quenched sample, as compared to the annealed sample, was suggested to be the origin of the change in χ. Unlike the effect of heat treatment the influence of cold work was found to be negligible [60]).

Hahn and Treutmann [36]) considered in detail the influence on the susceptibility of electron scattering, introduced by alloying Pd with Rh or Ag. Their calculations, based upon the theory by Jones [61]), incorporate a broadening of

the density of states, proportional to the residual resistivity of the alloy under consideration.

With a particular choice of the position of the Fermi level these authors could explain the increase in χ for pseudo-Pd. This result can only be obtained when E_F is located in a narrow energy range. Since E_F cannot be determined with this accuracy required for this problem, the calculation by Hahn and Treutmann is not conclusive. The same argument holds for the recent model calculation by Brereton [69], which is very similar to Hahn and Treutmann's calculation.

Norris and Myers [46] did observe distinctive blurring of structures in the optical spectrum of Pd-Ag alloys, indicative of the expected broadening.

Because the problem of alloys is too complicated, since E_F changes *and* electron scattering occurs, we have investigated $\chi(T)$ for three Pd samples with different residual resistivities (the residual resistivity is assumed to be a measure for the amount of electron scattering). In fig. 3.1 the susceptibility data are plotted versus temperature and the values of the residual resistivity ratio (RRR) are listed in table 3.1.

The sample with the highest RRR value (JM-S8750) has the highest value of the susceptibility (see fig. 3.1) except at low temperatures ($T < 20$ K). The sample with the lowest RRR value (JM W1774) has the lowest susceptibility above about 80 K, where χ reaches its maximum value, while at low temperatures it has the highest susceptibility. This behaviour is similar to the temperature dependence of χ for pseudo Pd (see ref. 36). Clearly there is a temperature dependent change between the different samples. Therefore we have plotted the susceptibility, normalized to its maximum value, in fig. 3.8. For comparison

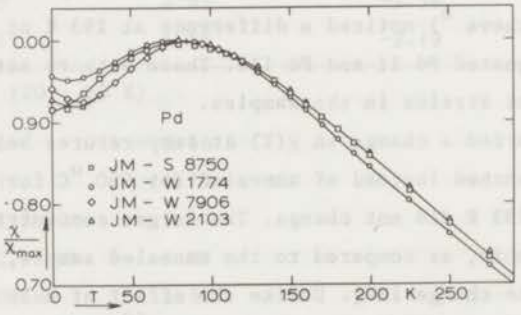

Fig. 3.8. χ/χ_{max} versus temperature for some "pure" Pd samples. The data for the JM-W7906 sample are from Schinkel et al. (ref. 58).

TABLE 3.3

COMPARISON OF THE SUSCEPTIBILITY (χ) OF PURE Pd FROM DIFFERENT SOURCES ($\chi_N(T) = \chi(T)/\chi(T_{max})$)

authors	RRR	T_{max} (K)	χ_{max} (10^{-4} emu/mol)	χ_N(20K)	χ_N(293K)	χ(20K) (10^{-4} emu/mol)	χ(293K) (10^{-4} emu/mol)
Hoare and Matthews[6]	(Pd I)	80	8.05	0.97	0.70	7.79	5.60
	(Pd III)	80	7.86	0.97	0.69	7.63	5.45
Manuel and St.Quenton[59]	(Pd IV)	85	7.90	0.92	0.71	7.30	5.61
Weiss and Kohlhaas[63]	-	80	7.67	-	0.72	-	5.56
Foner et al.[62]	∿4600 [64]	85	7.80	0.94	0.72	7.31	5.63
Donzé[60]	(quenched)	75	8.09	0.96	0.69	7.77	5.61
	(annealed)	85	7.90	0.94	0.71	7.42	5.61
Jamieson and Manchester[57]	1000	85	7.88	0.93	0.70	7.29	5.56
Schinkel et al.[58]	260	85	7.87	0.92	0.71	7.28	5.56
this work	150	80	7.92	0.92	0.71	7.44	5.60
	12 [2)]	90	7.77	0.92	0.71	7.16	5.51
	6	80	7.77	0.95	0.70	7.43	5.42
	12 [1)]	90	7.82	0.92	0.72	7.20	5.61

1) run 1 (16-5-68)

2) run 2 (21-1-70)

we also included data by Schinkel et al. [58]) on a sample with RRR = 260. (JM-W7996).

The picture of a regular increase of χ below T_{max} with increasing disorder scattering (decreasing RRR), which is apparent from the behaviour of the JM-W1774, JM-S8750 and JM-W7906 samples, is destroyed by the behaviour of the JM-W2103 sample. Although the RRR value for this latter sample is only two times larger than for the JM-W1774 sample the value of χ/χ_{max} at low temperatures is equal to the value of the JM- 7906 sample, which has an RRR value forty times that of the JM-W1774 sample.

Before drawing definite conclusions we have collected susceptibility data for pure Pd from different sources in table 3.3 and have listed also the susceptibilities at T = 20 K and T = 293 K, normalized to their maximum values.

From the data shown in table 3.3 the following picture emerges:

1. $\chi = (5.58 \pm 0.03) \times 10^{-4}$(emu/mol) for T = 293 K.

Foner's result deviates about +1.0 % from this value. Our results for the samples with low RRR value are systematically below this value: RRR 12(-1.2%), RRR 6(-3.0%). Also Hoare's data for the Pd III sample (which were confirmed in later experiments [59])) are lower (-2.5%). It is remarkable that the low value for our JM-W2103 sample (RRR = 12) apparently evolved with time since the first run did show a higher value.

2. $\chi = (7.88 \pm 0.04) \times 10^{-4}$(emu/mol) for $T = T_{max}$.

Foner's result is about 1.0% lower than this value, while our values for the "impure" samples also do not deviate very much (-1.2%). Donzé's result for the quenched sample deviates by +2.6%. The data by Hoare again deviate; Pd III (-0.3%) and Pd I (+2.1%).

3. $\chi = (7.30 \pm 0.02) \times 10^{-4}$(emu/mol) for T = 20 K.

Donzé's result for the quenched sample deviates strongly (+6.7%), while the annealed sample also shows a higher value (+1.7%). Hoare's data also deviate very much: Pd I (+7.0%), Pd III (+4.7%). Our results deviate by +2.0% (RRR 150), -2.0% (RRR 12) and +2.0% (RRR 6).

4. $\chi_N = 0.71 \pm 0.01$ for T = 293 K (see fig. 3.9).

The values of χ_N do not show a systematic variation with the RRR values. Only for the Pd III sample measured by Hoare and for the quenched sample of Donzé a definite deviation occurs.

5. $\chi_N = 0.93 \pm 0.01$ for T = 20 K (see fig. 3.9).

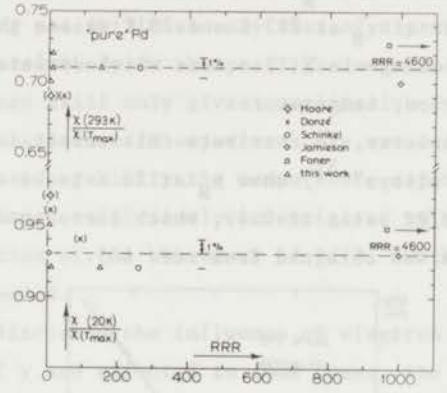

Fig. 3.9. $\chi(T)/\chi_{max}$, for T = 293 K and T = 20 K, versus the value of the residual resistivity ratio (RRR). Filled symbols ( ) are for Pd/H samples (see text). For references see table 3.3.

Again Hoare's data deviate strongly (+7.5%). Donzé's result for the quenched sample is off by +3.3%, while Manuel's data give a deviation of opposite sign (-2.2%). Our result for the sample with lowest RRR value shows a deviation of +2.2%.

Discussion.

The evaluation of the experimental data on the susceptibility of pure Pd presented above shows that in general the deviations in absolute values from the average values do not amount to more than 1%. The values of χ_N at 293 K do not show a dependence on the RRR values. The only exceptions are the data by Hoare and Donzé (quenched sample). Although the presence of magnetic impurities (reported by Manuel and St. Quinton [59]), for Hoare's samples) can influence the susceptibility around $T = T_{max}$, it cannot explain the deviation, totally. Since the RRR values of these samples is not known, a possible correlation between the observed deviations and the RRR value can not be established.

The presence of magnetic impurities becomes more influential at low temperatures as is clear in the samples by Hoare (see ref. 59) and Donzé. Manuel and St. Quinton [59]) tried to correct for the presence of the magnetic impurities (supposed to be Fe or Co atoms). However their procedure, describing the magnetization of the particles with a Brillouin-function, with high spin values, is subject to criticism [65]) and was shown to be incorrect by Doclo [19]).

Apparently too much is subtracted by this procedure (see also ref. 36). So we are left with the deviation of χ_N(20 K) observed for our sample with RRR = 6. Combining the behaviour of χ_N at 293 K and 20 K we see that in this case a real temperature dependent change in χ(T) occurs which deviates about -1.5% and +2% at high, respectively low, temperature.

It is doubtful, however, to attribute this effect to the low RRR value. Recent data for Pd-H "alloys" [57]) show χ_N at 20 K to be constant (and equal to pure Pd value) up to H/Pd ratio of 0.49, which corresponds to an RRR value of about 2 (this estimate was obtained from ref. 66).

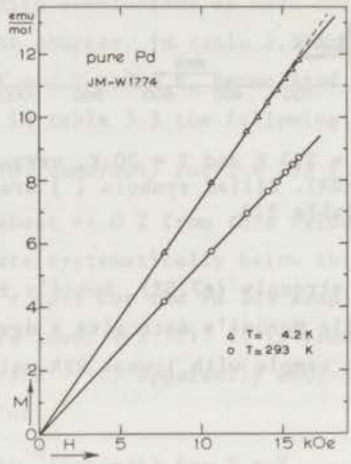

Fig. 3.10.M versus H for pure Pd-JM-W1774. Note the slight field dependence at T = 4.2 K.

Explanations in terms of (non)magnetic impurities or gases are improbable since the samples are nominally very pure. However, they could be introduced during the preparation of the samples. Actually, a slight field dependence of χ at 4.2 K can be noted, see fig. 3.10, which is absent in the other samples.

In view of the fact that the largest changes in the temperature dependence of χ of pure Pd at low temperatures result in a value of χ_N of 0.96, it is clear that electron scattering cannot explain the total disappearance of the maximum in χ(T) (corresponding to χ_N = 1.00) observed in dilute Pd-Rh and Pd-Ag alloys, which have similar RRR values as our "pure" Pd sample.

3.5. Conclusions.

It has been shown that the temperature dependence of χ for pure Pd, notably the occurrence of a maximum in χ(T) at about 85 K, cannot be accounted for quantitatively in terms of the suggestions listed in section 3.3. Since the

possibility of anti-ferromagnetic ordering can be disregarded [6,8,9,10]) the explanation must be in terms of one of the other mechanisms proposed in section 3.3. From the remaining possibilities only that of a particular bandstructure has been considered extensively in the past. The most accurate, recent calculations by Andersen [3]) can still only give a qualitative explanation (see fig. 3.3), although the deviations with experiment are not large (a few percent). The other possibilities, especially the temperature dependence of the exchange interaction I, are not yet sufficiently investigated to assess their importance for the explanation of the behaviour of $\chi(T)$. Further theoretical calculations are clearly needed.

Finally we have discussed the influence of electron scattering. Although the absolute values of χ are affected in some cases, the influence on $\chi(T)$ is very small (within 1%). The few cases for which a distinct influence on $\chi(T)$ has been found (Hoare, Donzé, our sample JM-W1774) are most probably due to magnetic impurities, which cause a too high χ at low temperatures; and to non-magnetic impurities, which cause a too low χ at room temperature.

The discrepancy which exists between the "established" γ values of Pd-Rh alloys and those obtained recently [33,34]) calls for a new investigation of this system. Optical measurements would be interesting to check the possibility of a virtual bound state on Rh in Pd [70]). These measurements could also provide the alloy parameter required in the calculations by Levin et al. [5]).

APPENDIX CHAPTER 3

MAGNETIC SUSCEPTIBILITY OF SOME PURE Pd SAMPLES

T (K)	JM S8750	JM W1774	JM 2103
0	7.26	7.44*	7.22*
10	7.28	7.40	7.16
20	7.44	7.43	7.16
30	7.58	7.49	7.26
40	7.68	7.57	7.38
50	7.78	7.66	7.52
60	7.85	7.73	7.63
70	7.89	7.76	7.71
80	7.91	7.77	7.76
90	7.90	7.76	7.77
100	7.86	7.70	7.74
110	7.81	7.64	7.68
120	7.74	7.56	7.61
130	7.65	7.46	7.53
140	7.55	7.35	7.42
150	7.43	7.23	7.30
160	7.31	7.10	7.18
170	7.19	6.96	7.05
180	7.07	6.82	6.93
190	6.94	6.69	6.80
200	6.82	6.56	6.69
225	6.48	6.24	6.37
250	6.15	5.92	6.06
275	5.83	5.62	5.74
293	5.60	5.42	5.51

*values at T = 2 K
unit of χ is 10^{-4}emu/mol (A = 106.4)

REFERENCES CHAPTER 3

1. Wolff, P.A., Phys. Rev. 120 (1960) 814.
2. Mueller, F.M., Freeman, A.J., Dimmock, J.O. and Furdyna, A.M., Phys. Rev. B1 (1970) 4617.
3. Andersen, O.K., Phys. Rev. B2 (1970) 883.
4. Soven, P., Phys. Rev. 156 (1967) 809; Phys. Rev. 178 (1969) 1136.
5. Levin, K., Bass, R. and Bennemann, K.H., Phys. Rev. B6 (1972) 1865.
6. Hoare, F.E. and Matthews, J.C., Proc. Roy. Soc. A212 (1952) 137.
7. van Vleck, J.H., J. Chem. Phys. 9 (1938) 85.
8. Crangle, J. and Smith, T.F., Phys. Rev. Letters 9 (1962) 86.
9. Abrahams, S.C., J. Phys. Chem. Solids 24 (1963) 589.
10. Cable, J.W. and Wollan, E.O., Phys. Rev. 140 (1965) A2003.
11. Mott, N.F. and Jones, H., The theory of the properties of metals and alloys. (Oxford University Press, 1936).
12. Elcock, E.W., Rhodes, P. and Teviotdale, A., Proc. Roy. Soc. A221 (1953) 53.
13. Rhodes, P., as quoted in ref. 14.
14. Shimizu, M., Takahashi, T. and Katsuki, A., J. Phys. Soc. Japan 18 (1963) 240.
15. Hoare, F.E., Matthews, J.C. and Walling, J.C., Proc. Roy. Soc. A216 (1953) 502.
16. Budworth, D.W., Hoare, F.E. and Preston, J., Proc. Roy. Soc. A257 (1960) 250.
17. Hoare, F.E. and Yates, B., Proc. Roy. Soc. A240 (1957) 42.
18. Star, W.M., de Vroede, E. and van Baarle, C., Physica 59 (1972) 128; Comm. K. Onnes Lab., Leiden No. 390 c.
19. Doclo, R., thesis, University of Gent 1968.
20. Doclo, R., Foner, S. and Narath, A., J. Appl. Phys. 40 (1969) 1206.
21. Friedel, J., Lenglart, P. and Leman, G., J. Phys. Chem. Solids 25 (1964) 781.
22. Vuillemin, J.J., Phys. Rev. 144 (1966) 396.
23. Allan, G., Leman, G. and Lenglart, P., J. de Physique 29 (1968) 885.
24. Mori, N., J. Phys. Soc. Japan 25 (1968) 72.
25. Lipton, D. and Jacobs, R.L., J. Phys. C. Metal Physics Suppl. 3 (1971) S389.

26. Andersen, O.K., private communication.
27. Wohlfarth, E.P., Phys. Letters 22 (1966) 280.
28. Andersen, O.K., J. Appl. Phys. 41 (1970) 1225.
29. Foner, S. and McNiff Jr., E.J., Phys. Rev. Letters 19 (1967) 1438.
30. Muller, F.A., Gersdorf, R. and Roeland, L.W., Phys. Letters 31A (1970) 424.
31. Foner, S. and McNiff Jr., E.J., Phys. Letters 29A (1969) 28.
32. Gersdorf, R. and Muller, F.A., (Proc. Magn. Conf. Grenoble 1970) J. de Physique 32 (1971) C1-995.
33. Nieuwenhuys, G.J., private communication.
34. Junod, A., private communication.
35. Boerstoel, B.M., Zwart, J.J. and Hansen, J., Physica 54 (1971) 442; Comm. K. Onnes Lab., Leiden No. 385 c.
36. Hahn, A. and Treutmann, W., Z. angew. Phys. 26 (1969) 129.
37. Cottet, H. and Peter, M., Solid State Commun. 8 (1970) 1601.
38. Rao, G.N., Matthias, E. and Shirley, D.A., Phys. Rev. 184 (1969) 325.
39. Narath, A. and Weaver, H.T., Phys. Rev. B3 (1971) 616.
40. Yu, A. Y-C. and Spicer, W.E., Phys. Rev. 169 (1968) 497.
41. Pierce, D.T. and Spicer, W.E., Phys. Rev. B5 (1972) 2125.
42. Christensen, private communication to P. Winsemius.
43. Janak, J.F., Eastman, D.E. and Williams, A.R., Solid State Commun. 8 (1970) 271.
44. Eggs, J. and Ulmer, K., Phys. Letters 26 A (1968) 246; Z.f.Physik 213 (1968) 293.
45. Myers, H.P., Walldén, L. and Karlsson, A., Phil. Mag. 18 (1968) 725.
46. Norris, C. and Myers, H.P., J. Phys. F: Metal Phys. 1 (1971) 62.
47. Hüfner, S., Wertheim, G.K. and Wernick, J.H., Solid State Commun. 11 (1-72) 259.
48. White, G.K. and Pawlowicz, A.T., J. Low Temp. Phys. 2 (1970) 631.
49. Vuillemin, J.J. and Bryant, H.J., Phys. Rev. Letters 23 (1969) 914.
50. Das, S.G., Koelling, D.D. and Mueller, F.M., Phys. Rev., to be published.
51. Edwards, D., Phys. Letters 20 (1966) 362.
52. Berk, N.F. and Schrieffer, J., Phys. Rev. Letters 17 (1966) 433.
53. Clogston, A.M., Phys. Rev. Letters 19 (1967) 583.
54. Schrieffer, J., Phys. Rev. Letters 19 (1967) 644.
55. Diamond, J.B., thesis U. Pennsylvania 1971 and Int. J. Magn., 2 (1972) 241.
56. Misawa, S., Phys. Letters 32A (1970) 541.

57. Jamieson, H.C. and Manchester, F.D., J. Phys. F: Metal Phys. 2 (1972) 323.
58. Schinkel, C.J., Hartog, R. and Klyn, R., unpublished results.
59. Manuel, A.J. and St. Quinton, J.M.P., Proc. Roy. Soc. A273 (1963) 412.
60. Donzé, P., thesis, University of Geneva 1968; Archives des Sciences, Genève, 22 (1969) fasc. 3.
61. Jones, H., Phys. Rev. 134 (1964) A958; Proc. Roy. Soc. A285 (1965) 461 and Proc. Roy. Soc. A294 (1966) 405.
62. Foner, S., Doclo, R. and McNiff Jr., E.J., J. Appl. Phys. 39 (1968) 551.
63. Weiss, W.D. and Kohlhaas, R., Z. angew. Physik 23 (1967) 175.
64. Hornfeldt, S., Ketterson, J.B. and Windmiller, L.R., J. Crystal Growth 5 (1969) 289.
65. Nieuwenhuys, G.J., Boerstoel, B.M., Zwart, J.J., Dokter, H.D. and van den Berg, G.J., Physica 62 (1972) 278; Comm. K. Onnes Lab., Leiden No. 395 c.
66. Fletcher, R., Ho, N.S. and Manchester, F.D., J. Phys. C. Metal Phys. Suppl. 1 (1970) S59.
67. Sato, Y., Sivertsen, J.M. and Toth, L.E., Phys. Rev. B1 (1970) 1402.
68. Montgomery, H., Pells, G.P. and Wray, E.M., Proc. Roy. Soc. A301 (1967) 261.
69. Brereton, M.G., Phil. Mag. 25 (1972) 1019.
70. the possible occurrence of a virtual bound state in dilute Pd-Rh alloys has been suggested by H.P. Myers (private communication).

CHAPTER 4

THE MAGNETIC SUSCEPTIBILITY OF Pd-Cr AND Pt-Cr ALLOYS.

Abstract.

In this chapter results of magnetic susceptibility measurements on Pd-Cr and Pt-Cr alloys are presented. From these data it is very clear that a change in the magnetic properties of the Cr atoms occurs when the concentration of these atoms is increased. In the low concentration regime ($c \leq 1$ at.%Cr) the Cr atoms can be considered as nonmagnetic, while for higher concentrations a magnetic moment develops at the Cr sites. Interaction between these moments gives rise to the maximum in the susceptibility, observed for $c > 7$ at.%Cr. Due to the complex behaviour of the Pd susceptibility an accurate quantitative determination of the impurity contribution is impossible. A qualitative explanation of the susceptibility in terms of potential scattering and local spin fluctuations is discussed. An analysis of the specific-heat data is shown to be consistent with the susceptibility results. Finally the properties of the Pd-Cr and Pd-Ni systems are computed and it is concluded that both systems can be described in terms of the local spin fluctuation model.

4.1 Introduction.

The first indications that the Pd-Cr system behaved similar to a "classic" Kondo system like Cu-Fe (e.g. minimum in the resistivity [1]), "giant" value of the thermopower [2])) motivated a detailed study of this alloy system. The first results of a combined effort to determine the resistivity, specific heat and the magnetic susceptibility were already reported [3]). Recently the detailed results for the resistivity and the thermopower of Pd-Cr and Pt-Cr alloys, including also the specific heat data, were published [4]). In this chapter we will present the results of the susceptibility measurements, which show in a direct way the weakly magnetic behaviour at low concentrations ($c < 1$ at.%Cr) and the strongly magnetic character of the Cr atoms for higher concentrations.

In order to appreciate the peculiar properties of the Pd-Cr system one has to consider the very complex behaviour revealed by most Pd-based alloys.

This complexity is related directly to the unique properties of Pd itself, especially the large exchange-enhanced susceptibility (see chapter 3).

If Mn, Fe, Co or Ni is solved in Pd the susceptibility (at room temperature) of the alloy is larger than that of pure Pd, while most other elements as solute, including Cr, bring about a smaller susceptibility. This behaviour was established in the almost exhaustive work by Gerstenberg [5]. From his observations Gerstenberg concluded that Mn, Fe, Co and Ni retain their (d) electrons, while the other elements lose their electrons (at least partly) when solved in Pd. The latter effect results in a decrease of the susceptibility caused by a decrease in $N(E_F)$ as the Pd d-band is filled by these electrons. In the case of Cr three electrons were estimated to remain localized, while the other three filled the Pd d-band causing a decrease of the susceptibility, but also a temperature dependence different from pure Pd. In this respect Cr can be considered as intermediate between e.g. Mn and Ag. (The latter is supposed to give up its s-electron to the Pd d-band.)

At low temperatures the difference between Mn, Fe, Co, Ni and Cr become more pronounced. Pd-Co and Pd-Fe alloys are ferromagnetically ordered at very low concentrations [6] featuring "giant-moments". Pd-Mn is also ferromagnetically ordered at low concentrations ($c \leq 2$ at.%) but for higher concentrations the ordering changes character and finally becomes anti-ferromagnetic [7]. Pd-Ni alloys show an enhanced Pauli paramagnetism at low concentrations ($c \leq 0.5$ at.%). When the concentration is increased the temperature dependence becomes larger, revealing the tendency to local moment behaviour. Above about 2% the Pd-Ni alloys are ferromagnetically ordered (see chapter 2) due to the presence of local moments at the Ni sites.

Qualitatively the properties of dilute Pd-Cr alloys are very similar to those of dilute Pd-Ni alloys (see chapter 2 and section 4.5). For Pd-Cr above a certain concentration (about 7 at.%) also magnetic ordering occurs. The nature of the ordering is probably anti-ferromagnetic, although ferromagnetic [8] interactions are also present, resulting in a behaviour similar to that exhibited by Cu-Mn [9].

Recently, the resistivity of Rh based alloys [10] containing Cr, Mn, Fe, Co and Ni were found to be analogous to the Pd based alloys. Similar to Pd-Cr also Rh-Cr [10,11] exhibits a resistivity minimum, the other elements showing the behaviour characteristic for Rh-Fe [12] which is similar to that of Pd-Ni [13]. The presence of magnetic ordering in Pd-Mn, Pd-Co and Pd-Fe at very low concentrations ($c \sim 0.1$ at.%) makes a comparison with Rh alloys of similar concentration impossible.

The properties of Pd-Ni have been succesfully explained in terms of local spin fluctuations (LSF) (see chapter 2). An extension of the LSF model to finite temperatures was made by Kaiser and Doniach [14]), who could fit the temperature dependence of the resistivity of Rh-Fe quite satisfactorily. These authors also pointed out [15]) that inclusion of a virtual bound state (due to potential scattering) could explain the decrease of the resistivity as observed e.g. in Al-Mn [16]). Very recently it was shown by Rivier and Zlatić [17]) that the presence of resonant potential scattering indeed results in a decreasing resistivity with increasing temperature. These authors obtained a universal curve for $\rho(T)$ as a function of T/T_{sf}, showing a T^2 behaviour for $T << T_{sf}$ and a variation as $\ln T$ for $T >> T_{sf}$. Around the inflexion point of this curve occurs a region where the resistivity is linear in T. When resonant potential scattering is accounted for, the resistivity at $T = 0$ is finite and decreases with temperature according to the universal curve, while for zero potential scattering $\rho(T = 0) = 0$ and ρ increases with temperature.

In view of these theoretical developments we will apply the concepts of LSF theory also to Pd-Cr and Pt-Cr alloys, although only qualitative comparisons are possible.

The advantage of the LSF concept is the explanation of a "non-magnetic" behaviour without using the idea of "spin-compensation". This idea has been used frequently in the past to visualize the gradual transition to the non-magnetic state which occurs below the Kondo temperature. (Taken literally this notion is incorrect since the spin polarization induced in the conduction-electron gas is an order of magnitude smaller than the local spin polarization, see e.g. ref. 18). The negative exchange coupling between the local spin and the conduction electrons required for "spin-compensation" is thought to be impossible in Pd due to its high polarizibility, hence the original difficulty in considering Pd alloys as possible Kondo alloys. The high susceptibility of Pd is certainly the reason why only Cr and Ni show non-magnetic behaviour at concentrations of about 0.5 at.%. For Pt based alloys the observation of LSF effects is probably much more likely [19]). Also the specific heat shows the presence of LSF effects according to the measurements of Costa-Ribeiro et al. [43]) However, the evidence of these measurements is less convincing.

4.2 Previous experiments.

The magnetic susceptibility of many Pd alloys, including Pd-Cr, has been measured in the temperature range from 90 to 1100 K by Gerstenberg [5]). In order to explain the differences in behaviour of the various alloys Gerstenberg

considered two mechanisms:

1. filling of the Pd band.
2. existence of local moments.

The first mechanism results in a large decrease of the susceptibility since the density of states decreases with increasing energy near the Fermi energy of pure Pd (which is near the top of the d-band). In a rigid band picture the density of states at the Fermi energy, $N(E_F)$, is a function of the electron concentration, i.e. number of electrons per atom (Z) multiplied by the atomic concentration (c). Accordingly, the susceptibility is also a function of Zc. All the alloy data, for which a decrease in the susceptibility occurs, were shown to fit a universal curve χ vs. Zc based on the results for Pd-Ag (Z = 1). The results for Pd-Cr conformed to the universal curve when the effective valency was chosen to be equal to 3. From this behaviour it was concluded that Cr apparently retains the other three outer electrons. The presence of these localized electrons gives rise to an extra temperature dependence of the susceptibility.

After we published [3]) the first low temperature susceptibility results, Nagasawa [20]) reported the susceptibility of dilute Pd-Cr and Pt-Cr alloys from liquid helium temperatures up to 300 K.

He showed that the decrease in χ at room temperature for a 0.5 at.% and a 0.8 at.% Pd-Cr alloy persisted to low temperatures. Furthermore the decrease $\Delta\chi$ ($\equiv \chi_{Pd} - \chi_{alloy}$) turned out to be proportional with the concentration for these two alloys. The temperature dependence of $-\Delta\chi$ appeared to be mainly determined by the temperature dependence of the host susceptibility, as was deduced by Nagasawa from a plot of $\Delta\chi$ vs. $\chi^2_{Pd}(T)$. A similar relation was shown to hold for a Pd-Mo (1.6 at.%) and a Pd-V (2.0 at.%) alloy, indicating the essentially non-magnetic character of the Cr atoms too.

The susceptibility of Pt-Cr was measured for alloys containing 0.5 to 3.5 at.%Cr. The alloys exhibit a larger susceptibility than that observed for pure Pt. The extra susceptibility ($\Delta\chi$) was fitted to a Curie-Weiss law, $\Delta\chi(T) \propto \mu^2/(T + \Theta)$, with $\Theta \sim 50$ K and $\mu \sim 1.2\ \mu_B$. However, large deviations occurred for $T < 50$ K.

In order to account for the decrease of χ of dilute Pd-Cr alloys Nagasawa considered a possible decrease of $N(E_F)$ (like suggested by the experiments of Gerstenberg) and a negative polarization of the Pd atoms surrounding the Cr atoms. The first possibility was ruled out since the specific heat was reported [3]) to increase upon alloying Pd with Cr. Therefore the second possibility,

theoretically proposed by Moriya [21]), seemed more likely. The precise nature of this negative polarization in relation to the presence of potential scattering remained unclear, however.

Donzé [22]) also obtained some accurate results for the susceptibility of dilute Pd-Cr alloys (0.1, 0.3, 0.5, 1.0 and 2.0 at.%) in the temperature range from 1.5 to 300 K. For low concentrations $c \leq 0.5$ at.%, $\chi(T)$ exhibits a maximum at about 85 K characteristic for pure Pd (see chapter 3), in agreement with Nagasawa's data. For higher concentrations this maximum gradually disappeared, indicating an increasing temperature dependence of $\Delta\chi$ with concentration. Donzé analyzed his results by assuming the susceptibility of Pd-Mo alloys to be equal to the "host" susceptibility of Pd-Cr alloys of equal concentration (assuming thereby Z = 6 for Cr). The "local" susceptibility of the Cr atoms $\Delta\chi(T)$ was therefore obtained by subtracting χ(Pd-Mo) from χ(Pd-Cr) at each temperature. Plotting $(\Delta\chi)^{-1}$ vs. temperature it appeared that $\Delta\chi(T)$ followed a Curie-Weiss law ($\theta \sim 200$ K, $\mu \sim 4.9\ \mu_B$) above about 100 K, while a deviation occurred below this temperature. The value for the magnetic moment is in good agreement with the measurements by Burger [23]) of Pd-Cr and Pd-H-Cr and is equal to the moment of a free Cr^{++} ion. However the large θ value indicates anti-ferromagnetic interactions. The behaviour at low temperatures, which shows a flattening off to a finite value at T = 0, was tentatively ascribed to "spin-compensation".

4.3 Experimental data.

The magnetic susceptibility measurements were performed with the apparatus described in chapter 1.

Sample preparation.

The samples consisted of small pieces (about 100 mg) cut from the same material used for the drawing of wires for the resistivity measurements by Star et al. [4]). The alloys were prepared by melting appropriate amounts of the pure metals in Al_2O_3 crucibles with an induction furnace in an Argon atmosphere. The purity of the starting materials, as quoted by Johnson Matthey, is as follows: (in brackets): Pd (JM-W2103): Si (2 ppm), Fe (4 ppm), all other elements < 4 ppm; Pd (JM-W2231): Si (7 ppm), Fe (4 ppm), all other elements < 4 ppm; Pt (JM-S3389): Si (1 ppm), all other elements < 6 ppm; Cr (JM-S4765): Si (200 ppm), Fe (200 ppm), Mo (80 ppm), Al (40 ppm), Mn (1 ppm), all other elements < 2 ppm; Mo (JM-24796): Si (20 ppm), Fe (60 ppm), Ni (20 ppm), Cr (10 ppm), all other elements < 1 ppm.

Pd (JM-W2103) was used for the preparation of the 2.0 and 4.0 at.% Pd-Cr alloys, while Pd (JM-W2331) was the solvent for all the other Pd alloys.

The data about some of the sample characteristics are collected in table 4.1.

After solidification the alloys were annealed in vacuum at 1000 °C for 24 hours and subsequently quenched in water. The Pt-Cr samples were again annealed, prior to the susceptibility measurements, for about 3 hours at 600 °C (see table 4.1).

TABLE 4.1

SAMPLE DATA

sample no.	nominal concentration	KOL	analysed concentration	heat treatment time, temp.
a. Pd-Cr alloys				
1	0.5	68102	0.29	
2	2	6820	2.02;1.8	
3	4	6821	3.49;3.42	
4	5	68105	4.61	24^h; 1000 °C
5	7	68106	6.75	
6	10	68107	7.95	
7	15	68108	13.3	
8	20	68109	16.0	
b. Pd-V				
9	1	68116	0.94	24^h; 1000 °C
c. Pd-Mo				
10	2	6915	1.97	24^h; 1000 °C
d. Pt-Cr				
11	0.5	6929	0.48	2^h; 600 °C
12	1.0	6952	0.89	3^h; 600 °C
13	0	6951	-	3^h; 650 °C

Before the susceptibility was measured the samples were carefully etched in boiling aqua regia.

The concentrations of the solute atoms have been determined by Dr. Kragten and collaborators (Natuurkundig Laboratorium, University of Amsterdam) using

an atomic-absorption spectrophotometric method. As far as the Pd-Cr alloys are concerned, it turned out that the presence of Pd atoms disturbed the determination of the Cr concentration. This necessitated the removal of the Pd atoms from the solution injected into the spectrophotometer, before a proper determination of the Cr concentration was carried out. For Pt-Cr alloys no difficulties were encountered. The accuracy of this concentration analysis is about 3%. The differences between the nominal and analysed concentrations, are large for the samples 1, 6, 7 and 8. Smaller deviations were determined for the resistivity samples (see ref. 4), which were analysed by Johnson Matthey. Using the latter concentrations our results at T = 293 K are in better agreement with the other data (see fig. 4.5).

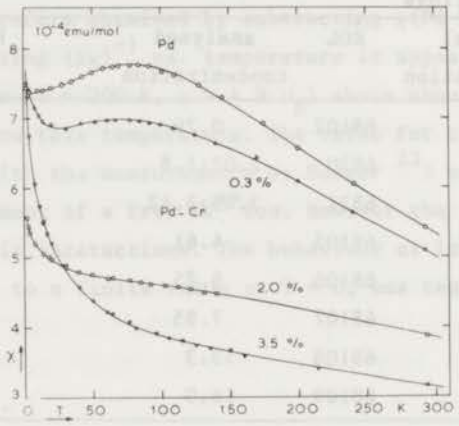

Fig. 4.1 Temperature dependence of the susceptibility of pure Pd (JM W2103) and three Pd-Cr alloys.

Susceptibility results.

The susceptibility data of the alloys we have investigated are shown in figs. 1, 2, 3 and 4 and listed in tables in the appendix.

In fig. 1 we have plotted the results for the 2 at.% and 3.5 at.% (nominal 4.0 at.%) Pd-Cr alloys published earlier [3]) (corrected for an error of about 5% in the preliminary calibration constant based on the susceptibility of Cr $K(SO_4)_2.12\ H_2O$) together with the data for the Pd-Cr 0.3 at.% alloy.

In this figure the strong decrease of the susceptibility at room temperature for the 3.5 at.% alloy is seen to be compensated at liquid helium temperatures. The change in the qualitative temperature dependence when the concentration is increased from 0.3 at.% to 3.5 at.% is also reflected in the gradual disappearance of the maximum in $\chi(T)$ around 85 K, characteristic for

pure Pd (see chapter 3). Due to the high purity of the Pd (4 ppm Fe) starting material this effect can be attributed to the influence of the Cr impurities with more certainty than in previous measurements, which showed an appreciable

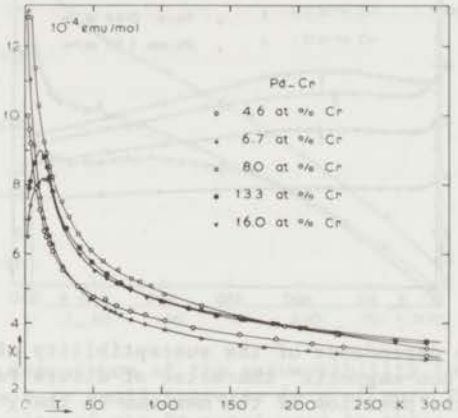

Fig. 4.2 Temperature dependence of the susceptibility of several Pd-Cr alloys.

temperature dependence at low temperatures due to magnetic contamination (mainly Fe).

Another check on the absence of large amounts of magnetic contamination in our samples is provided by the slight field dependence which occurs at low temperatures ($T \leq 4$ K). The alloys show a field dependence in the susceptibility which is nearly the same in each alloy and of comparable magnitude as observed in the pure Pd (JM W1774) sample (see fig. 3.10). Only the 0.3 at.% Pd-Cr alloy shows a somewhat larger field dependence, explaining the relatively large increase of χ at low temperatures for this alloy.

The values of χ indicated in the figures 1, 2 and 3 for $T < 4$ K are (M/H) values evaluated at 16 kOe (see however below).

In fig. 2 the temperature dependence of the higher concentrated alloys is plotted. At room temperature the susceptibility decrease starts to diminish for concentrations above about 7 at.%, in agreement with the observations of Gerstenberg (see fig. 4.5). At low temperatures χ increases steadily with increasing concentration until about 8 at.%. For the latter concentration a maximum in $\chi(T)$ occurs at about 2 K. This maximum is more evident, as it shifts to higher temperatures for the two most concentrated alloys. For these alloys, where apparently magnetic interactions between the Cr impurities take place, "low" field values (4 kOe) for the susceptibility are plotted in the

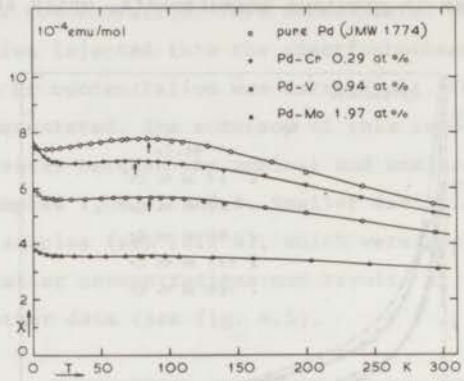

Fig. 4.3 Temperature dependence of the susceptibility of several Pd alloys and of pure Pd. The "non-magnetic" character of dilute Pd-Cr is clearly seen. The arrows indicate the position of the maximum in the χ vs. T curve.

figure.

In fig. 3 the results for pure Pd and the most dilute Pd-Cr alloy are plotted for comparison with our data for a Pd-V (0.94 at.%) and a Pd-Mo (1.97 at.%) alloy. The qualitative behaviour of dilute Pd-Cr is seen to be very similar to that shown by Pd-V or Pd-Mo. The arrows indicate the location of the maximum in $\chi(T)$, which is absent in the Pd-Mo alloy. Again, the small increase of χ at low temperatures can be explained by the presence of Fe contamination ($\sim$ 4 ppm).

In fig. 4 our data for pure Pt and two Pt-Cr alloys (0.5 at.% and 0.9 at.%) are shown. Our data for pure Pt show a slight maximum in $\chi(T)$ at 90 K confirming the results by Foner et al. [24]). The small increase of χ at low temperatures is an indication of the very low magnetic impurity content ($\sim$ 1 ppm Fe) of the sample we have investigated. The temperature dependence of the impurity contribution to the susceptibility of the Pt-Cr alloys can therefore, in principle, be established with more certainty than in the earlier investigation by Nagasawa [20]). In Nagasawa's data the alloy susceptibility for $c \leq 1$ at.%Cr is dominated below 100 K by the large and strongly temperature dependent contribution of the host, due to a large amount of magnetic contamination.

It is remarkable that the room temperature susceptibility of our 0.3 at.% alloy is smaller than that of pure Pt. The difference is small ($\sim$ 1%), so we cannot draw any firm conclusions about this behaviour, which is analogous to that observed in Pd-Cr.

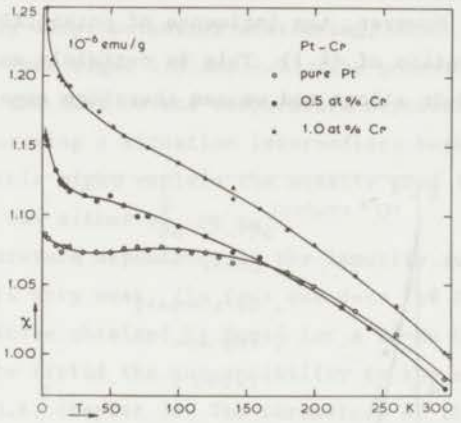

Fig. 4.4 Temperature dependence of the susceptibility for pure Pt and two Pt-Cr alloys. Note the very small increase in χ of pure Pt at low temperatures, indicating the high purity of the Pt metal used in these experiments.

4.4 Discussion.

In the introduction of this chapter we have argued that the concept of localized spin fluctuations (L.S.F.) can be applied, at least qualitatively, to the dilute Pd-Cr and Pt-Cr alloys. The theoretical calculations by Lederer and Mills [25]) (see also Lederer [26])) indicate that in the case of a local suppression of the exchange interaction of the host (e.g. in the case of Pd-Pt) the temperature dependence of the impurity susceptibility is dominated by that of the host. They found the following relation:

$$\Delta\chi(T) \propto -|\Delta U|\ \chi^2_{host}(T) \qquad (4.1)$$

where $\Delta\chi(T)$ is the impurity susceptibility and ΔU the local change in the exchange interaction of the host. This behaviour must be compared to that exhibited by an alloy where the local susceptibility is enhanced over that of the host (e.g. Pd-Ni). In the latter case the temperature dependence of the impurity susceptibility is determined by the local susceptibility:

$$\Delta\chi(T) \propto +\ |\Delta U|\ \chi_{loc}(T) \qquad (4.2)$$

Pd-Cr.

The large decrease of χ for Pd-Cr alloys suggests that in this case we can apply formula 4.1. However, the influence of potential scattering was neglected in the derivation of (4.1). This is certainly an unrealistic assumption in the case of Pd-Cr alloys and we can therefore expect deviations from formula (4.1).

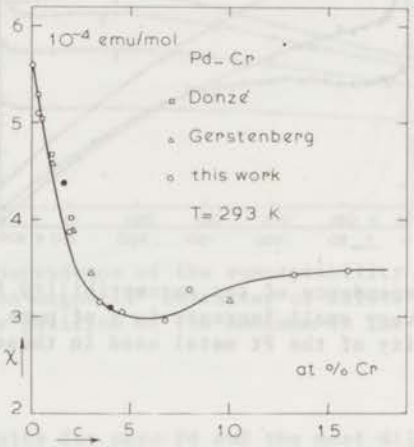

Fig. 4.5 Concentration dependence of χ (at T = 293 K) for the Pd-Cr alloys. Our data are plotted according to the analyzed concentrations (see section 4.3). Data from Donzé (ref. 22) and Gerstenberg (ref. 5) are also indicated.

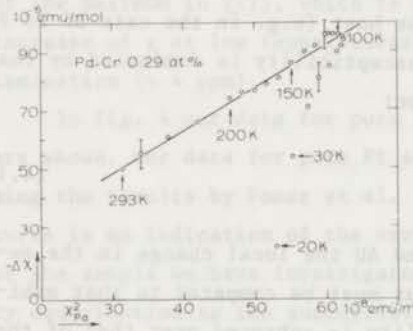

Fig. 4.6 $-\Delta\chi$ versus χ^2_{host}

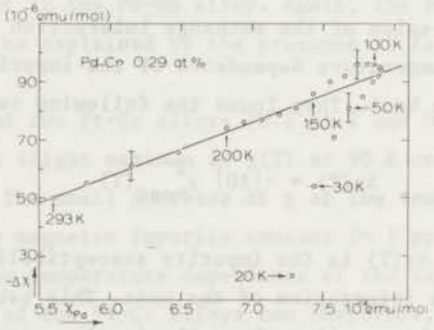

Fig. 4.7 $-\Delta\chi$ versus χ_{host}

Analysis of the temperature dependence of χ for the Pd-Cr 0.29 at.% alloy.

We have plotted $-\Delta\chi(T)$ versus $\chi^2_{Pd}(T)$ with temperature as an implicit parameter in fig. 4.6 (for the 0.3 at.% alloy $\chi_{Pd}(T)$ of Pd JM-S8750 was chosen). Up to about 100 K $\Delta\chi(T)$ varies linearly with $\chi^2_{Pd}(T)$. However, from fig. 4.7 it can be concluded that $\Delta\chi(T)$ varies linearly with $\chi_{Pd}(T)$ as well.

A similar conclusion can be drawn for the Pd-Cr 1.9 at.% alloy, comparing figs. 4.8 and 4.9. As expected above this is most probably related with the presence of relatively large potential scattering, which also occurs for the Pd-Mo and Pd-V alloy (see figs. 4.8 and 4.9). The potential scattering decreases the influence of the host on the temperature dependence of the impurity susceptibility [27]), causing a situation intermediate between that described by (4.1) and (4.2). This might explain the equally good linear fits above about 100 K of $\Delta\chi(T)$ vs. either χ^2_{Pd} or χ_{Pd}.

Still, the temperature dependence of the impurity susceptibility for the dilute Pd-Cr alloys is very weak. (In fact our data for Pd-Cr 0.3 at.% are almost identical to those obtained by Donzé for a Pd-Mo 0.3 at.% alloy)

We have therefore fitted the susceptibility to the expression given by Misawa [28]) (formula 3.6, chapter 3). The parameters of the computer fit (least-squares procedure) to this expression in the temperature range from 20 - 300 K have the following values: $\chi_o = 6.93 \times 10^{-4}$ emu/mol, $a = +3.21 \times 10^{-8}$, $T_1 = 85.9$ K, $b = +1.36 \times 10^{-13}$ and $T_2 = 63.1$ K. The value for T_1, which determines the position of the maximum in $\chi(T)$, has a similar value as calculated for pure Pd (see chapter 3), indicating the nearly non-magnetic character of the Cr atoms. (a is in emu $mol^{-1}K^{-2}$; b in emu $mol^{-1}K^{-4}$).

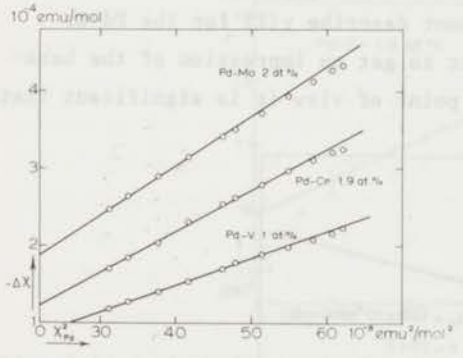

Fig. 4.8 $-\Delta\chi$ versus χ^2_{host}

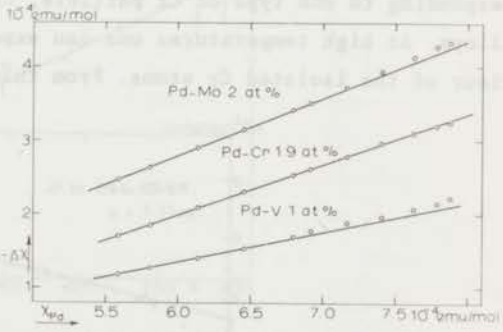

Fig. 4.9 $-\Delta\chi$ versus χ_{host}

Analysis of the temperature dependence of $\Delta\chi$ for a Pd-V, Pd-Mo and Pd-Cr alloy.

The weakly magnetic nature of the Cr impurities in dilute Pd-Cr alloys changes into a more magnetic one when the Cr-concentration is increased. This kind of behaviour has been noted in many dilute alloys (for a discussion see chapter 1) and can be considered as due to impurity-impurity interactions resulting in the increase of the local spin fluctuation lifetime (τ_{sf}) or, equivalently, the decrease of the LSF temperature T_{sf}.

In the case of the 3.45 at.% alloy and higher concentrated alloys the temperature dependence of χ has become quite large, which justifies an analysis in terms of a Curie-Weiss behaviour. We have fitted our data by computer, using a least-squares programme to the following expression:

$$\chi(T) = \chi_o + \frac{C}{T + \Theta} \qquad (4.3)$$

where χ_o is a constant susceptibility, Θ the apparent Weiss temperature and C is proportional to the concentration and the value of the magnetic moment (μ) of the Cr impurities.

In order to see whether Cr impurities with different magnetic behaviour (characterised by the value of Θ) did contribute to the susceptibility of the alloys, we performed an analysis similar to the one applied in the case of Au-V alloys (see chapter 1).

The results of the computerfits in the different temperature ranges are listed in table 4. In the case of samples for which a maximum occurred the temperature range was limited to temperatures above 20 K (7.95 at.% and 13.3 at.%) or 30 K (16.0 at.%). Comparing the values of the parameters in the high- and low-temperature range it is clear that one Curie-Weiss term, corresponding to one type of Cr particle, cannot describe $\chi(T)$ for the Pd-Cr alloys. At high temperatures one can expect to get an impression of the behaviour of the isolated Cr atoms. From this point of view it is significant that

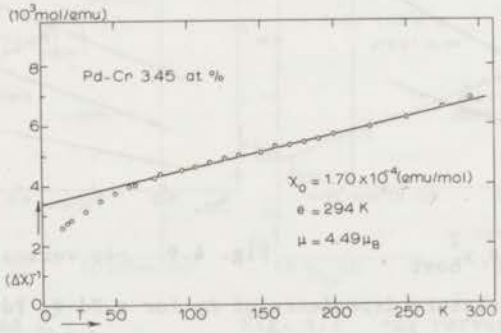

Fig. 4.10 Curie-Weiss analysis of $\Delta\chi (= \chi - \chi_o)$ for Pd-Cr 3.45 at.%.

the Θ and μ values in range c for the 3.45 at.% and 4.61 at.% alloy are close to the values obtained by Donzé [22]) for dilute alloys (c ≤ 1 at.%Cr). The results of a graphical evaluation of Θ and μ, using χ_o obtained from the computer fit in range c for the 3.45 at.% and the 4.61 at.% alloy, are shown

in figs. 4.10 and 4.11 respectively. The deviations below about 50 K indicate clearly the existence of Cr impurities with lower Θ values ("more" magnetic).

We have also analysed the susceptibility of the 1.9 at.% alloy by subtracting at each temperature the value we obtained for the Pd-Mo 2 at.% alloy. (This is the procedure used by Donzé [22]). In this way one hopes to get a fair impression of the local susceptibility ($\delta\chi$) at the Cr impurity. In fig. 4.12

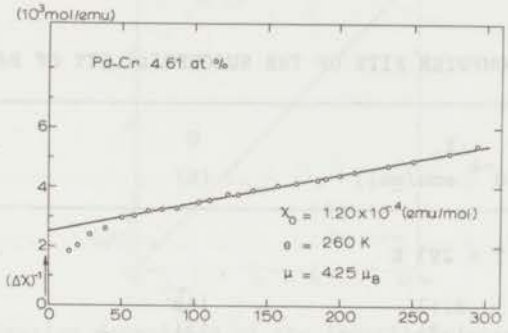

Fig. 4.11 Curie-Weiss analysis of $\Delta\chi(= \chi - \chi_o)$ for Pd-Cr 4.61 at.%.

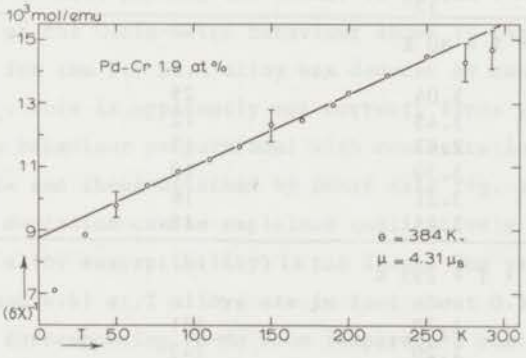

Fig. 4.12 Curie-Weiss analysis of $\delta\chi(= \chi - \chi(\text{Pd-Mo}))$ for Pd-Cr 1.9 at.%.

the result of our analysis is shown as a plot of $(\delta\chi)^{-1}$ versus T. A good description of these data can be given by a Curie-Weiss term, except for the lowest temperatures (T < 50 K). The parameters of the Curie-Weiss term are in agreement with those obtained for the two alloys discussed above.

When the value of Θ is identified with T_{sf} there is also an agreement with the value deduced for T_{sf} (or T_K, the Kondo temperature) from the resistivity [4]).

Unfortunately the Cr concentration of these alloys is too high to observe

the flattening-off of the susceptibility, predicted by L.S.F. theory for $T << T_{sf}$ (see chapter 1). This kind of behaviour has been deduced by Donzé for his dilute alloys [22]). However the low temperature data were corrected for Fe contamination, which introduces an unknown error, and are therefore not reliable.

TABLE 4.2

PARAMETER VALUES OF COMPUTER FITS OF THE SUSCEPTIBILITY OF Pd-Cr TO EQ. 4.3.

conc. (at.%)	χ_o (10^{-4} emu/mol)	θ (K)	μ (μ_B)
range a: 14 K < T < 293 K			
3.45	2.13	168	3.3
4.61	1.81	131	2.9
6.75	2.44	25	1.4
7.95	1.43	115	2.6
13.3	2.21	83	1.6
16.0	2.18	113	1.6
range b: 14 K < T < 80 K			
3.45	3.04	29	1.6
4.61	3.45	12	1.2
6.75	2.87	13	1.2
7.95	3.30	19	1.4
13.3	3.21	16	1.0
16.0	3.25	18	0.9
range c: 80 K < T < 293 K			
3.45	1.70	281	4.4
4.61	1.20	242	4.1
6.75	2.18	72	1.9
7.95	1.03	162	3.3
13.3	1.28	246	2.6
16.0	1.56	220	2.2

The values of χ_o obtained by the computerfits are much smaller than the room temperature values (the χ_o values are close to the Pd-Mo room temperature values) indicating a substantial contribution due to the magnetic character of the Cr impurities as compared with Mo impurities. A similar conclusion was drawn by Cottet [29]). The variation of χ_o with concentration is similar to that

of χ(293 K) (fig. 4.5).

The difference between $\chi(T)$ and χ_o can be considered as the local susceptibility (χ_{Cr}) of the Cr impurity, when $\chi_{Cr}(T)$ dominates the temperature dependence of the host. This can be supposed to be correct for the 3.45 at.% and the 4.61 at.% alloy.

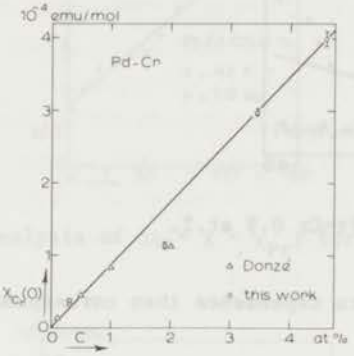

Fig. 4.13 Concentration dependence of the impurity susceptibility χ_{Cr}(at T = 0) for some Pd-Cr alloys. Data by Donzé are from ref. 22.

In fig. 4.13 we have plotted the values of χ_{Cr} at T = 0, calculated from an extrapolation of the Curie-Weiss behaviour shown in figs. 4.10 and 4.11. The value of χ_{Cr} for the 1.9 at.% alloy was deduced by considering $\delta\chi$ (see fig. 4.12) as χ_{Cr}. This is apparently not correct, since χ_{Cr} for this alloy deviates from the behaviour proportional with concentration, which is consistent with our data and those obtained by Donzé (see fig. 4.13) for lower concentrations. The deviation can be explained qualitatively by supposing χ_o ($\equiv$ Pd-Mo 2 at.% alloy susceptibility) is too large. The values of χ_o for the Pd-Cr 3.45 at.% and 4.61 at.% alloys are in fact about 0.5×10^{-4} emu/mol smaller than the corresponding Pd-Mo room temperature susceptibilities. (This difference would almost explain the deviation of χ_{Cr} for the 2 at.% alloy quantitatively).

Pt-Cr.

The Pt-Cr alloy system behaves very similar to the Pd-Cr system as was demonstrated for the resistivity and the specific heat [4]). The quantitative difference is mainly caused by the smaller value of the exchange enhancement of the susceptibility; $\sim$3.8 compared to about 10 for Pd [30]). Taking this fact into consideration we do not expect formula 4.1 to hold, which is demonstrated in fig. 4.14 for the Pt-Cr 0.9 at.% alloy. At "low" temperatures (T < 170 K)

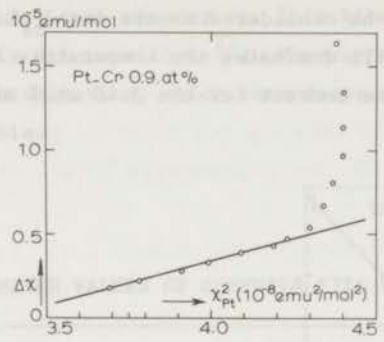

Fig. 4.14 $\Delta\chi$ vs. χ^2_{host} for Pt-Cr 0.9 at.%.

$\Delta\chi$ shows a larger temperature dependence than corresponds with the $\chi(T)$ of pure Pt.

For comparison with the analysis by Nagasawa [20]) the temperature dependence of the impurity susceptibility ($\Delta\chi = \chi_{alloy} - \chi_{Pt}$) is shown in figs. 4.15 and 4.17 for the 0.48 at.% and the 0.89 at.% alloy. For the 0.48 at.% alloy $\Delta\chi$ is negative at room temperature but positive at liquid helium temperatures, therefore $(\Delta\chi)^{-1}$ becomes very large around 100 K. So, only below about 100 K we can look for a Curie-Weiss behaviour. From fig. 4.15 it is clear that a description of $\Delta\chi$ by a Curie-Weiss term is rather uncertain. The parameters representing the solid line are similar to those derived by Nagasawa [20]). The temperature dependence of $\Delta\chi$ for the 0.89 at.% alloy cannot be described by a Curie-Weiss term over a wide temperature range either. Although the presence of magnetically different Cr atoms can qualitatively explain this behaviour, the identification of $\Delta\chi$ as χ_{Cr} is most probably incorrect. As in the case of Pd-Cr we believe $\delta\chi$ (being χ(Pt-Cr) - χ(Pt-Mo)), to be a better approximation for χ_{Cr} in Pt-Cr alloys.

Recently, Inoue and Nagasawa [31]) reported some results for χ(Pt-Mo 2.4 at.%). Assuming the decrease in χ at T = 293 K of pure Pt upon alloying with Mo to be proportional with concentration ($d\chi/dc = -0.20 \times 10^{-4}$ emu/mol-at.%Mo) we have evaluated for our Pt-Cr alloys $\delta\chi$, taking for χ(Pt-Mo) the susceptibility for pure Pt minus a constant, equal to $(d\chi/dc)_{Pt-Mo}$ multiplied by the Cr concentration.

The temperature dependence of $\delta\chi$ is shown in figs. 4.16 and 4.18. The fit to a Curie-Weiss term is considerably improved, although still not adequate. (The deviation observed in fig. 4.16 at temperatures below about 50 K are due

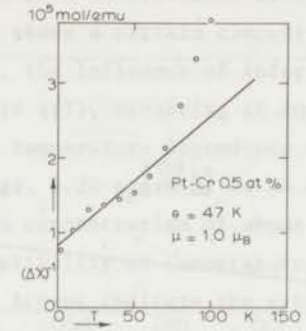

Fig. 4.15 Curie-Weiss analysis of $\Delta\chi (= \chi - \chi_{Pt})$ for Pt-Cr 0.5 at.%.

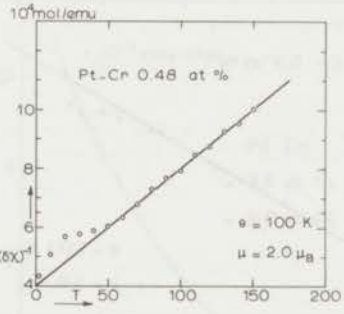

Fig. 4.16 Curie-Weiss analysis of $\delta\chi$ (see text) for Pt-Cr 0.5 at.%.

to the temperature dependence in pure Pt; since $\delta\chi$ is very small this has a large influence on $(\delta\chi)^{-1}$).

The parameters of the Curie-Weiss relation between $\delta\chi$ and T deduced from figs. 4.16 and 4.18 are also more in agreement with those of Pd-Cr than those obtained from $(\Delta\chi)^{-1}$ vs. T (figs. 4.15 and 4.17).

In fig. 4.19 we have collected the values of $\Delta\chi(o)$ as obtained from our results (figs. 4.15 and 4.17) and those of Nagasawa (fig. 12, ref. 20) and Inoue and Nagasawa (fig. 3, ref. 31). Taking into account the inaccuracy of these results, $\Delta\chi(o)$ is proportional to concentration up to 3.5 at.%Cr.

We have also plotted $\delta\chi(o)$ for our alloys. It is seen from fig. 4.19 that $\delta\chi(o)$ is consistently higher than $\Delta\chi(o)$. The dashed line in fig. 4.19 corresponds to a variation of $\delta\chi(o)$ proportional with concentration.

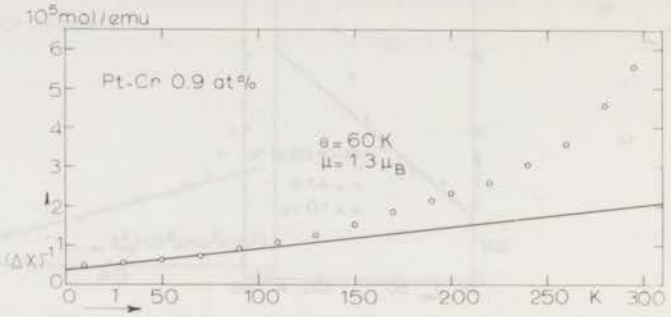

Fig. 4.17 Curie-Weiss analysis of $\Delta\chi(= \chi - \chi_{Pt})$ for Pt-Cr 0.9 at.%.

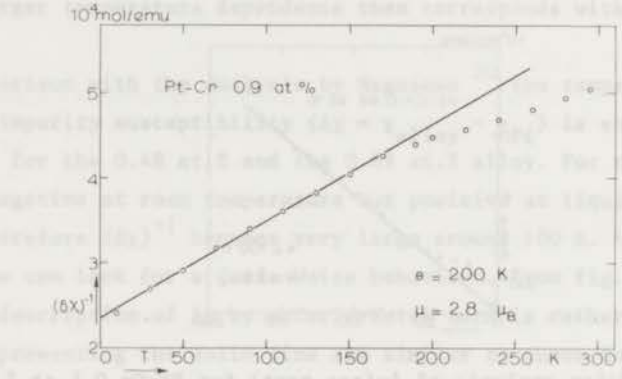

Fig. 4.18 Curie-Weiss analysis of $\delta\chi$(see text) for Pt-Cr 0.9 at.%.

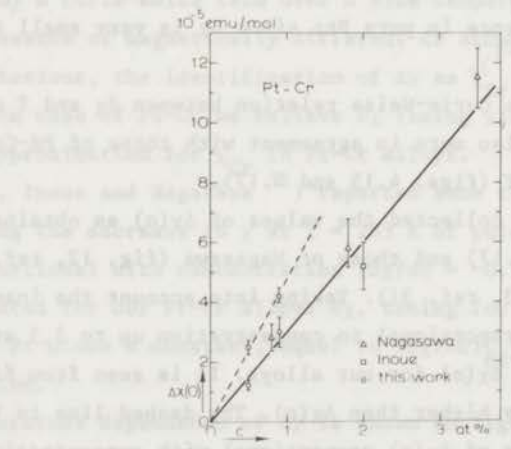

Fig. 4.19 Concentration dependence of $\Delta\chi$(at T = 0) for some Pt-Cr alloys. Data by Nagasawa are deduced from ref. 20, by Inoue from ref. 31. The crosses indicate the values of $\delta\chi$(see text).

Magnetic interactions between the Cr impurities in Pd-Cr alloys.

We also investigated more concentrated alloys in order to see whether magnetic ordering occurs above a certain concentration. As was remarked in the beginning of section 4.3, the influence of inter-impurity interactions was evident from the maxima in $\chi(T)$, occurring at low temperatures for the most concentrated alloys. The temperature dependence of χ at low temperatures (< 18 K) is shown in figs. 4.20 and 4.21 on an expanded scale. The appearance of a maximum in $\chi(T)$ at a concentration of about 8 at.% is very clear from these figures. The susceptibility at temperatures near T_{max} is field dependent as noted in section 4.3. Arrows indicate the estimated position of the maximum in the $\chi(T)$ vs. T curves. The values of T_{max} are plotted as a function of concentration in fig. 4.22. Extrapolation of T_{max} versus c to $T_{max} = 0$ gives a "critical" concentration c_o of about 7 at.%Cr. It is significant that the

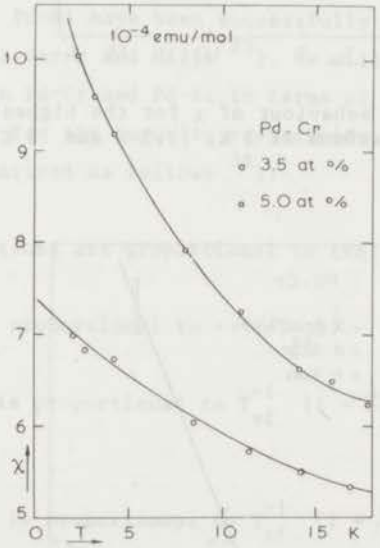

Fig. 4.20 Low temperature behaviour of χ for two Pd-Cr alloys of intermediate concentration.

temperature dependence of the resistivity does change its character also at about 7 at.%. For $c < 7$ at.% large minima in $\rho(T)$ are observed, while for 10 at.% a maximum occurs at about 25 K. For still higher concentrations $\rho(T)$ shows only a change in slope but increases monotonously with temperature. This behaviour is qualitatively the same as observed in e.g. Cu-Mn [9]) and Au-Fe [32]) and was attributed to inter-impurity interactions. The temperature

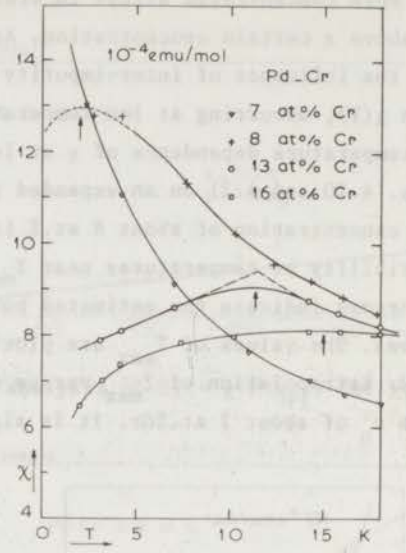

Fig. 4.21 Low temperature behaviour of χ for the highest concentrated Pd-Cr alloys, which exhibit a maximum at 2 K, 11.5 K and 15 K respectively, as indicated by the arrows.

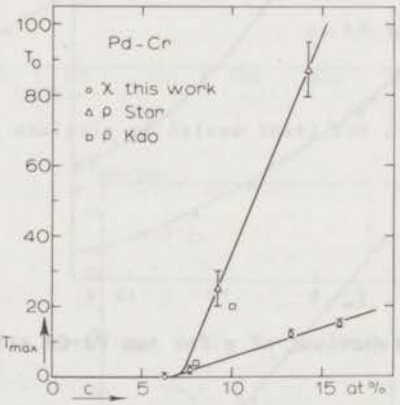

Fig. 4.22 Concentration dependence of T_{max} (deduced from our susceptibility data) and T_o (deduced from the resistivity results by Star et al.[4]) and Kao and Williams [33]) for Pd-Cr alloys. The critical concentration is about 7 at.%.

of the maximum in $\rho(T)$ or the change in slope can be considered as the "ordering" temperature T_o. This temperature has also been plotted in fig. 4.22 as obtained from data by Star et al. [4]) and Kao and Williams [33]). It is

interesting to see that these temperatures also extrapolate to zero at about 7 at.%, although they are much larger than T_{max} deduced from χ_{max}. This difference between T_o and T_{max} has been noted before in many alloy systems e.g. Au-Fe [32]), Rh-Co [34]). The full explanation of these "ordering" effects, i.e. the nature of the magnetic ordering, which is a complex mixture of anti-ferromagnetic and ferromagnetic interactions, has yet to be given. Recently this problem has even received a generic name: "mictomagnetism" [35]) or "spin-glass" [36]), indicating the renewed interest in the properties of these alloys.

An important difference between Pd-Cr and e.g. Au-Fe is the large value of the critical concentration. This is clearly related to the non-magnetic character of most of the Cr atoms below c_o. In this respect Pd-Cr has to be compared with Rh-Fe [37]) and Pd-Ni [39]).

Comparison between Pd-Cr and Pd-Ni.

Many properties of Pd-Ni have been successfully explained by the LSF theory as developed by Lederer and Mills [25]). We will compare in this section the similarities between Pd-Cr and Pd-Ni in terms of this theory. The predictions of the LSF theory for the impurity resistivity, specific heat and susceptibility can be summarized as follows [38]):

1. All extra contributions are proportional to the impurity concentration.

2. The resistivity is proportional to $+ (T/T_{sf})^2$.

3. The specific heat is proportional to $T_{sf}^{-1} \{1 - \frac{4\pi^2}{5} (\frac{T}{T_{sf}})^2\}$, for $T << T_{sf}$

4. The susceptibility is proportional to $T_{sf}^{-1} \{1 - \frac{\pi^2}{3} (\frac{T}{T_{sf}})^2\}$, for $T << T_{sf}$

The above predictions have been verified for dilute ($c \leq 0.5$ at.%) Pd-Ni alloys (see ref. 39 and chapter 2).

For Pd-Cr and Pt-Cr alloys the *resistivity* [4]) satisfies the LSF prediction also, if one takes account of the potential scattering, which causes $\rho(T)$ to decrease monotonously with temperature. Also the *specific heat* can be explained by the LSF theory (see ref. 4). We have made a computer analysis of the specific-heat data of Pd-Cr alloys (see appendix chapter 2) and found a change in the T^3 term comparable to that observed for Pd-Ni. Contrary to the case of

Au-V (chapter 1) this analysis provides a variation of $\Delta\gamma$ stronger than proportional with concentration (see fig. 4.23), confirming the earlier conclusions [4]). Also shown in fig. 4.23 are the values of $\Delta\gamma$, corrected for the change in $N(E_F)$, due to alloying ($\gamma - \gamma^1$). The values of γ^1 were obtained from data by Heiniger [40]) on a Pd-1.0 at.%Mo alloy. ($d\gamma/dc = -1.0$ mJ/mol K^2-at.%Mo). The change in $d\gamma/dc$ of Pd-Cr alloys due to this correction is about 100%.

The *susceptibility* is difficult to evaluate since the value of the host susceptibility is uncertain. We have used two approximations for the host susceptibility in the foregoing to obtain χ:

1. χ_o, as derived from the computerfits.
2. χ(Pd-Mo) or χ(Pt-Mo).

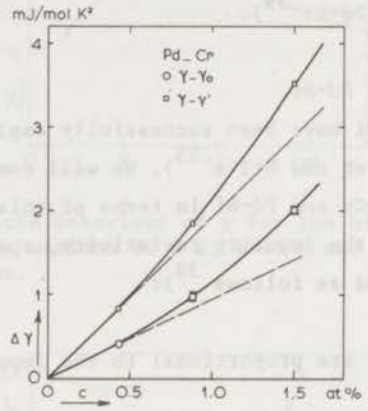

Fig. 4.23 Concentration dependence of γ, obtained from our computerfits of the specific heat data by Boerstoel (see ref. 4). The value of γ_o is of pure Pd (see ref. 42); γ^1 refers to the value of Pd-Mo (see text).

Our results combined with those of Donzé give $\Delta\chi \propto c$ up to about 5 at.% for Pd-Cr and $\Delta\chi \propto c$ up to about 3 at.% for Pt-Cr. The temperature dependence of $\Delta\chi$(or $\delta\chi$) for $T << T_{sf}$ is not in agreement with LSF predictions. This is certainly due to the presence of strongly magnetic Cr impurities (also the Fe contamination plays a role) in the higher concentrated ($\sim$ 5 at.%) alloys. It is remarkable that Donzé [22]) obtained a temperature dependence which is qualitatively in agreement with the LSF theory, although his method of analysis is subject to criticism. At higher temperatures, $T \sim T_{sf}$, the susceptibility can be described by a Curie-Weiss relation. The Θ values, when identified with T_{sf}, are in agreement with those deduced from resistivity [4]) and specific heat (see table 4.3). From the Curie-Weiss behaviour it is clear that there is an important local contribution (the χ_o values also indicate this). The

TABLE 4.3

Summary of LSF effects in specific heat and susceptibility

alloy	$d\chi/dc$ (10^{-3}emu/mol)	$T_{sf}^{\dagger}$ (K)	$\chi^{-1}\frac{d\chi}{dc}$	$d\gamma/dc$ (mJ/molK^2)	T_{sf}^{*} (K)	$\gamma^{-1}\frac{d\gamma}{dc}$	$\xi^{\P}$	$\beta^{-1}\frac{d\beta}{dc}$
Pd-Ni	65	20	87	150	170	16	0.2	-12
Pd-Cr	8.5	150	12	95	800	10	0.8	-12
				193	400	20	0.8	
Pt-Cr	3.0	400	15	57	500	9	0.6	- 4.5
	$4.7^{\dagger}_{\dagger}$	250	24				0.4	
Au-V	3.7	330	-	68	370	100	0.3	- 4

† obtained from $T_{sf} \simeq \frac{10}{8}\left(\frac{d\chi}{dc}\right)^{-1}$; * obtained from $T_{sf} \simeq (5) \times 25 \times 10^{3}\left(\frac{d\gamma}{dc}\right)^{-1}$

¶ $\xi = N_{\gamma}(E_F)/N_{\chi}(E_F) = \gamma^{-1}(d\gamma/dc)/\chi^{-1}(d\chi/dc)$; $^{\dagger}_{\dagger}$ from $\delta\chi/dc$

§ for the derivation of T_{sf} from $(d\chi/dc)$ or $(d\gamma/dc)$ see ref. 38.

decrease of the bulk susceptibility of Pd-Cr alloys at room temperature (see fig. 4.5) is therefore caused by potential scattering, which gives rise to a strong decrease of the local density of states on the surrounding Pd atoms. This latter effect has been noted in NMR measurements on Pd-V [27] (also for Pt-Cr [31]) and Pt-Mo [41])), which probed the local susceptibility around the impurities. This strong deviation from rigid-band behaviour can also be expected in Pd-Cr, since the charge difference between host and impurity is large. With this microscopic model one can understand, at least qualitatively, the paradox noted by Nagasawa [20]): the increase of γ and the decrease of χ when Pd is alloyed with Cr. The decrease in $N(E_F)$ of the Pd atoms surrounding Cr results in a decrease of γ. Apparently the contribution due to LSF at Cr is larger than this decrease, so the total change is positive. For the susceptibility the decrease in $N(E_F)$ will cause a substantial decrease in χ, due to the large exchange enhancement (see chapter 3) of the pure Pd. Apparently this decrease cannot be compensated (at room temperature) by the local contribution of the Cr impurities. When the concentration of Cr is increased the decrease in $N(E_F)$ will saturate, while the local contribution of each Cr atom

increases. These two effects cause the bulk susceptibility to increase again as is observed for $c \geq 7$ at.%. It is perhaps not coincidental that this concentration is equal to the "critical" concentration for the occurrence of a maximum in $\chi(T)$.

From table 4.3 we draw the conclusion that the Pd-Cr and Pd-Ni alloys are also quantitatively very similar, as far as the specific heat is concerned. The quantitative difference in the susceptibility indicates a stronger magnetic character for the Ni atoms, resulting in a smaller value for the critical concentration c_o.

APPENDIX CHAPTER 4

MAGNETIC SUSCEPTIBILITY OF SOME Pd-Cr ALLOYS. *

	concentration (at.%Cr)							
T	0.29	1.90	3.45	4.61	6.75	7.95	13.3	16.0
	106.1	105.3	104.5	103.9	102.9	102.0	99.3	97.7
2	7.53	5.58	7.52	10.00	13.40	12.8	7.69	6.45
10	7.05	5.14	5.83	7.40	8.00	10.3	8.95	8.00
20	6.90	4.98	5.21	6.08	6.30	8.23	7.80	7.78
30	6.87	4.86	4.82	5.44	5.50	7.20	6.75	6.49
40	6.89	4.80	4.58	5.06	5.06	6.55	6.17	6.00
50	6.93	4.75	4.37	4.80	4.66	6.03	5.75	5.58
60	6.95	4.71	4.23	4.60	4.41	5.71	5.44	5.32
70	6.97	4.68	4.10	4.45	4.24	5.45	5.16	5.11
80	6.97	4.66	4.01	4.33	4.07	5.24	4.95	4.94
90	6.95	4.63	3.94	4.21	3.95	5.07	4.78	4.79
100	6.90	4.60	3.86	4.10	3.86	4.91	4.65	4.67
110	6.85	4.58	3.82	4.01	3.75	4.76	4.54	4.56
120	6.78	4.55	3.78	3.94	3.65	4.63	4.44	4.46
130	6.73	4.52	3.73	3.85	3.57	4.51	4.34	4.38
140	6.65	4.48	3.69	3.77	3.52	4.39	4.25	4.30
150	6.57	4.44	3.65	3.73	3.45	4.28	4.17	4.23
160	6.50	4.41	3.61	3.67	3.39	4.18	4.10	4.16
170	6.40	4.38	3.57	3.62	3.35	4.10	4.03	4.09
180	6.30	4.34	3.54	3.56	3.30	4.02	3.97	4.02
190	6.18	4.30	3.50	3.53	3.26	3.92	3.92	3.96
200	6.08	4.26	3.46	3.47	3.22	3.85	3.86	3.92
225	5.82	4.15	3.38	3.35	3.13	3.70	3.73	3.78
250	5.54	4.05	3.30	3.25	3.06	3.56	3.60	3.67
275	5.28	3.96	3.21	3.14	2.99	3.38	3.50	3.56
293	5.10	3.88	3.16	3.07	2.96	3.27	3.43	3.49

* smoothed values obtained from fig. 4.1 and 4.2; unit 10^{-4} emu/mol

the atomic weights are also indicated above each column.

APPENDIX CHAPTER 4

MAGNETIC SUSCEPTIBILITY OF Pt, Pt-Cr ALLOYS, Pd-Mo AND Pd-V.*

T	Pt		Pt-0.48 Cr		Pt-0.89 Cr		Pd-1.97 at.%Mo	Pd-0.94 at.%V
	A=195.1		A=194.4		A=193.8		A=106.2	A=105.8
	χ_m	χ_A	χ_m	χ_A	χ_m	χ_A	χ_A	χ_A
2	1.086	2.119	1.157	2.249	1.250	2.422	3.80	5.95
10	1.079	2.105	1.132	2.201	1.207	2.339	3.62	5.65
20	1.075	2.097	1.118	2.173	1.190	2.306	3.57	5.60
30	1.073	2.093	1.114	2.166	1.179	2.285	3.55	5.60
40	1.073	2.093	1.112	2.162	1.171	2.269	3.55	5.61
50	1.073	2.093	1.110	2.158	1.164	2.256	3.55	5.63
60	1.074	2.095	1.107	2.152	1.157	2.242	3.55	5.64
70	1.075	2.097	1.103	2.144	1.152	2.232	3.55	5.65
80	1.076	2.099	1.099	2.136	1.148	2.225	3.55	5.65
90	1.076	2.099	1.095	2.129	1.142	2.213	3.55	5.65
100	1.075	2.097	1.092	2.123	1.138	2.205	3.55	5.65
110	1.075	2.097	1.088	2.115	1.132	2.194	3.52	5.63
120	1.073	2.093	1.084	2.107	1.127	2.184	3.51	5.60
130	1.072	2.091	1.080	2.099	1.121	2.172	3.50	5.55
140	1.070	2.087	1.076	2.092	1.116	2.163	3.48	5.50
150	1.068	2.084	1.072	2.084	1.110	2.151	3.47	5.43
160	1.066	2.080	1.067	2.074	1.105	2.141	3.46	5.36
170	1.063	2.074	1.062	2.064	1.098	2.128	3.45	5.28
180	1.059	2.066	1.057	2.055	1.092	2.116	3.43	5.20
190	1.054	2.056	1.052	2.045	1.085	2.103	3.41	5.14
200	1.049	2.046	1.045	2.031	1.078	2.089	3.38	5.10
225	1.034	2.017	1.030	2.002	1.060	2.054	3.31	4.92
250	1.018	1.986	1.012	1.967	1.041	2.017	3.24	4.73
275	1.001	1.953	0.993	1.930	1.020	1.977	3.17	4.53
293	0.987	1.926	0.977	1.899	1.003	1.944	3.12	4.40

* Smoothed values obtained from fig. 4.3 and 4.4; units: χ_m (10^{-6}emu/g); χ_A (10^{-4}emu/mol); T(K).

REFERENCES CHAPTER 4

1. Schwaller, R. and Wucher, J., C.R. Acad. Sc. Paris 264 (1967) 116.
2. Gainon, D. and Sièrro, J., Phys. Letter 26 A (1968) 601; Helv. Phys. Acta 43 (1970) 541.
3. Star, W.M., Boerstoel, B.M., van Dam, J.E. and van Baarle, C., Proc. 11th Int. Conf. on Low Temp. Phys. (LT 11), St. Andrews, 1969, p. 1280.
4. Star, W.M., de Vroede, E. and van Baarle, C., Physica 59 (1972) 128; Commun. Kamerlingh Onnes Laboratorium, Leiden No. 390 c.
5. Gerstenberg, Ann. Physik 2 (1958) 236.
6. see e.g. Nieuwenhuys, G.J., Boerstoel, B.M., Zwart, J.J. and van den Berg, G.J., Physica 62 (1972) 278; Commun. Kamerlingh Onnes Laboratorium, Leiden No. 395 c.
7. Rault, J. and Burger, J.P., C.R. Acad. Sc. Paris 269 (1969) 1085.
8. Rault, J. and Burger, J.P., C.R. Acad. Sc. Paris 267 (1968) 750.
9. see e.g. Gerritsen, A.N. and Linde, J.O., Physica 18 (1952) 887; Kouvel, J.S., J. Phys. Chem. Solids 24 (1963) 795.
10. Coles, B.R., Mozumder, S. and Rusby, R., Proc. 12th Int. Conf. on Low Temp. Phys., Kyoto, 1970, p. 737.
11. Nagasawa, H. and Inoue, N., Proc. 12th Int. Conf. on Low Temp. Phys., Kyoto, 1970, p. 741.
12. Coles, B.R., Phys. Letters 8 (1964) 243.
13. Schindler, A.I. and Coles, B.R., J. Appl. Phys. 39 (1968) 956.
14. Kaiser, B. and Doniach, S., Int. J. Magnetism 1 (1970) 11.
15. A similar suggestion was communicated to the author by Lederer in 1969.
16. Caplin, A.D. and Rizzuto, C., Phys. Rev. Lett. 21 (1968) 746.
17. Rivier, N. and Zlatić, V., J. Phys. F: Metal Phys. 2 (1972) L 99; see also loc. cit. p. L 87.
18. Fischer, K., in "Springer Tracts in Modern Physics" (ed. G. Höhler) vol. 54, p. 1 (Springer Verlag, Berlin) 1970.
19. van Dam, J.E. and van den Berg, G.J., Phys. Stat. Sol. (a) 3 (1970) 11.
20. Nagasawa, H., J. Phys. Soc. Japan 28 (1970) 1171.
21. Moriya, T., Proc. Theor. Phys. 33 (1965) 157.
22. Donzé, P. thesis University of Geneva, 1970 (Archives des Sciences, Genève, vol. 22, fasc. 3, 1969).
23. Burger, J.P., Ann. Physique 9 (1964) 345.
24. Foner, S., Doclo, R. and McNiff, Jr., E.J., J. Appl. Phys. 39 (1968) 551.
25. Lederer, P. and Mills, D.L., Phys. Rev. 165 (1968) 837.

26. Lederer, P., Proc. Nato Advanced Study Institute "Magnetism-Current Topics", La Colle sur Loup, 1970, to be published.
27. Kohzuki, S. and Asayama, K., J. Phys. Soc. Japan, 32 (1972) 1237.
28. Misawa, S., Phys. Letters 32A (1970) 541.
29. Cottet, H., thesis, University of Geneva, 1971.
30. Andersen, O.K., Phys. Rev. B2 (1970) 883.
31. Inoue, N. and Nagasawa, H., J. Phys. Soc. Japan 31 (1971) 477.
32. see e.g. Cannella, V. and Mydosh, J.A., Phys. Rev., to be published.
33. Kao, F.C.C. and Williams, G., Phys. Rev. B, to be published.
34. Coles, B.R., Tari, A. and Jamieson, H.C., preprint.
35. Beck, P.A., Met. Trans. 2 (1971) 2015.
36. Coles, B.R., as quoted by Anderson, P.W., Mat. Res. Bull. 5 (1970) 549.
37. Murani, A.P. and Coles, B.R., J. Phys. C: Metal Phys. Suppl. 2 (1970) S 159.
38. see Saint-Paul, M., Souletie, J., Thoulouze, D. and Tissier, B., J. Low Temp. Phys. 7 (1972) 129.
39. Schindler, A.I., Naval Research Laboratory Report 7057, Washington, D.C., 1970.
40. Heiniger, F., unpublished results.
41. Weisman, I.D. and Knight, W.D., Phys. Rev. 169 (1968) 373.
42. Boerstoel, B.M., Zwart, J.J. and Hansen, J., Physica 54 (1971) 442.
43. Costa-Ribeiro, P., Saint-Paul, P., Thoulouze, D. and Tournier, R., preprint LT 13.

SAMENVATTING

De in dit proefschrift beschreven metingen van de magnetische susceptibiliteit (χ) in het temperatuurgebied van 2 - 300 K vormen een deel van het onderzoek dat in de Metalengroep ondernomen is om een beter inzicht te krijgen in het gedrag van verdunde magnetische legeringen.

De motivatie van dit onderzoek was gelegen in de vele, verschillende, theoretische voorspellingen omtrent de temperatuurafhankelijkheid van verscheidene eigenschappen bij lage temperaturen, d.w.z. ver beneden de zogenaamde Kondo temperatuur. De nauwkeurige meting van enkele eigenschappen (de elektrische weerstand, de soortelijke warmte en de magnetische susceptibiliteit) als funktie van de temperatuur zou kunnen bijdragen tot een keuze tussen de verschillende theorieën.

De legeringen (Au-V, Pd-Cr en Pt-Cr) waarvan bovenstaande eigenschappen zijn gemeten, zijn gekozen vanwege de hoge waarde van T_K ($\sim$ 300 K), zodat gemakkelijk aan de voorwaarde $T << T_K$ voldaan kon worden.

De resultaten van de soortelijke warmte en de weerstandsmetingen toonden aan dat deze grootheden met de temperatuur variëerden als T, resp. T^2, wanneer voldaan was aan de volgende voorwaarden:

a. $T < 0.1\ T_K$

b. $c < c_o$

De waarde van de concentratie c_o bleek evenredig te zijn met de Kondo temperatuur. Wanneer $c > c_o$ traden interaktie verschijnselen aan het licht, die geïnterpreteerd kunnen worden als het afnemen van de Kondo temperatuur met toenemende concentratie.

Onze metingen van de susceptibiliteit van Au-V legeringen zijn in overeenstemming met de hierboven genoemde resultaten (zie hoofdstuk 1). Voor de legeringen met een concentratie lager dan 0.5 at.% bleek de extra susceptibiliteit voor $T \leq 0.2\ T_K$ evenredig te zijn met T^2, terwijl voor hogere concentratie interaktie effekten, leidend tot een lagere T_K waarde, konden worden vastgesteld. Het gedrag van de extra susceptibiliteit als funktie van de concentratie duidt echter ook op interakties die aanleiding geven tot een toeneming van T_K. Voor dit complexe gedrag wordt een verklaring gesuggereerd, uitgaande van een wisselwerking tussen de opgeloste atomen die van karakter verandert als funktie van de afstand.

De temperatuurafhankelijkheid van de extra susceptibiliteit ($\Delta\chi$) van de legering met de laagste concentratie (0.2 at.%) wordt goed beschreven met een uitdrukking afgeleid door Schotte en Schotte. Hieruit blijkt dat de temperatuur-

afhankelijkheid van $\Delta\chi$ bepaald wordt door de effectieve breedte van het energieniveau behorende bij het opgeloste atoom. Deze breedte is van de grootte orde kT_K en voor lage T_K waarden veel kleiner dan de breedte (Δ) van de virtueel gebonden toestand ($\Delta \sim 20.000$ k).

De metingen door ons verricht aan Pd-Cr en Pt-Cr legeringen (zie hoofdstuk 4) hebben duidelijk de geleidelijke overgang tussen een zwak magnetisch en een sterk magnetisch karakter van de opgeloste Cr atomen bij toenemende concentratie aangetoond. (Dit kan geïnterpreteerd worden als de afneming van T_K met toenemende concentratie). De temperatuurafhankelijkheid van $\Delta\chi$ bij lage temperaturen wordt overheerst door de bijdrage van geringe hoeveelheden magnetische verontreinigingen ($\sim$ 4 ppm Fe). Bij hogere temperaturen voldoet $\Delta\chi(T)$ redelijk aan een Curie-Weiss relatie. Wanneer de effectieve Neél temperatuur gelijkgesteld wordt aan T_K zijn de gevonden waarden in overeenstemming met die afgeleid uit de weerstandsmetingen en uit een soortelijke warmte.

Voor Pd legeringen met een concentratie groter dan ongeveer 7 at.%Cr treden maxima op in $\chi(T)$, duidend op magnetische ordening. De invloed van deze ordening is ook waargenomen in de weerstand, waarvan het gedrag als funktie van de temperatuur qualitatief grote overeenkomst vertoont met dat waargenomen in een systeem als Cu-Mn.

Bij de analyse van $\chi(T)$ van de Pd-Cr legeringen is een goed begrip van het gedrag van zuiver Pd onontbeerlijk. Aan het Pd probleem hebben we apart aandacht geschonken in hoofdstuk 3. De susceptibiliteit van Pd is erg groot en vertoont een maximum als funktie van de temperatuur bij ongeveer 85 K. Voor de verklaring hiervan zijn vele suggesties gedaan, o.a. het optreden van een scherpe piek in de toestandsdichtheid, vlak bij de Fermi energie. Uit een vergelijking van onze resultaten met een recente bandstructuurberekening van Andersen blijkt dat er nog geen volledige quantitatieve overeenstemming bestaat tussen deze theorie en het experiment. De metingen blijken wel goed aangepast te kunnen worden aan een uitdrukking afgeleid door Misawa, die Pd als een Fermivloeistof beschouwt. Door het grote aantal parameters (5) is de significantie van deze aanpassing niet erg groot.

In hoofdstuk 2 worden soortelijke warmte metingen aan Pd-Ni legeringen gepresenteerd. Deze metingen hadden tot doel de invloed van lokale spin fluctuaties LSF op de soortelijke warmte bij hogere temperaturen te bestuderen. De reeds bekende resultaten waren meestal waren meestal beperkt tot 4 K. Onze metingen, uitgevoerd in het temperatuurgebied van 1.3 - 25 K, hebben de volgende nieuwe resultaten opgeleverd:

a. de anomalie in de temperatuurafhankelijkheid van de Debye temperatuur van Pd wordt niet veroorzaakt door een LSF bijdrage.

b. in Pd-Ni legeringen is er behalve een negatieve T^3 term ook een positieve T^5 term ten gevolge van LSF bijdragen.

c. uit de concentratieafhankelijkheid van de lineaire term kan een critische concentratie c_o voor het optreden van ferromagnetisme afgeleid worden ($c_o \sim$ 2.7 at.%Ni).

d. een uitwendig magneetveld van 20 kOe heeft slechts een geringe invloed ($\Delta\gamma/\gamma \sim 4\%$ voor Pd 2.2 at.%Ni).

Een vergelijking van Pd-Cr en Pd-Ni op basis van het LSF model leert dat beide systemen grote gelijkenis vertonen.

Op verzoek van de Faculteit der Wiskunde en Natuurwetenschappen volgt hier een overzicht van mijn studie.

Nadat ik in 1960 het diploma gymnasium β behaald had aan het Christelijk Lyceum „Zandvliet" te Den Haag, ben ik mijn studie begonnen aan de Rijksuniversiteit te Leiden. In 1963 legde ik het kandidaatsexamen af in de Wis- en Natuurkunde met als bijvak Sterrekunde. Sinds mijn kandidaatsexamen ben ik werkzaam geweest op het Kamerlingh Onnes Laboratorium in de werkgroep Mt-IV van de werkgemeenschap „Metalen F.O.M.-T.N.O." Vanaf 1964 ben ik in dienst van de Stichting F.O.M., tot 1966 als wetenschappelijk assistent, daarna als wetenschappelijk medewerker. De leiding van deze werkgroep berust bij Prof. dr. C.J. Gorter, terwijl dr. G.J. van den Berg als adjunct-werkgroepleider met het dagelijks toezicht is belast.

Mijn intrede in het laboratorium deed ik in kamer H, waar ik aanvankelijk bij dr. W.M. Star assisteerde bij het meten van zgn. anomale thermospanningen. In 1964 ben ik begonnen met het ontwikkelen van kool-thermometers. Dit onderzoek kon in samenwerking met dr. W.M. Star en dr. C. van Baarle afgesloten worden.

Voor mijn doctoraalexamen, dat ik in 1966 aflegde, heb ik de verschillende methoden van het meten van magnetische susceptibiliteit bestudeerd, ter voorbereiding van het bouwen van een meetopstelling. Na de overgang (begin 1967) naar de nieuwe vleugel van het laboratorium kon dan ook direct met de bouw van deze opstelling begonnen worden. Eind 1967 werd de opstelling in bedrijf gesteld en na de nodige ijkingen begin 1968 de eerste meting verricht worden. Bij de constructie van deze opstelling heb ik van de waardevolle adviezen van dr. C. van Baarle geprofiteerd, terwijl de uitvoering ervan op vakkundige wijze geschied is door de heren M.C. Zonneveld en J. Turenhout.

Sinds 1964 heb ik geassisteerd op het natuurkundig practicum (vanaf 1967 als assistent bij het werkcollege voor 1^e jaars chemici).

Bij de uitvoering van de metingen heb ik de waardevolle medewerking van drs P.C.M. Gubbens en Marike Pikart zeer op prijs gesteld. Ook drs. J.J. Zwart en drs. C.W.M. Dessens ben ik erkentelijk voor de steun die zij mij verleend hebben.

De nauwe samenwerking en de vele discussies met dr. W.M. Star zijn voor mij een grote stimulans geweest bij het bepalen van de richting van het onderzoek, dat als onderdeel van één project gezien kan worden om van van dezelfde

legeringen verschillende eigenschappen te bepalen. Dr. Boerstoel ben ik erkentelijk voor het suggereren van het soortelijke warmte onderzoek.

De legeringen zijn vervaardigd door de heren C.E. Snel, H.J. Tan en T.J. Gortenmulder.

De concentratiebepalingen zijn uitgevoerd door dr. J. Kragten en medewerkers van het Natuurkundig Laboratorium der Universiteit van Amsterdam.

De tekeningen en foto's zijn vervaardigd door de heren H.J. Rijskamp, W.J. Brokaar en W.F. Tegelaar, terwijl de tekst van dit proefschrift op vaardige wijze getypt is door mevrouw E. de Haas-Walraven.

7301584

STELLINGEN

1. De suggestie, dat in Ag-Pd legeringen de veronderstelde scherpe overgang van virtueel gebonden toestanden op de Pd-atomen naar een Pd d-band zou samenhangen met een kritische concentratie, analoog aan de kritische percolatie-waarschijnlijkheid, pleit eerder tegen dan voor een scherpe overgang.
   C. Norris en H.P. Myers, J. Phys. F; Metal Phys. 1 (1971) 62.
   M.F. Sykes en J.W. Essam, Phys. Rev. 133 (1964) A310.

2. De verklaring van de anomale temperatuurafhankelijkheid van de effectieve Debije-temperatuur van Pd die in dit proefschrift gegeven wordt, kan worden getoetst door de meting van de fonon-dispersie in een niet-magnetische Pd-legering, b.v. Pd-5at.%Cu.
   Dit proefschrift, hoofdstuk 2.

3. De door Pells en Shiga uit hun metingen afgeleide brede piek in het optische absorptiespectrum van Au bij 1 eV kan worden toegeschreven aan een onjuiste analyse.
   G.P. Pells en Shiga, J. Phys. C. 2 (1969) 1835.

4. Meting van het Mössbauer-effekt in Pd-Ni legeringen dient te worden uitgevoerd om opheldering te verschaffen over de discrepantie tussen de verschillende bepalingen van de kritische concentratie voor het optreden van ferromagnetisme.
   Dit proefschrift, hoofdstuk 2.

5. Het optreden van een maximum in de magnetische susceptibiliteit van vloeibare Ge-Fe legeringen als funktie van de temperatuur kan niet worden verklaard met het Kondo-effekt, zoals door Wachtel en Maier gesuggereerd wordt.
   E. Wachtel en J. Maier, Phys. Letters 39A (1972) 131.

6. De bewering van Robbins en Claus, dat het magnetische gedrag van Ni_3Al moet worden verklaard in termen van clusters in plaats van met een bandenmodel, is gebaseerd op onjuiste conclusies en op te weinig experimenten.
   C.G. Robbins en H. Claus, Proc. 17^{th} Int. Conf. on Magn. (A.I.P., New York) 1972, p. 527.

7. De opmerking, dat de temperatuurafhankelijkheid van de magnetische susceptibiliteit van Cu-Fe legeringen ($\chi = \chi_o + C/(T+29)$), geëxtrapoleerd naar $T = 0$, in strijd is met de derde hoofdwet van de thermodynamica, is irrelevant voor het gedrag van χ bij $T \approx 1$ K.
   B. Triplett en N.E. Phillips, Phys. Rev. Letters 27 (1971) 1001.

8. De conclusie, die White en Pawlowicz trekken uit de geringe drukafhankelijkheid van het gedeelte van het Fermi-oppervlak van Pd met overwegend s-p karakter, namelijk dat de totale toestandsdichtheid aan het Fermi-oppervlak weinig zou variëren met het volume, is aanvechtbaar.
G.K. White en A.T. Pawlowicz, J. Low Temp. Phys. 2 (1970) 631.

9. In Pd-Cr legeringen neemt bij toenemende concentratie van chroom de bijdrage van de elektronen tot de soortelijke warmte toe, terwijl de magnetische susceptibiliteit afneemt. Dit kan kwalitatief worden verklaard met de aanwezigheid van een virtueel gebonden toestand op de Cr-atomen.
H. Nagasawa, J. Phys. Soc. Japan 28 (1970) 1171.

10. Voor de vergelijking van berekeningen van de eigenschappen van legeringen met de experimentele resultaten verdient in het geval van Pd-legeringen de soortelijke warmte de voorkeur boven de magnetische susceptibiliteit.
K. Levin, R. Bass en K.H. Benneman, Phys. Rev. B6 (1972) 1865.

11. In het gedeelte van het Kamerlingh Onnes laboratorium waar roken verboden is dient het lopen in schoenen met rubberen zolen te worden vermeden.
Dr. S.W. Tromp, "Wichelroede en Wetenschap", Kosmos, 1950.